

Identification and Functional Characterization of Novel p38
MAPK and PIKfyve Inhibitors

January 2018

Masaomi TERAJIMA

Identification and Functional Characterization of Novel p38
MAPK and PIKfyve Inhibitors

A Dissertation Submitted to
the Graduate School of Life and Environmental Sciences,
the University of Tsukuba
in Partial Fulfillment of the Requirements
for the Degree of Doctor of Philosophy in Biological Science
(Doctoral Program in Biological Sciences)

Masaomi TERAJIMA

Table of Contents

Abstract	1
Abbreviations	4
General introduction.....	6
Chapter-I	10
Anti-inflammatory effect and selectivity profile of AS1940477, a novel and potent p38 mitogen-activated protein kinase inhibitor	
Summary	11
Introduction	13
Materials and Methods	15
Results	21
Discussion	25
Tables and Figures	31
Chapter-II.....	40
Inhibition of c-Rel DNA binding is critical for the anti-inflammatory effects of novel PIKfyve inhibitor	
Summary	41
Introduction	42
Materials and Methods	45
Results	57
Discussion	67
Tables and Figures	73
General discussion.....	103
Acknowledgement	108
References	110

Abstract

Chronic inflammation is characterized by infiltration of inflammatory cells and persistent activation of immune system, leading to aberrant production of proinflammatory cytokines. Numerous studies have provided the evidence that proinflammatory cytokines, including TNF α , IL-6, and IL-23, play key roles in chronic inflammation, and many biologic drugs targeting these cytokines have shown excellent therapeutic effects in clinical, however, they still have some problems the presence of nonresponsive patients and a low remission rate in monotherapy. To elucidate the immunological mechanisms of chronic inflammation and identify potential targets for novel anti-inflammatory drugs, in this study, I have focused attention on the intracellular signaling pathway regulating proinflammatory cytokine production.

In the first chapter, I have screened and identified a novel p38 MAPK inhibitor, AS1940477, and its anti-inflammatory effect and selectivity profile have been evaluated. AS1940477 selectively inhibited enzyme activity against p38 α and β isoforms, and suppressed proinflammatory cytokine production in human peripheral blood mononuclear cells and signal activation in synovial stromal cells. AS1940477 also potently inhibited LPS-induced TNF α production *in vivo*, and its inhibitory effect was confirmed even after 20h of administration.

In the second chapter, I have screened and identified two novel IL-12p40 production inhibitors, AS2677131 and AS2795440, and functional characterization and target identification of these compounds have been performed. Interestingly, these compounds inhibited not only

proinflammatory cytokine production in macrophages but also BCR-mediated B cell activation, and a significant preventive effect was also confirmed on experimental arthritis in rats. In addition, PIKfyve, a class III lipid kinase, was identified as a target molecule by molecular biological analysis using photoreactive linker-conjugated probes. PIKfyve was also found to selectively control the binding activity of c-Rel, an NF κ B family transcription factor, to the promoters of the target genes, IL-12p40 and IL-1 β .

In conclusion, the current study has demonstrated that p38 MAPK and PIKfyve play key roles in the development of chronic inflammation, and the inhibition of their kinase activity by novel small molecule inhibitors (AS1940477, AS2677131, and AS2795440) could be a new therapeutic approach for treating chronic inflammatory diseases. It is also expected that new molecules as anti-inflammatory drug targets will be found in future from PIKfyve-c-Rel pathway.

Abbreviations

TNF α	tumor necrosis factor alpha
IL	interleukine
RA	rheumatoid arthritis
DC	dendritic cell
Th17	T helper 17
MAPK	mitogen-activated protein kinase
ERK	extracellular signal-regulated kinase
JNK	c-Jun N-terminal kinase
PIKfyve	phosphoinositide kinase, FYVE-type zinc finger containing
PI	phosphoinositide
LPS	lipopolysaccharide
PHA	phytohemagglutininA
PGE ₂	prostaglandin E ₂
PBMC	peripheral blood mononuclear cell
SSC	synovial stromal cell
MMP-3	metallopeptidase-3
Con A	Concanavalin A
IRF	interferon regulatory factor
TNP	2,4,6-trinitrophenol
DMF	N,N-di-methylformamide
MALDI-TOFMS	MALDI-TOF mass spectrometry

siRNA	small interfering RNA
APC	allophycocyanin
MDP	muramyl dipeptide
TLR	Toll-like receptor
Poly(I:C)	polyinosinic-polycytidylic acid
AIA	adjuvant-induced arthritis

General introduction

With an expanding aging population in the world, the number of patients suffering from various aging-related diseases, including autoimmune diseases, atherosclerotic diseases, cancer, and neurodegenerative diseases, is predicted to increase in the future. Chronic inflammation is commonly associated with the development and progression of those diseases [1]. Chronic inflammation is characterized by infiltration with inflammatory cells (mononuclear cells, macrophages, lymphocytes) into the affected tissue and persistent activation of immune system, which consequently leads to aberrant productions of proinflammatory cytokines, chemokines, and autoantibodies.

Numerous experimental studies have provided that the expression levels of proinflammatory cytokines, such as tumor necrosis factor alpha (TNF α), IL-1 β , IL-6, IL-23, and IL-17, is strictly controlled, especially in amount, timing, and place of production, and positively correlated with the severity in many inflammatory diseases [2-4]. For instance, TNF α and IL-6 are rapidly released from activated macrophages and facilitate tissue inflammation, fibrosis and damage in rheumatoid arthritis (RA). IL-23 is also produced from activated macrophages and dendritic cells (DCs), and induce IL-17 production from T helper 17 (Th17) cells important as an inflammation initiator in the pathogenesis of several inflammatory diseases, such as psoriasis. In addition to advances of understanding in biology as described above, recent remarkable advance in antibody engineering technology has

brought many biologic drugs to market [2].

The excellent therapeutic effect of the biologic drugs that can neutralize the activity of target cytokines have indicated that inflammatory cytokines play an important role in the development of chronic inflammatory diseases, while monotherapy for individual cytokines still has some problems, such as the presence of nonresponsive patients and a low remission rate. Another problem is also that biological therapy is relatively expensive and inconvenient compared to oral drugs. Therefore, I thought that there were unmet medical needs for oral drugs that could simultaneously inhibit multiple inflammatory cytokines and fundamentally improve the formation of chronic inflammation.

As described above, inflammatory cytokines are predominantly produced by activated macrophages. Therefore, I focused on two different mechanisms regulating inflammatory cytokine production in macrophages and screened for small molecule inhibitors. The first is p38 mitogen-activated protein kinase (MAPK) as an important signal for the production of multiple inflammatory cytokines such as $\text{TNF}\alpha$, $\text{IL-1}\beta$ and IL-6 . The second is a production inhibitor of IL-12p40 , a common component of IL-12 and IL-23 . MAP kinases are serine/threonine protein kinases that include extracellular signal-regulated kinases (ERK), c-Jun N-terminal kinases (JNK), and p38 isoforms [5]. Among of them, p38 isoforms are responsible for the step of production and activation signal of multiple proinflammatory cytokines. On the other hand, IL-23 containing IL-12p40 subunit as a component play a key role in the expansion and survival of Th17 cells, which is one of helper T

cell subsets. Th17 is thought to activate effector cells such as macrophages and B cells, thereby contributing to the promotion of chronic inflammation.

In the first chapter, I have identified a novel p38 MAPK inhibitor AS1940477, and investigated the functional characteristics of AS1940477. Especially, the *in vitro* and *in vivo* characteristics regarding kinase selectivity and potency were evaluated in detail, and compared with those of previously reported p38 MAPK inhibitors in discussion section.

In the second chapter, I have identified two novel IL-12p40 production inhibitors, AS2677131 and AS2795440, and extensively investigated their pharmacological characteristics. Thereby, it has been found that those inhibitors exert unique immunoregulatory functions, including selective proinflammatory cytokine inhibition and B cell activation inhibition. I have also identified phosphoinositide kinase, FYVE-type zinc finger containing (PIKfyve), a Class III phosphoinositide kinase, as a direct target molecule of these inhibitors by chemical biological approach. PIKfyve is one of mammalian lipid kinases that act on phosphoinositide (PI) and PI3P to generate PI5P and PI(3,5)P₂, respectively [6], and involved in normal endosome processing and membrane trafficking, while immunological function of PIKfyve has remained almost unknown. So, I have explored the mechanism of action of PIKfyve inhibitors, and revealed a novel mechanism regulating cytokine production which is mediated by PIKfyve-c-Rel pathway.

Taken together, in this study, I have obtained multiple small molecule compounds with different mechanisms, including p38 MAPK inhibitor (AS1940477) and PIKfyve inhibitors (AS2677131, AS2795440), which all

have shown potent anti-inflammatory activity. The results of functional characterization of these inhibitors have provided strong evidence that p38 MAPK and PIKfyve play an important role in the production of inflammatory cytokines involved in the development of chronic inflammation. The inhibition of their activity was also indicated the possibility to become a new therapeutic approach for chronic inflammatory diseases.

Chapter I

Anti-inflammatory effect and selectivity profile of AS1940477, a novel and potent p38 mitogen-activated protein kinase inhibitor

Summary

Given the key role p38 MAPK plays in inflammatory responses through the production of cytokines and inflammatory mediators, its inhibition is considered a promising therapeutic strategy for chronic inflammatory diseases such as rheumatoid arthritis, psoriasis, inflammatory bowel disease, and chronic obstructive pulmonary disease. Here, I evaluated the anti-inflammatory effect and selectivity profile of the novel p38 MAPK inhibitor AS1940477. AS1940477 inhibited the enzymatic activity of recombinant p38 α and β isoforms but showed no effect against other 100 protein kinases including p38 γ and δ isoforms. I also confirmed the selectivity of AS1940477 in the intracellular signaling pathway. In human peripheral blood mononuclear cells, AS1940477 inhibited lipopolysaccharide (LPS)- or phytohemagglutininA (PHA)-induced production of proinflammatory cytokines, including TNF α , IL-1 β , and IL-6 at low concentrations (LPS/TNF α , IC₅₀ = 0.45 nM; PHA/TNF α , IC₅₀ = 0.40 nM). In addition, equivalent concentrations of AS1940477 that inhibited cytokine production also inhibited TNF α - and IL-1 β -induced production of IL-6, PGE₂, and MMP-3 in human synovial stromal cells. AS1940477 was also found to potently inhibit TNF α production in whole blood (IC₅₀ = 12 nM) and effectively inhibited TNF α production induced by systemically administered LPS in rats at less than 0.1 mg/kg (ED₅₀ = 0.053 mg/kg) with an anti-inflammatory effect lasting for 20 h after oral administration. Overall, this study demonstrate that AS1940477 is a novel and potent p38 MAPK

inhibitor and may be useful as a promising anti-inflammatory agent for treating inflammatory disorders.

Introduction

Chronic inflammatory diseases such as rheumatoid arthritis, psoriasis, and inflammatory bowel disease are characterized by autoimmune responses, leading to the destruction of normal tissues [7-9]. While the underlying immunological mechanisms and pathogenic factors contributing to the initiation and development of chronic inflammatory diseases have not been fully elucidated, the therapeutic success of cytokine-neutralizing agents (e.g. infliximab, adalimumab, etanercept, anakinra, and tocilizumab) suggests that proinflammatory cytokines such as $\text{TNF}\alpha$, $\text{IL-1}\beta$ and IL-6 play a central role in the pathogenesis of certain inflammatory diseases [3, 4]. However, despite their therapeutic efficacy, these biological therapies are expensive and relatively inconvenient to administer, leaving an unmet need for developing novel anti-inflammatory therapies and more effective and orally available small molecule inhibitors.

MAPKs are serine/threonine protein kinases that include ERK, JNK, and p38 isoforms [5]. p38 isoforms are responsive to various cellular stress stimuli, including shock, inflammatory cytokines, endotoxins, and growth factors. To date, four isoforms ($\text{p38}\alpha$, $\text{p38}\beta$, $\text{p38}\gamma$, and $\text{p38}\delta$) have been identified in mammalian cells and are expressed in differential, tissue-specific patterns. Of these four, $\text{p38}\alpha$ is mainly expressed in immune and inflammatory cells and is associated most closely with inflammatory responses [10, 11] and the synthesis of a variety of proinflammatory mediators such as $\text{TNF}\alpha$, $\text{IL-1}\beta$, IL-6 , and prostaglandin E_2 (PGE_2) regulated

by p38 α -dependent signaling. In addition, p38 α acts downstream of TNF α and IL-1 β [12], thereby mediating many of these molecules' biological effects such as pain, cell recruitment and bone metabolism. The targeted inhibition of p38 α using small molecule inhibitors is therefore believed to be an attractive strategy for treating inflammatory disorders.

To date, many p38 α inhibitors have been generated and characterized by a number of pharmaceutical companies, and several inhibitors, including BIRB796, VX-745, SCIO-469, and VX-702, have been found to exert beneficial effects in various animal models and have advanced to clinical trials. However, in light of inadequate clinical efficacy or unacceptable safety profiles attributed to low kinase selectivity and chemical structure-based toxicity, the clinical development of these compounds was eventually discontinued [13, 14].

Here, in order to evaluate a potential as an anti-inflammatory drug, I describe the pharmacological activity of the novel p38 inhibitor AS1940477 and demonstrate its potent and highly selective inhibitory activity against p38 MAPK both *in vitro* and *in vivo* acute inflammation model.

Materials and Methods

Preparation of AS1940477

The p38 MAPK inhibitor AS1940477 [6-[(6R)-2-(4-fluorophenyl)-6-(hydroxymethyl)-4,5,6,7-tetrahydropyrazolo[1,5-a]pyrimidin-3-yl]-2-(2-methylphenyl)pyridazin-3(2H)-one] was synthesized by Astellas Pharma (Tsukuba, Japan), and SB203580 [4-(4-fluorophenyl)-2-(4-methylsulfinyl)-phenyl-5-(pyridin-4-yl)-1H-imidazole] was purchased from Sigma-Aldrich (St. Louis, MO, USA)

Kinase isoform selectivity assays

The human p38 α and p38 β kinase activities of AS1940477 were evaluated using a Z'-Lyte™ kinase assay system (Life Technologies, Madison, FL, USA), and the activities of 99 other protein kinases (including p38 γ and p38 δ) were evaluated using a Kinase Profiling Assay (Carna Biosciences, Kobe, Japan). JNK2 kinase activity was examined by following an in-house protocol. Preactivated recombinant human JNK2 α 2/SAPK1a (40 ng/well; Upstate Biotechnology, Lake Placid, NY, USA) was diluted in 1.5 \times Assay Dilution Buffer-I (1 \times ADB-I; 20 mM MOPS, pH 7.2, 25 mM β -glycerol phosphate, 5 mM EGTA, 1 mM sodium orthovanadate, 1 mM DTT), and then 20 μ L of 1.5 \times ADB-I (containing recombinant JNK2) was mixed with 20 μ L of Mg/ATP/1 \times ADBI buffer (37.5 mM MgCl₂, 2 μ M ATP diluted with 1 \times ADB-I) and 10 μ L of AS1940477 at final concentrations of 10 to 1000 nM in a 96-well MaxiSorp Immuno Plate (Nalge Nunc International, Rochester, NY, USA) pre-coated

with recombinant human ATF-2 (0.1 µg/well; Upstate Biotechnology). After a 30-min incubation at 30 °C, the plate was washed three times with phosphate-buffered saline buffer containing Tween 0.05% and then incubated with 1:1000 diluted anti-phospho-ATF-2 (Thr71) (Cell Signaling Technology, Danvers, MA, USA) antibody for 60 min at room temperature. Subsequently, the plate was washed as described above and reacted with 1:5000 diluted anti-rabbit IgG conjugated HRP (Zymed Laboratories, South San Francisco, CA, USA) for 30 min at room temperature. After the plate was washed, TMB substrate (BD Biosciences Pharmingen, San Diego, CA, USA) was added, and the plate was incubated for 20 min in the dark. The reaction was stopped by adding 50 µL of 2 N H₂SO₄, and sample absorbance was measured with a microplate reader at 450 nm.

Cellular selectivity assays using human monocytic THP-1 cells

The selectivity of p38, JNK, and NFκB pathways in a cellular context was determined by measuring the phosphorylation of HSP-27 and c-Jun or IκBα degradation in THP-1 cells (ATCC TIB202). THP-1 cells were collected by centrifugation and resuspended in RPMI 1640 (Invitrogen, Carlsbad, CA, USA) containing 10% fetal bovine serum (BioWest, Nuaille, France) and 1% (v/v) penicillin-streptomycin solution. After a 30-min pretreatment with AS1940477 (final concentration: 1 to 1000 nM), the cells were incubated in presence or absence of LPS (*Escherichia coli*, 055:B5, 10 µg/mL, Sigma-Aldrich) for 30 min at 37 °C; the reaction was stopped by adding ice-cold phosphate-buffered saline. The cells were collected by centrifugation,

lysed in 300 μ L of 1 \times Lysis buffer (PathScan Kit contents; Cell Signaling Technology), sonicated for 30 sec on ice, and then centrifuged at 12,000 g for 5 min at 4 $^{\circ}$ C. The supernatants were then stored at -80 $^{\circ}$ C until ELISA analysis. Phospho- and total HSP-27 (Ser78), and c-Jun (Ser63) levels were determined by ELISA (PathScan ELISA kit, #7290, #7145, #7150, Cell Signaling Technology, Immunoassay kit, #KHO0331; Biosource International, Camarillo, CA, USA) following the manufacturer's instructions. Total I κ B α amount was also determined via ELISA (Cell Signaling Technology).

Cellular selectivity was also examined by Western blotting, THP-1 cells, pretreated with or without AS1940477 for 30 min, were stimulated with LPS (10 μ g/mL) for a period of 30 min followed by a rapid lysis in RIPA buffer (Sigma) containing Protease and Phosphatase inhibitor (Thermo Scientific, Yokohama, Japan) for Western blot analysis. THP-1 cell RIPA lysates were evaluated for HSP-27 and c-Jun phosphorylation by Western blotting using phospho-specific antibodies [phospho-HSP-27 (Ser78) and phospho-c-Jun (Ser63)] or total recognizing antibodies [HSP-27, c-Jun, and I κ B α]. All antibodies were purchased from Cell Signaling Technology.

Inhibition of LPS- or PHA-induced cytokine production in THP-1 and human PBMCs

THP-1 cells with or without 30-min AS1940477 pretreatment were stimulated with LPS (10 μ g/mL) for 16 h, and the concentration of TNF α in the supernatant was determined by ELISA. Blood was collected from healthy volunteers into sodium heparin-treated tubes, and human peripheral blood

mononuclear cells (PBMCs) were isolated by Ficoll density gradient centrifugation using Ficoll-Paque Plus (Amersham Biosciences, Piscataway, NJ, USA) according to the manufacturer's instructions. PBMCs were stimulated in absence or presence of AS1940477 (0.01 to 1000 nM) with LPS (1 µg/mL) or PHA for 16 h, and cytokine concentrations (TNF α , IL-1 β , IL-6, and IL-10) in the medium were measured by ELISA. The following reagents (antibodies, standard proteins, ELISA kits) were used in the assay: purified mouse anti-human TNF, biotin mouse anti-human TNF, and recombinant human TNF (BD Biosciences Pharmingen); DuoSet human IL-1 β (R&D Systems, Minneapolis, MN, USA); purified rat anti-human IL-6 (PeproTech, Rocky Hill, NJ, USA); biotin rat anti-human IL-6 and recombinant human IL-6 (BD Biosciences Pharmingen); purified rat anti-human IL-10 (PeproTech); biotin anti-human and viral IL-10; and recombinant human IL-10 (BD Biosciences Pharmingen).

Inhibition of LPS-stimulated TNF α production in human whole blood

AS1940477 was pre-dispensed and diluted as described for the THP-1 assay above, and human whole blood (275 µL/sample) obtained from healthy volunteers was incubated with diluted AS1940477 and LPS (0.01 µg/mL) for 2 h at 37 °C. After centrifugation, the plasma concentration of TNF α was measured by ELISA as described above.

Effect of AS1940477 on IL-6, PGE $_2$, and MMP-3 production in human synovial stromal cells

Human Synovial Stromal Cells (SSCs) were purchased from Applied Cell Biology Research Institute and cultured in DMEM containing 10% fetal bovine serum (BioWest) and 1% (v/v) penicillin-streptomycin solution. SSCs pretreated with AS1940477 (0.01 to 100 nM) for 30 min were stimulated with or without human TNF α (1 ng/mL)/IL-1 β (2 pg/mL) for 24 h, and levels of IL-6, PGE $_2$, and matrix metalloproteinase-3 (MMP-3) in the medium were measured by ELISA as per the PBMC assay (IL-6) or following the manufacturer's instructions (PGE $_2$, EIA kit Cayman Chemical, Ann Arbor, MI, USA; MMP-3, Human Total MMP-3 Immunoassay, R&D Systems)

Animals

Six- to seven-week-old female Lewis rats were purchased from Charles River Laboratories (Yokohama, Japan) and housed under 12-h light/dark cycles at a controlled temperature (23 ± 1 °C), with tap water and standard laboratory chow available *ad libitum*. Rats were allowed to habituate to the housing facilities for at least 3 days before compound treatment or mitogen stimulation. All experiments were conducted in accordance with the Astellas Pharma Inc. guidelines for the care and use of animals and under approved protocols of the Institutional Animal Care and Use Committee of Astellas Pharma Inc.

Rat acute LPS or Con A-induced cytokine production models

Female Lewis rats were utilized for *in vivo* LPS- or Concanavalin A (Con A)-stimulated inflammatory cytokine production studies with four and three

animals in the vehicle and AS1940477-treated groups, respectively. AS1940477 was suspended in 0.5% methyl cellulose and orally administered to animals in a volume of 5 mL per kg of body weight. Rats were orally administered vehicle or the indicated dose of AS1940477 4 h before LPS or Con A (Vector Labs, Burlingame, CA, USA) intravenous injection. LPS and Con A were challenged at a dose of 10 µg/animal or 3 mg/animal in each study. Animals were anesthetized 1.5 and 2 h after LPS injection or 4 h after Con A injection, and blood was collected. TNF α , IL-1 β , and IL-6 levels in the collected plasma were measured via ELISA 1.5 h, 1.5 h, and 2 h after LPS injection, respectively, and IL-2 levels were measured 4 h after Con A injection. TNF α was detected using an in-house ELISA system with purified hamster anti-mouse/rat TNF α , biotin anti-mouse/rat TNF α (BD Biosciences Pharmingen), and recombinant rat TNF α (R&D Systems). IL-1 β , IL-6, and IL-2 were also detected via a rat IL-1 β /IL-1F2 DuoSet kit, rat IL-6 Quantikine kit (R&D Systems), and rat IL-2 Immunoassay Kit (Biosource International), respectively.

In the study on the long-lasting effects of AS1940477, vehicle or the indicated dose of AS1940477 were administered 4 or 20 h after LPS injection, and TNF α levels in the collected plasma were measured via ELISA in the same way as described above.

Results

Selective inhibition of p38 MAPKs activity by AS1940477

I identified novel p38 MAPK inhibitors by performing a cell-based screening in a 96-well format of in-house chemical libraries, including over 16,000 compounds, to obtain a lead compound that inhibit TNF α production in LPS-stimulated human PBMCs, optimization of which yielded AS1940477 (Fig. 1). AS1940477 potently inhibited p38 α kinase activity with an IC₅₀ value of 11.2 nM (Fig. 2) and showed slightly weaker inhibition of p38 β (IC₅₀ 36.5 nM) but did not inhibit 100 representative protein kinases, including other p38 isoforms (p38 γ , p38 δ) and JNK2, at concentrations up to 1 μ M (Table 1).

Inhibition of the p38 pathway but not JNK or NF κ B pathways in THP-1 cells by AS1940477

Given that p38, JNK, and NF κ B pathways are closely associated with inflammatory responses and the cross-talk between the p38 pathway and other signal transduction pathways such as JNK and NF κ B, I examined the selectivity of AS1940477 in cell-based assay. I first stimulated a human monocytic THP-1 cell line with LPS for 30 min and then measured phospho-HSP-27, phospho-c-Jun, and total I κ B α levels in cell lysates via ELISA, as HSP-27 and c-Jun are known to be located downstream of p38 and JNK, respectively [15, 16]. I κ B α degradation level is also known to reflect the activation status of the NF κ B pathway [17]. AS1940477 suppressed

LPS-induced phosphorylation of HSP-27 with an IC₅₀ value of 4.1 nM (Fig. 3 A), a value greater than that observed for the p38 kinase inhibitor SB203580 (360-fold weaker IC₅₀ value, data not shown), while no inhibitory effect was observed on either the phosphorylation of c-Jun or IκBα degradation at concentrations up to 1 μM (Fig. 3 B, 3 C). The similar selectivity profile was confirmed in Western blot analysis (Fig. 3 D). These results indicated that AS1940477 has no effect on JNK or NFκB pathways and that its inhibitory effect was highly selective for the p38 pathway in the cellular context.

Blockade of cytokine production by AS1940477 in endotoxin-stimulated human cells

I next studied the effects of AS1940477 on cytokine production (TNFα, IL-6, IL-1β, and IL-10) in LPS- or PHA-stimulated human cells. LPS and PHA were used as activators of monocytes/macrophages and T cells, respectively. LPS-induced TNFα production in THP-1 cells and human PBMCs was blocked by AS1940477 with IC₅₀ values of 0.6 nM and 0.45 nM, respectively, in a concentration-dependent manner (Fig. 4, Table 2). I then assessed the effect of AS1940477 on LPS-induced TNFα release in human whole blood. The results showed that AS1940477 potently inhibited TNFα release from LPS-stimulated whole blood with an IC₅₀ value of 12 nM (Table 2). In addition to TNFα, LPS-induced IL-1β and IL-6 production was also suppressed in human PBMCs at almost the same concentration which induced TNFα suppression (IC₅₀ values: 0.55 nM and 3.5 nM, respectively) (Table 2). Further, AS1940477 inhibited PHA-induced cytokine production

(TNF α , IL-6, and IL-10) in human PBMCs with respective IC₅₀ values of 0.40 nM, 1.2 nM, and 6.1 nM for each cytokine, whereas PHA-induced IL-2 production was not inhibited by AS1940477 at concentrations up to 10 μ M (Table 2).

Effect of AS1940477 on TNF α and IL-1 β -induced production of inflammatory mediators in healthy human synovial stromal cells

In addition to its critical role in inflammatory cytokine production, p38 MAPK is also an important signal transduction molecule activated by inflammatory cytokines such as TNF α and IL-1 β [18]; therefore, I examined whether AS1940477 blocked the TNF α and IL-1 β signaling cascades in healthy human SSCs. TNF α and IL-1 β synergistically stimulated SSCs to produce large amounts of IL-6, PGE₂, and MMP-3, with expression levels peaking at 24 h after stimulation. AS1940477 inhibited the production of IL-6, PGE₂, and MMP-3 in a concentration-dependent manner (Fig. 5 A-C), with IC₅₀ values of 0.64 ± 0.55 nM, 0.76 ± 1.0 nM, and 0.88 ± 0.88 nM, respectively.

Inhibitory effect of AS1940477 on cytokine production in a rat model of acute inflammation

I then studied the ability of AS1940477 to suppress acute inflammation *in vivo* by evaluating LPS- and Con A-stimulated cytokine production in rats (Fig. 6). In this model, TNF α , IL-1 β , and IL-6 plasma levels peaked between 1.5 and 2 h after LPS treatment. At doses of 0.03 to 1 mg/kg, orally

administered AS1940477 significantly decreased the plasma concentrations of TNF α , IL-1 β , and IL-6 in a dose-dependent manner (Fig. 6 A-C). Of note is the fact that AS1940477 exerted a suppressive effect on LPS-induced TNF α and IL-6 production at an extremely low dose, with ED₅₀ values of 0.053 mg/kg against both cytokines. In the Con A-stimulated model, the plasma concentration of IL-2 peaked at 5 h after stimulation, and AS1940477 had no inhibitory effect on IL-2 production (Fig. 6 D). These results suggest that AS1940477 has the ability to regulate inflammatory cytokine production *in vivo*, consistent with *in vitro* studies.

I also evaluated the long-lasting inhibitory effect of AS1940477 on cytokine production in a rat model of LPS-stimulated production of TNF α . AS1940477 was administered 20 h before LPS injection, and plasma TNF α levels were measured. AS1940477 significantly suppressed LPS-induced TNF α production in a dose-dependent manner ($p < 0.01$ for each dose vs. vehicle), which was comparable with the inhibitory activity of AS1940477 4 h before LPS injection (Fig. 7). These findings indicated that the *in vivo* inhibitory effect of AS1940477 on cytokine production lasted for 20 h.

Discussion

p38 MAPK plays a key role in chronic inflammation, and its therapeutic potential has been extensively studied [19]. Over the past decade, many small molecule inhibitors of p38 MAPK have been generated and advanced to clinical trials; however, undesirable side effects or low efficacy have led to the withdrawal of most compounds after initial clinical trials. For example, development of BIRB-796, AMG-548, and VX-745 was discontinued due to side effects such as gastrointestinal disorders, elevated liver enzyme levels, and central nervous system disorders [20], while VX-702 was withdrawn due to insufficient efficacy, with only around 40% of rheumatoid arthritis patients achieving an ACR20 response [21]. These adverse effects relate to the chemical structure or differing kinase selectivity patterns of these agents and are believed to be unrelated to p38 α inhibition. As such, the next generation of p38 MAPK inhibitors needs to be more selective and potent than currently available compounds.

The current study demonstrated the *in vitro* and *in vivo* pharmacological profiles of a novel small molecule inhibitor of p38 MAPK, AS1940477. I evaluated its selectivity against over 100 kinases, in contrast to previous reports of p38 inhibitors which featured selectivity data for only a limited number of kinases. AS1940477 showed potent inhibition of p38 α and p38 β in cell-free enzymatic assay and high selectivity for p38 α and p38 β in a kinase assay profiling against 100 representative protein kinases, including c-Jun N-terminal kinase and p38 γ and p38 δ isoforms (Table 1). In contrast,

clinically advanced p38 MAPK inhibitors such as BIRB796 and Pamapimod inhibit not only p38 α but also JNK activity in enzymatic assays [22, 23]. I also tested the selectivity of AS1940477 for the intracellular signaling pathway in THP-1 cells. When the p38, JNK, and NF κ B pathways were activated in LPS-stimulated THP-1 cells, AS1940477 selectively inhibited only the p38 pathway without affecting the JNK or NF κ B pathways (Fig. 3), indicating selective inhibition of the p38 pathway by AS1940477 in both cell-free and cell-based conditions and therefore low likelihood of off-target effects compared with other p38 inhibitors such as BIRB796 and Pamapimod.

As the p38 MAPK signaling pathway is closely associated with the production of various pro- and anti-inflammatory cytokines and other inflammatory mediators [24, 25], I examined the effects of AS1940477 on the production of typical inflammatory cytokines and mediators. The results showed that AS1940477 reduced the levels of TNF α , IL-1 β , and IL-6 produced from LPS- or PHA-stimulated human monocytic cells and/or whole blood (Table 2). LPS is a principal component of gram-negative bacteria [26], and PHA is a lectin found in plants, particularly legumes. LPS and PHA activate mainly monocytes/macrophages and T cells, respectively [27], suggesting that AS1940477 inhibits both monocyte/macrophage- and T cell-dependent inflammatory cytokine production. Interestingly, IL-2 production in PHA-stimulated PBMCs was not affected by AS1940477 at concentrations up to 10 μ M (Table 2). Although SB203580 was previously reported to inhibit IL-2 production in activated T cells [28, 29], another

report showed no change in IL-2 production or proliferation in T cells with specific inhibition of p38 α by dominant negative p38 α [30], findings consistent with the results of the present study. These results suggest that AS1940477 is highly selective for p38 α , possessing an anti-inflammatory effect without immunosuppression. In addition, a reduction in TNF α - and IL-1 β -induced IL-6 (Fig. 5 A), PGE $_2$ (Fig. 5 B) and MMP-3 (Fig. 5 C) production was observed in human SSCs, indicating that AS1940477 plays an important role in the downstream signaling and production of TNF α and IL-1 β . IL-6 and PGE $_2$ are representative inflammatory cytokines/mediators for inflammation and pain, respectively, while MMP-3 is associated with joint destruction. Taken together, these findings suggest that AS1940477 can inhibit the production and signaling of proinflammatory cytokines, resulting in affecting monocytes, T cells, and synovial cells, which are involved in the pathogenesis of rheumatoid arthritis.

I also used a rat model of acute LPS- and Con A-induced cytokine production to examine the anti-inflammatory effect of AS1940477 *in vivo*. In the LPS-treated model, AS1940477 significantly reduced plasma concentrations of TNF α and IL-6 at doses below 0.1 mg/kg and also partially decreased plasma IL-1 β levels at 1 mg/kg (Fig. 6 A-C). The lesser effect on IL-1 β production compared with TNF α and IL-6 production in this model may be attributed to the differential contribution of p38 α in the generation of cytokines. In contrast, AS1940477 did not significantly affect Con A-induced IL-2 production at 1 mg/kg (Fig. 6 D). Although the IL-2 level appeared to be slightly reduced at 0.3 to 1 mg/kg, the effect was not statistically significant

($p > 0.05$). The cytokine selectivity of AS1940477 was consistent with that observed in the *in vitro* assay (Table 2); thus, AS1940477 is believed to be specific for p38 α *in vivo*.

In the present study, I showed that AS1940477 potently inhibited the production of various inflammatory cytokines such as TNF α from LPS-stimulated THP-1 cells and human PBMCs with IC₅₀ values of 0.6 nM and 0.45 nM, respectively (Fig. 4, Table 2). The potency of AS1940477 in these mononuclear cells is stronger than those of p38 inhibitors in clinical testing such as BIRB796, VX-702, Pamapimod, and PH-797804 (IC₅₀ = 3.4 to 60 nM) [14, 23, 31]. Further, the activity of AS1940477 in whole blood assay was more potent than those of other p38 inhibitors; for example, SCIO-469, Pamapimod, and PH-797804 inhibited LPS-induced TNF α production in whole blood with IC₅₀ values of 300, 400, and 85 nM, respectively [14, 23, 32], which were weaker than that of AS1940477 (IC₅₀ = 12 nM). From the results of the *in vitro* study, I expected AS1940477 to show potent activity *in vivo* and tested this in a rat acute inflammation model, where the compound suppressed LPS-induced TNF α production at extremely low doses (ED₅₀ = 0.052 mg/kg, Fig. 6). In comparison, Pamapimod and PH-797804 have been reported to inhibit TNF α production in LPS-treated rats with ED₅₀ values of 0.3 and 0.07 mg/kg, respectively. To the best of my knowledge, no other studies have reported on p38 inhibitors with greater potency *in vivo* than AS1940477.

Given the good pharmacokinetic profile of AS1940477 with no metabolic concerns (data not shown), I examined its long-lasting effect using an *in vivo*

acute inflammation model. When AS1940477 was orally administered to rats 20 h before LPS injection, its suppressive effect was almost the same as that seen when given 4 h before LPS injection. This result suggests that the potent anti-inflammatory effect of AS1940477 may last for almost one day after a single administration.

Recently, several second generation p38 inhibitors, including VX-702, SCIO-469, and ARRY-797, were tested in clinical trials and were found to be ineffective in treating rheumatoid arthritis [20, 33-35]. Despite a temporary decrease in the plasma CRP levels in the drug-treated groups, levels eventually reverted to those of the placebo group. A p38 inhibitor BMS-582949 also showed therapeutic effectiveness against rheumatoid arthritis in a Phase IIB study without CRP rebound phenomenon [36]; unlike SCIO-469 or VX-702, BMS-582949 potentially blocks not only p38 kinase activity but also p38 activation [37], which may contribute to its continuous anti-inflammatory effect. Thus, the role of p38 MAPK in chronic inflammatory disease remains controversial and further clinical data will be necessary to resolve this issue.

In summary, I documented the pharmacological profile of AS1940477, a novel p38 MAPK inhibitor, and found it to have potent inhibitory activity for p38 α and p38 β without affecting other protein kinases. AS1940477 also inhibited LPS- and PHA-stimulated proinflammatory cytokine production in human PBMCs and TNF α /IL-1 β -induced liberation of inflammatory mediators in SSCs and has potent inhibitory activity in whole blood as well as in a rat model of acute inflammation with effects lasting for almost one

day. Taken together, these results suggest that AS1940477 may be a promising anti-inflammatory agent for use in treating chronic inflammatory diseases.

Tables and Figures

Table 1.

Kinase selectivity of AS1940477

Kinases	IC ₅₀ ^a , (nM)	IC ₇₅ ^a , (nM)
p38 α	11.2	18.4
p38 β	36.5	65.8
p38 γ	>1000	>1000
p38 δ	>1000	>1000
JNK2	>1000	>1000
other 97 kinases ^b	>1000	>1000

^a IC₅₀ and IC₇₅ values are expressed.

^b Ninety-seven kinases: ABL, ACK, AXL, BMX, BTK, CSK, DDR2, EGFR, EphA2, FAK, FES, FGFR1, FGFR3, FLT1, FLT3, FLT4, FMS, FYN, HER2, IGF1R, INSR, IRR, ITK, KDR, KIT, LTK, LYN_a, MER, MET, MUSK, PDGFR_a, PDGFR_b, RET, RON, ROS, SRC, SYK, TEC, TIE2, TRKA, TYRO3, ZAP70, AKT1, AKT2, AurC, BMPR1A, BRAF, CaMK2_a, CaMK4, CDK2, CDK3, CHK1, CHK2, CK1_a, COT, CRIK, DAPK1, DLK, Erk5, GSK3_a, GSK3_b, IKK_a, IKK_b, JNK3, MAP2K1, MAP2K2, MAP2K4, MAP2K5, MAP2K7, MAP3K1, MAP3K2, MAP3K3, MAP3K4, MAP3K5, MAPKAPK3, MAPKAPK5, MINK, MLK1, MLK2, MLK3, MNK1, MNK2, MSK1, NEK2, p70S6K, PAK6, PHKG1, PIM1, PKAC_a, PKD2, RAF1, ROCK1, RSK1, RSK2, SRPK2, TAK1, TTK

Table 2.

***In vitro* effect of AS1940477 on LPS- or PHA-induced cytokine production from human PBMCs and whole blood*.**

Cell type	Stimulus/cytokine	IC ₅₀ , (nM)
Human PBMC	LPS/TNF α	0.45
Human PBMC	LPS/IL-1 β	0.55
Human PBMC	LPS/IL-6	3.5
Human PBMC	PHA/TNF α	0.40
Human PBMC	PHA/IL-6	1.2
Human PBMC	PHA/IL-10	6.1
Human PBMC	PHA/IL-2	>10,000
Human WB*	LPS/TNF α	12

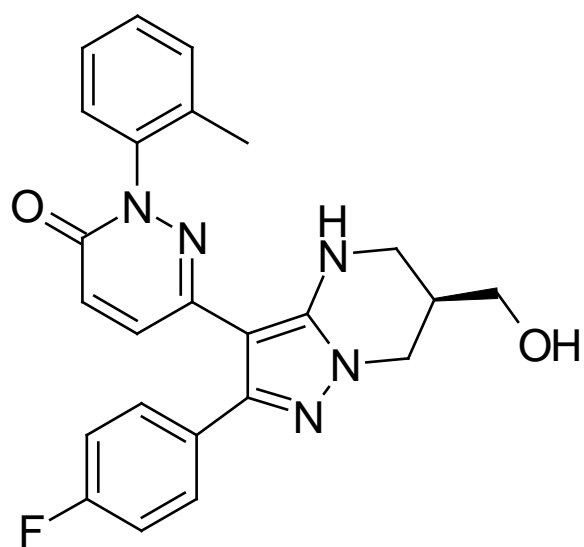


Fig. 1. Structure of AS1940477

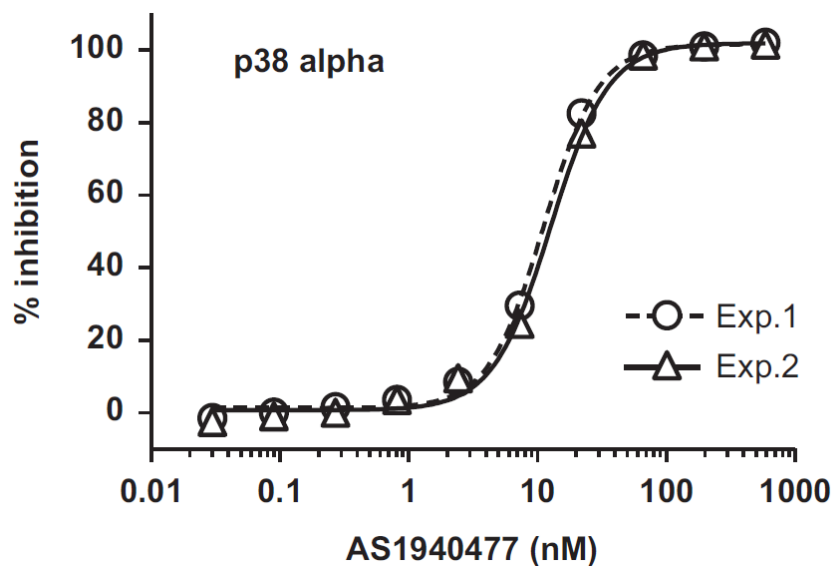


Fig. 2. Effect of p38 α MAPK enzyme inhibition by AS1940477. Human p38 α kinase activity of AS1940477 was evaluated using Z'-Lyte™ kinase assay system provided by invitrogen corporation. The presented data are average values of duplicate analysis obtained two independent experiments.

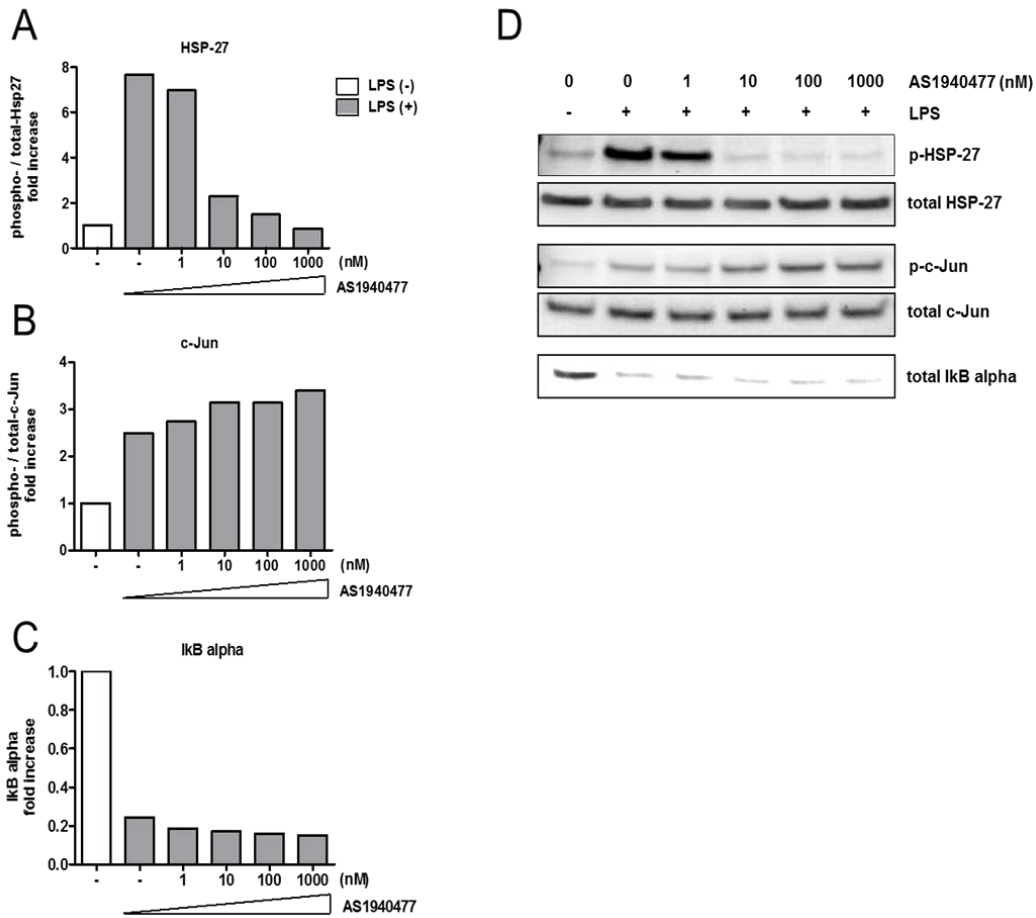


Fig. 3. Cellular selectivity of AS1940477 for p38 versus JNK and NFκB signaling pathways in THP-1 cells. THP-1 cells pre-treated with AS1940477 for 30 min were stimulated with or without LPS 10 μg/mL for 30 min at 37 °C. The reaction was stopped by adding cold phosphate-buffered saline, and cellular lysates were prepared as described in the Methods section. p38 activity was measured by assessing phosphorylation of HSP-27, JNK activity by assessing phosphorylation of c-Jun, and NFκB activity by assessing degradation of IκBα via ELISA (A–C) or Western blot (D). The presented data are representative of the results obtained from three independent experiments.

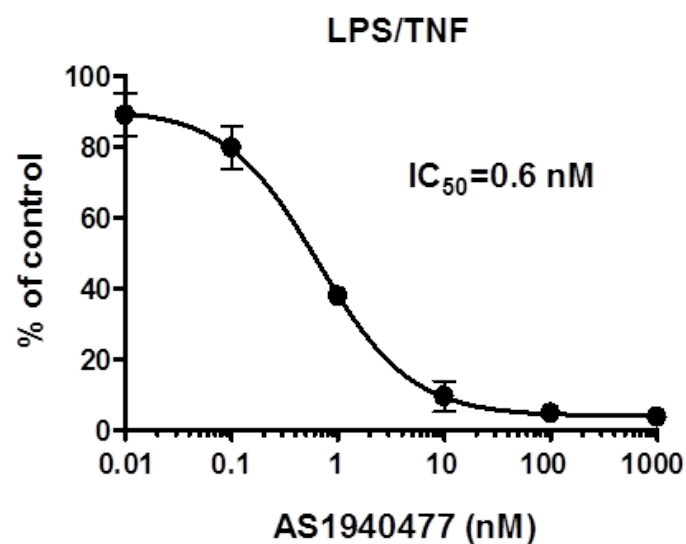


Fig. 4. Effect of AS1940477 on LPS-induced TNF α production in THP-1 cells. THP-1 cells were treated with AS1940477 and LPS 10 μ g/mL at the same time and incubated for 18 h at 37 $^{\circ}$ C. The concentration of TNF α in the supernatant was determined via ELISA. The presented values are expressed as the mean \pm S.E.M. of triplicate experiments, and the IC₅₀ value was calculated using GraphPad Prism 4.0 software.

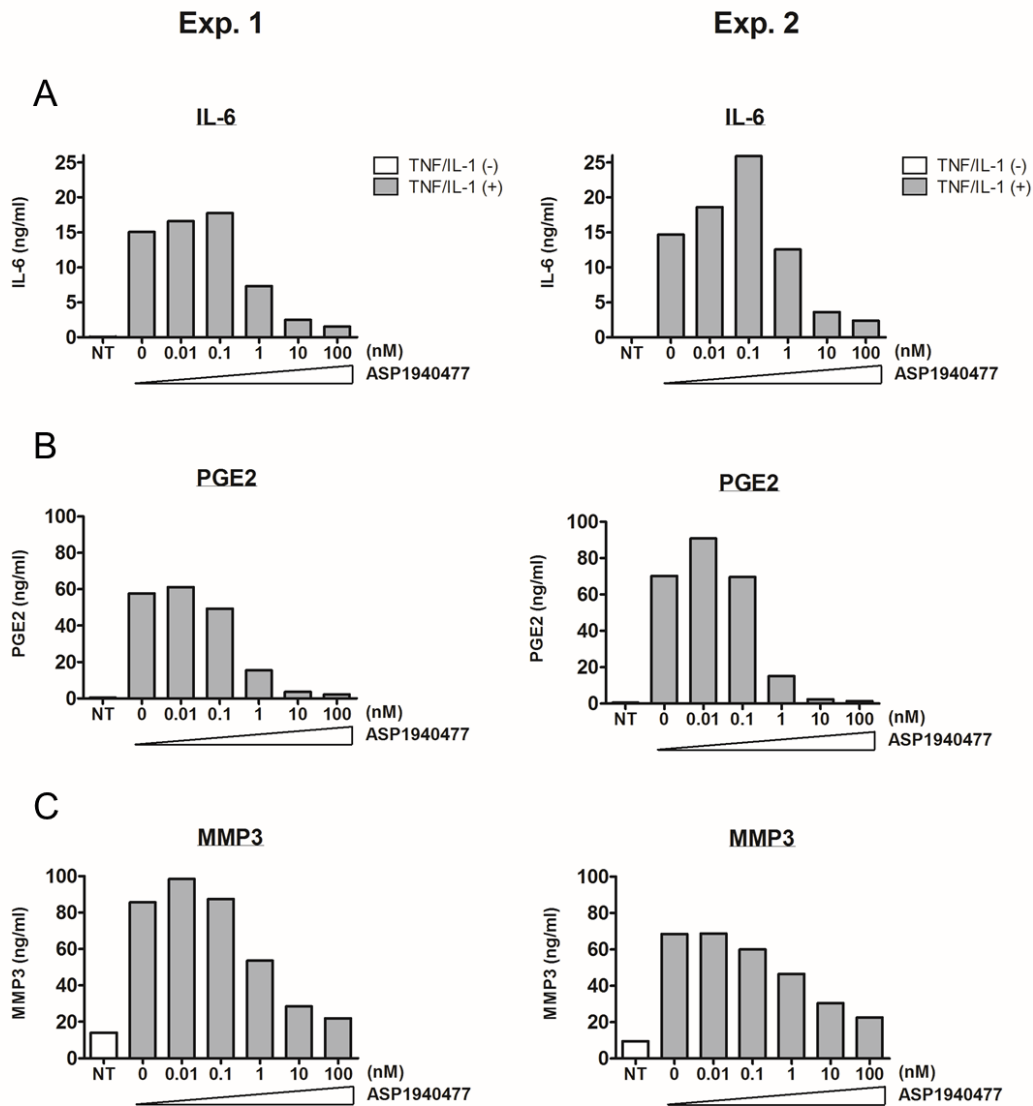


Fig. 5. Inhibitory effect of AS1940477 on TNF α /IL-1 β signaling transduction in human synovial stromal cells. Human synovial stromal cells were stimulated with TNF α (1 ng/mL) and IL-1 β (2 pg/mL) for 24 h after a 30-min preincubation in the presence or absence of the indicated concentrations of AS1940477. IL-6 (A), PGE₂ (B), and MMP-3 (C) levels in the culture media were determined by ELISA as described in the Methods. Two representative data of three independent experiments are displayed.

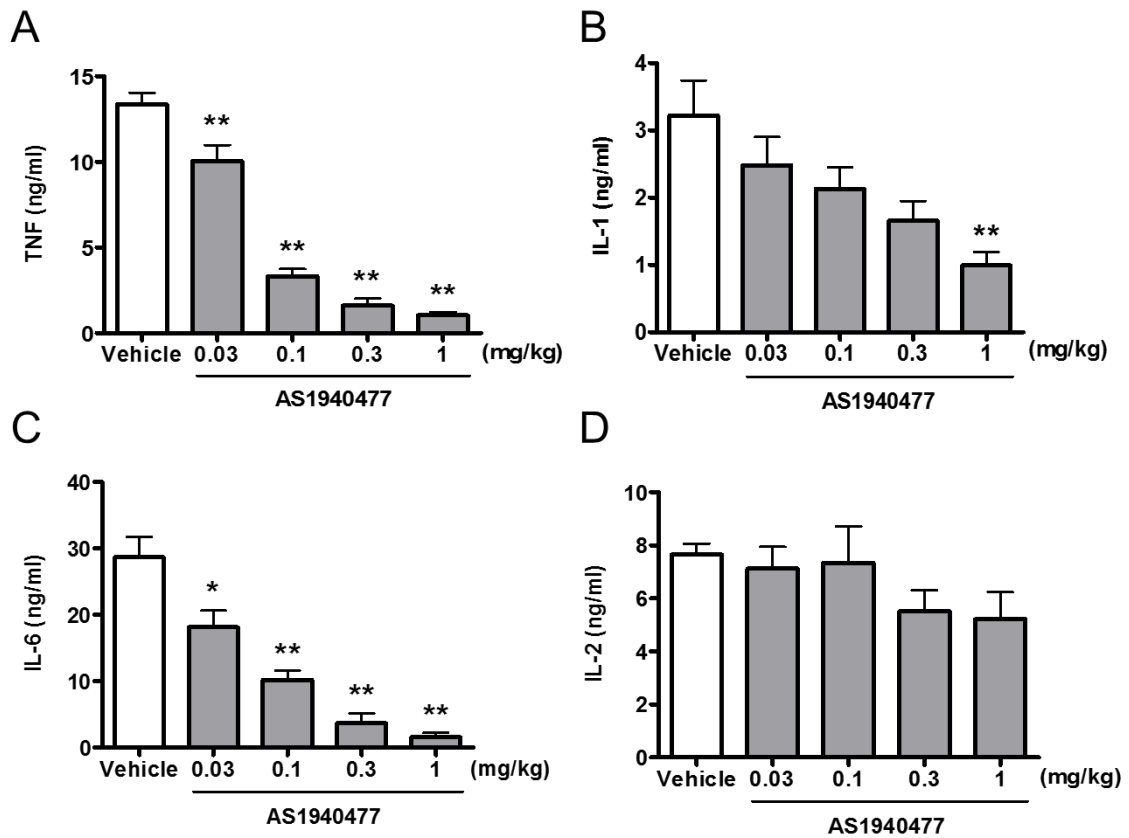


Fig. 6. Effect on *in vivo* LPS- and Con A-induced inflammatory cytokine production. AS1940477 or vehicle (0.5% methyl cellulose) were administered orally to female Lewis rats 4 h before i.v. injection of LPS (10 μ g/rat) or Con A (3 mg/rat). TNF α , IL-1 β , and IL-6 levels were measured in collected plasma 1.5, 1.5, and 2 h after LPS injection, respectively. IL-2 levels were also measured in collected plasma 4 h after Con A injection. The values are expressed as mean \pm S.E.M. Significant differences between vehicle and treated groups: * p < 0.05, ** p < 0.01 (one-way ANOVA followed by Dunnett's multiple range test).

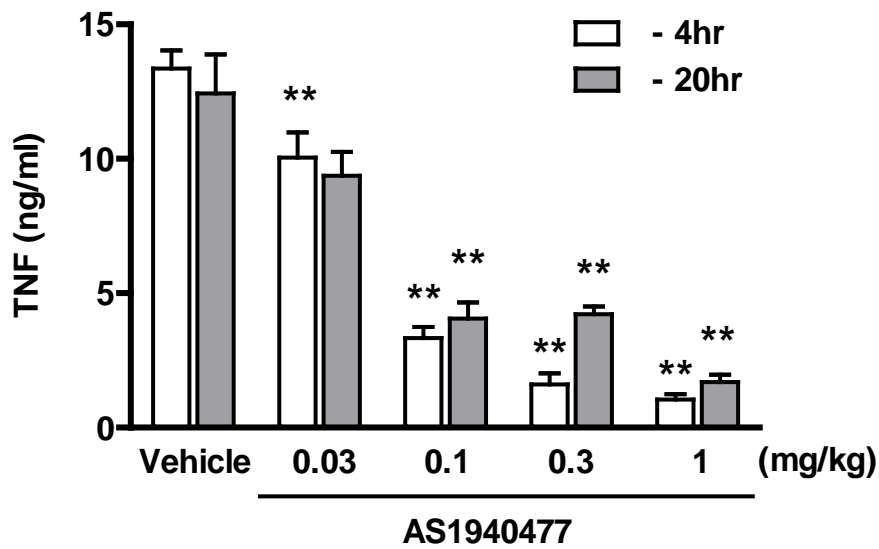


Fig. 7. Long-lasting effect of AS1940477 in an *in vivo* model of LPS-induced TNF α production. AS1940477 or vehicle (0.5% methyl cellulose) were administered orally to female Lewis rats 4 or 20 h before i.v. injection of LPS (10 μ g/rat). TNF α levels were measured in collected plasma 1.5 h after LPS injection. Values are expressed as mean \pm S.E.M. Significant differences between vehicle and treated groups: ** $p < 0.01$ (one-way ANOVA followed by Dunett's multiple range test)

Chapter II

**Inhibition of c-Rel DNA binding is critical for the anti-inflammatory effects
of novel PIKfyve inhibitor**

Summary

Aberrant production of proinflammatory cytokines is linked to many autoimmune diseases, and their inhibition by small molecule compounds is considered beneficial. Here, I performed phenotypic screening in IFN γ /LPS-activated RAW264.7, mouse macrophage cells, and discovered AS2677131 and AS2795440 as novel and potent inhibitors of IL-12p40, a subunit of IL-23. Interestingly, these compounds exhibited unique pharmacological activities in their inhibition of the production of IL-12p40, IL-6 and IL-1 β but not TNF α in activated macrophages or dendritic cells, and expression of IgM-induced MHC class II on B cells. To reveal these mechanisms, I synthesized two different activity probes which were structurally related to the AS compounds, and identified probe-specific binding proteins, including PIKfyve, a Class III PI kinase. The AS compounds inhibited PIKfyve activity and mimicked the properties of PIKfyve-deficient cells, eventually validating PIKfyve as target molecule. Regarding mechanism, AS2677131 regulated DNA binding activity of c-Rel on IL-12p40 and IL-1 β promoter. As expected, a PIKfyve inhibitor prevented the development of arthritis in rats. Taken together, my findings of the novel and potent PIKfyve inhibitors AS2677131 and AS2795440 reveal the critical role of PIKfyve in proinflammatory cytokine production and B cell activation, and may indicate a potential new therapeutic option for treatment of inflammatory diseases.

Introduction

Aberrant production of proinflammatory cytokines is critical to the development and progression of many autoimmune diseases, including rheumatoid arthritis, psoriasis, and inflammatory bowel disease [2]. IL-23 is an inflammatory cytokine that has recently been proposed to play a pathogenic role in development of some autoimmune diseases. IL-23 is composed of heterodimeric proteins of unique IL-23p19 and common IL-12p40 subunits which is shared with IL-12 [38]. IL-12p40-deficient mice do not develop arthritis, skin disease, or intestinal inflammation because of impaired production of IL-23 [39, 40]. Therefore, pharmacological inhibition of IL-12p40 production has been thought as a potential new therapeutic option for the treatment of these diseases.

IL-12p40 is produced primarily by activated macrophages and DCs, when these cells are stimulated by a variety of pathogenic or inflammatory agents. In particular, LPS and IFN γ are strong inducers of IL-12p40, and the signaling pathway in their induction of IL-12p40 expression has been well investigated [41]. Cells stimulated with LPS and IFN γ show activation of various intracellular signaling proteins, such as NF κ B and interferon regulatory factor (IRF), followed by binding of these protein to their response site on a target gene promoter, resulting in elevation of IL-12p40 mRNA. The mammalian NF κ B family proteins consist of five members, c-Rel, p65/RelA, RelB, p50/NF κ B1, and p52/NF κ B2. c-Rel is specifically expressed in lymphoid and myeloid cells, and is essential for expression of IL-12p40 in

macrophages [42].

Phosphoinositides play crucial roles in a variety of cellular processes [43], and their metabolism is controlled by highly specific kinases and phosphatases via reversible phosphorylation at positions 3, 4, and/or 5 of the inositol headgroup in PI. PIKfyve, a FYVE finger-containing phosphoinositide kinase, is an evolutionarily conserved mammalian lipid kinase that acts on PI and PI3P to generate PI5P and PI(3,5)P₂, respectively [6]. Functional impairment of PIKfyve leads to aberrant endosome enlargement and marked cytoplasmic vacuolation, as a consequence of impaired normal endosome processing and membrane trafficking [44-47]. Since PIKfyve regulates pleiotropic cell functions, a comprehensive understanding has yet to be obtained.

I here report the discovery of two small molecule compounds, AS2677131 and AS2795440, which exert unique immunoregulatory functions, selective cytokine inhibition and B cell activation inhibition. I also identified PIKfyve as a direct target molecule of these compounds by a chemical biological approach, and further study revealed that inhibition of intracellular PIKfyve activity by AS2677131 selectively decreased c-Rel binding to gene promoters of IL-12p40 and IL-1 β , indicating that AS2677131 regulates cytokine production through a PIKfyve-c-Rel pathway. Oral administration of AS2677131 suppressed chronic inflammation, as indicated by the inhibition of development of adjuvant-induced arthritis in rats. Collectively, my findings describe novel and selective PIKfyve inhibitors which show potent anti-inflammatory effects, and may indicate that PIKfyve is a potential new

therapeutic target for the treatment of various inflammatory diseases.

Materials and Methods

Reagents

AS2677131

(rel-N-{6'-[(2R,6S)-2,6-dimethylmorpholin-4-yl]-3,3'-bipyridin-5-yl}-3-ethyl-2-methyl-1H-pyrrolo[3,2-b]pyridine-5-carboxamide), AS2795440
(N-(1"-isopropyl-6-methyl-1",2",3",6"-tetrahydro-3,3':6',4"-terpyridin-5-yl)-2,3-dimethyl-1H-pyrrolo[3,2-b]pyridine-5-carboxamide), and AS2559819
(N,2,3-trimethyl-N-(5-{4-[2-(morpholin-4-yl)ethoxy]phenyl}pyridin-3-yl)-1H-indole-5-carboxamide) were synthesized by Astellas Pharma Inc. (Ibaraki, Japan). The general synthetic routes of AS2677131 and AS2795440 were previously described [48].

Cell culture

A mouse macrophage cell line, RAW264.7, was routinely cultured in DMEM/F12 supplemented with 5% FCS (BioWest) and 1% penicillin/streptomycin [10,000 units of penicillin per mL, 10,000 µg of streptomycin per mL]. Peritoneal macrophages were prepared as previously described with minor modification [49]. Mice were injected i.p. with 2 mL of 3% thioglycolate (Difco) and cells were harvested from the peritoneal cavity 4 days after by lavage with cold PBS. DCs were obtained by differentiating bone marrow with RPMI supplemented with 10% FCS, 1% penicillin/streptomycin [10,000 units of penicillin per mL, 10,000 µg of streptomycin per mL], 5 ng/mL GM-CSF, and 5 ng/mL IL-4 for 7 d.

Peritoneal macrophages and DCs were cultured in RPMI medium 1640 supplemented with 10% FCS and 1% penicillin/streptomycin [10,000 units of penicillin per mL, 10,000 µg of streptomycin per mL]. RAW264.7 cells were pre-stimulated with 100 ng/mL of mouse IFN γ (Peprotech) for 7-10 h and stimulated with 10 µg/mL LPS (Sigma) in the presence or absence of compounds overnight. Peritoneal macrophages were costimulated with 3 ng/mL of mouse IFN γ and 1 µg/mL of LPS in the presence or absence of compounds overnight. DCs were pre-stimulated with 3 ng/mL of mouse IFN γ for 7-10 h and stimulated with 1 µg/mL LPS and 10 µg/mL muramyl dipeptide/MDP (Peptide Institute, Inc.) overnight.

Cytokine mRNA analysis and ELISA

Total RNA was sequentially extracted from RAW264.7 cells at 0, 0.5, 1, 2, and 4 h after stimulation with IFN γ and LPS. cDNA was prepared, labeled, and hybridized to the commercial GeneChip according to the manufacturer's standard protocols (Agilent Technologies). Cytokine analysis was performed according to the manufacturer's instructions (PharMingen, Biosource, or R&D Systems). Supernatants and plasma sample were subjected to ELISA for IL-12p40, IL-6, and TNF α using a sandwich ELISA system. Following antibodies were purchased from PharMingen: purified rat anti-mouse IL-12 p40/p70, biotin rat anti-mouse IL-12 (p40/p70), purified rat anti-mouse IL-6, biotin rat anti-mouse IL-6, purified hamster anti-mouse/rat TNF, and biotin rabbit anti-mouse/rat TNF. The following ELISA standard proteins were purchased from Peprotech: recombinant murine IL-12, recombinant murine

IL-6, recombinant murine TNF- α , and recombinant rat TNF- α . Rat IL-12p40 and rat IL-6 were quantified using CytoSet (Biosource) and DuoSet (R&D Systems), respectively.

Intracellular Ca²⁺ measurement

Ramos cells were loaded with 1 μ M Fluo-4-AM (Dojinkagaku) for 60 min at room temperature in HBSS (20 mM HEPES; pH7.4) in the presence of 0.01% pluronic acid. Cells were dispensed in 384-well clear-plate (Greiner) in the presence of DMSO or compounds. After acquisition of a baseline value, the cells were stimulated with anti-IgM, and Ca²⁺ was measured with a FDSS 7000 kinetic plate reader (Hamamatsu Photonics) using a standard Fluo-4 480-nm excitation and 530-nm emission filter set.

***In vivo* antibody production model**

TNP(90)-AECM-Ficoll (Biosearch Technologies) was diluted with saline to 200 μ g/mL, and injected into female Lewis rats (500 μ L/head, i.v., $n = 5$) on day 0. Vehicle (0.5% MC) or AS2795440 were orally administrated to rats at indicated concentrations from day 0 to day 6. The concentration of anti-TNP IgM antibody was measured by ELISA. The anti-TNP IgM was bound to plates precoated with TNP-BSA (Biosearch Technologies), and then detected by HRP-conjugated rat anti-IgM antibody (American Qualex).

Synthesis of photoreactive affinity capture probe

Tool compounds High and Low were synthesized in-house and the Linker

was kindly provided by Prof. Akito Tanaka, Hyogo University of Health Science. The tool compounds and Linker were reacted with 1-ethyl-3-(3-dimethylaminopropyl) carbodiimide and 1-hydroxybenzotriazole in DMF at room temperature. After purification with SepPak plus C18 (Waters), the acquired amides were used as photoreactive affinity capture probes.

Pull down experiments with photoreaction

RAW264.7 cells were lysed in 0.2% CHAPS lysis buffer (0.2% CHAPS, one tablet of cOmplete EDTA-free Protease Inhibitor Cocktail Tablets (Roche) per 50 mL of HBS-N (GE Healthcare)). The centrifuged lysates (5 mg/mL) were incubated with Dynabeads MyOne Streptavidin C1 (Invitrogen) for preclearing. After removal of the beads with a magnetic block, 1 μ L of a competitor (10 mM), the tool compound High in DMF, or DMF only was added to the lysates (100 μ L/test) and they were incubated for 30 min at 4 °C. Then, 1 μ L of the probes (0.1 mM) was added to the solution and they were incubated for 2 h at 4 °C. After dilution with 900 μ L of 0.2% CHAPS lysis buffer, the solutions were exposed to UV light (wave length 302 nm) for 1 min at 4 °C. The solutions were then incubated with Dynabeads MyOne Streptavidin C1 (50 μ L slurry/test) for 30 min at 4 °C. The beads were collected with the magnetic block, and washed three times with 0.1% SDS in HBS-EP (GE Healthcare) and once with water.

Protein digestion and mass spectrometry

Nine microliters of digestion buffer (0.01% SDS and 0.5 mM CaCl₂ in 50 mM ammonium bicarbonate) and 1 μL of trypsin solution (0.5 μg/μL, Promega) were added to the collected beads, and they were incubated for 16 h at 37 °C. After dilution with 100 μL 0.1% formic acid/46% acetonitrile, they were applied to the Stage tip purification method [50] with SCX and SDB-XC Empore discs (3M). For the SCX stage tip, the applied samples were washed with 0.1% formic acid/46% acetonitrile, eluted with 500 mM ammonium formate/45% acetonitrile (pH 3.0 by TFA) and diluted 20 times with water. For the SDB-XC stage tip, they were washed with 0.1% formic acid/2% acetonitrile (LC-A solution), eluted with 0.1% formic acid/90% acetonitrile (LC-B solution) and then evaporated. The desalted samples were dissolved with LC-A and loaded directly onto a C18 analytical column (3 μm, 0.075 mm x 150 mm, Nikkyo Technos). The experiments were performed using an Ultimate 3000 liquid chromatography system (Dionex) connected with an LTQ Orbitrap XL mass spectrometer (Thermo Fisher) utilizing a nano-electrospray ion source. LC separation was performed at a flow rate 400 nl/min with a linear gradient of 2-45% LC-B over 80 min, followed by an additional 5 min at 90% LC-B. Mass spectrometric analysis was performed in data-dependent mode to take up to three product ion scans for the three highest intensity peaks in each full scan (m/z : 400-1500, set resolution: 60000), with the lock mass option at m/z 445.1200. Protein identification was performed using Mascot software (Version 2.3, Matrix Science Inc.) against a protein database based on an NCBI REFSEQ protein sequence (ftp://ftp.ncbi.nlm.nih.gov/refseq/M_musculus/mRNA_Prot/mouse.protein.faa

.gz, built in 2010 Oct; 25163 sequences). Identification results from the Mascot software were summarized and integrated with gene annotations using an original program developed in-house. Acetylation (protein N-term), oxidation [51] and pyro-Glu (N-term Glu and Gln) were set for variable modifications. Precursor ion and fragment ion mass tolerances were set to 10 ppm and 0.8 Da, respectively. Up to three missed trypsin cleavages were allowed. Peptide identification criteria was $p < 0.05$, where p was the probability that the observed match was a random event.

Immunoprecipitation for PIKfyve enzyme assay

The lysate of RAW264.7 cells was immunoprecipitated with anti-PIKfyve antibody (ProteinTech). Control immunoprecipitates with normal rabbit IgG (Cell Signalling Technology) were run in parallel in every experiment. Prior to the immunoprecipitations, the cells were lysed in RIPA buffer (Sigma) supplemented with protease & phosphatase inhibitor cocktail (Thermo). The centrifuged lysates (2 mg/1 mL/test) were incubated with antibodies (5 μ g/test) overnight at 4 °C. Protein G Mag sepharose beads (50 μ L slurry/test, GE Healthcare) were added to the final 2 h of incubation at 4 °C. Immunoprecipitates were washed three times with HBS-EP buffer (GE Healthcare) and twice with kinase assay buffer (50 mM Tris pH 7.5, 1 mM EGTA, 1.5 mM MgCl₂) for PIKfyve enzyme assay.

PIKfyve enzyme assay with MALDI-TOF mass spectrometry

(MALDI-TOFMS) analysis

For PIKfyve enzyme assay, immunoprecipitates were used after washing without the elution step. The kinase reaction using endogenous PIKfyve-binding beads (20 μ L final volume) was carried out for 6 h at 37 $^{\circ}$ C in kinase assay buffer supplemented with 300 μ M ATP (Promega), 300 μ M PI(3)P diC8 (Echelon, P-3008) and the AS compounds (0, 50, and 200 nM). The matrix solution for MALDI-TOFMS analysis was prepared with 90 μ L of norharmane and 10 μ L of harmaline (4 mg/mL in acetonitrile/water/TFA = 50/50/1 for both) [52]. One microliter of the reacted samples were mixed with 4 μ L of the matrix and the mixture was spotted at 1 μ L each on three wells of a 384-well MALDI-TOFMS plate (AB Sciex). Negative ion mass spectra were recorded on a 4800 MALDI-TOF/TOF analyzer (AB Sciex) using the manufacturer's standard parameter setting for reflector mode with a mass range of m/z 500-2000 and 4000 laser shots/well. Signal to noise ratio (S/N) of m/z 745.2 for the enzymatic reaction product, PI(3,5)P2 diC8, was automatically calculated from the obtained spectra. The S/Ns of the product at 50 and 200 nM inhibitor concentrations were compared to that at 0 nM (no inhibition) to calculate a % inhibition rate of this assay. The % inhibition rate was averaged from the three measurements in each sample.

PI3K enzyme assay

Catalytic activity of PI3K α was measured by Kinase-Glo Assay. In brief, the kinase reactions were performed in 384-well plates (Greiner). Each well was loaded with 0.5 μ L of test compounds (in 10% DMSO) and 4 μ L of reaction buffer (2.5 μ M ATP, 12.5 mM MnCl₂, 50 mM HEPES, pH7.3, 100

mM NaCl, 10 mM MgCl₂, 2 mM EGTA, 2 mM DTT). The reaction was initiated by the addition of 5 μ L of enzyme/substrate mix (14 ng/ μ L of PI3K α and 40 μ g/mL of L-alpha-phosphatidylinositol) and terminated by the addition of Kinase-Glo buffer (Promega) after incubation for 3 h at 37 °C. The plates were read in a plate reader (SPECTRAMax) for luminescence detection. PI3K β and PI3K δ kinase activities were evaluated following the manufacturer's instructions, PI3-Kinase HTRF™ Assay Kit (Millipore).

Western blotting

The samples were resolved by SDS-PAGE and transferred to PVDF membranes (BioRad). The membranes were blocked and incubated sequentially with the primary then secondary antibodies. The blots were developed using the ECL system (GE Healthcare) in accordance with the manufacturer's instructions. The primary antibodies used for this study are listed in Table 3.

Microscopy

RAW264.7 cells were stimulated with IFN γ and LPS in the presence of DMSO or compounds (100 nM) as described above. After 2 h, cells were fixed with 4% paraformaldehyde phosphate buffer solution (Wako). Images were acquired using a phase-contrast microscope (ECLIPSE Ni-E, Nikon) equipped with 100x oil objective. NIS-Elements AR software was used for image analysis.

ChIP Assay

The ChIP assay was performed with a SimpleChIP® Enzymatic Chromatin IP Kit (Cell Signaling Technology). Cells were used for RAW264.7 cells stimulated with 100 ng/mL IFN γ and 1 μ g/mL LPS for 2 h. c-Rel- or PU.1-DNA complexes were immunoprecipitated using anti-c-Rel or anti-PU.1 antibody (Table 3). Precipitated, purified DNA was used as a template for PCR amplification using primers (Table 4).

Promoter-luciferase reporter assay

For the luciferase reporter assay, I used the promoter fragment (-313/+12) of the mouse p40 gene, which contains several essential response site for IL-12p40 functional expression, such as ets-2, PU.1, NF κ B, C/EBP, and interferon-stimulated response element (ISRE) [53, 54]. A fragment of the p40 promoter prepared from mouse genomic DNA (Clontech) by a PCR-based method was ligated into the *XhoI/HindIII* cleavage site of a pGL4.10 vector (Promega). RAW264.7 cells were transiently co-transfected with reporter gene plasmid and phRL-null *Renilla* plasmid (Promega) using Nucleofector (Lonza). Five hours after transfection, the cell culture medium was changed to complete medium containing 10% FBS and stimulated with IFN γ (100 ng/mL) for 16 h, followed by LPS (10 μ g/mL) for an additional 6 h. Dual-Luciferase Reporter Assays (Promega) were performed according to the manufacturer's instructions. Firefly luciferase activity was normalized to *Renilla* activity. Reporter activity is shown as the average of three determinations and standard error.

siRNA transfection

c-Rel and scrambled control small interfering RNA (siRNA) were purchased from RNAi Co. or Invitrogen (Table 5). Peritoneal macrophages were transfected with 20 nM siRNA using Lipofectamine™ RNAiMax Transfection Reagent (Life Technologies) overnight. Medium was then changed to DMEM containing 10% FCS, penicillin/streptomycin-free. After 48 h, cells were stimulated with 3 ng/mL mouse IFN γ and 1 μ g/mL LPS for 8 h, and IL-12p40 and TNF α concentrations in the supernatants were measured by ELISA.

Flow cytometry

Whole blood from AS2795440 or vehicle-treated rats was diluted ten times with RPMI medium and stimulated with anti-IgM (10 μ g/mL) (Southern Biotechnology) in a 48-well plate. After incubation for 4 h at 37 °C, samples were washed with PBS and then stained with PE-conjugated anti-rat CD45R antibody (Pharmingen) and FITC-conjugated anti-rat MHC class II antibody (eBioscience) for 30 min at room temperature, then analyzed using a FACSCalibur™ instrument (Becton Dickinson) with CELL Quest software. Whole blood collected from AIA at day 25 was stained with allophycocyanin (APC)-conjugated anti-rat CD45RA antibody, FITC-conjugated rat CD3, and PE-conjugated anti-rat CD62L (Pharmingen) for 30 min at 4 °C and analyzed using a FACSCantoII™ instrument (Becton Dickinson) with BD FACSDiva™ software.

Arthritis model

All animals were held under sterile pathogen-free conditions, and animal experiments were approved by the Institutional Animal Care and Use Committee of Astellas, in accordance with AAALAC guidelines. AIA was achieved by immunization of 6-week-old Lewis rats (Charles River Laboratory) with complete Freund's adjuvant as described previously [55]. Normal untreated (NT) or vehicle-treated (CT) rats were used as negative or positive controls, respectively. After arthritis induction, the left hind paw volume was measured on days 1, 11, 15, and 25 by a water displacement method using a plethysmometer for rats (MK-550; Muromachi Kikai Co., Ltd.). Rats were orally administered AS2795440 (1-10 mg/kg) or vehicle (0.5% MC) once per day from day 1 to 24. Vehicle and AS2795440-treated groups consisted of 5-10 animals per group. The normal untreated group consisted of 2 animals per group. Histologic evaluation of arthritis severity was performed on the formalin-fixed left hindlimb joint by Sapporo General Pathology Laboratory. The severity of disease in joints was graded on a scale of 0-3, according to an in-house scoring system: 0: normal, 1: slight change, 2: moderate change, 3: severe change (for details see Table 6)

Statistics

Statistical analysis using Student's *t*-test (for single comparisons) or one-way ANOVA (for multiple comparisons) was performed using Prism software (version 4; GraphPad Software, Inc.). Data that satisfied the

confidence levels of $p < 0.05$, 0.01, and 0.001 are noted. Data are presented as means \pm S.E.M., unless otherwise noted.

Results

AS2677131 and AS2795440 inhibited proinflammatory cytokine production both *in vitro* and *in vivo*.

I first conducted cell-based phenotypic screening for IL-12p40 production inhibitors, optimized chemical structure, and obtained two novel inhibitors, AS2677131 and AS2795440. These compounds potently inhibited IL-12p40 production in IFN γ /LPS-stimulated RAW264.7 cells, a mouse macrophage cell line, with IC₅₀ values of 2.4 and 2.0 nM, respectively. AS2559819, an inactive compound, induced no change in IL-12p40 production (IC₅₀, > 10 μ M) and was used as a negative control in the following studies (Fig. 8 and 9 A). To examine the effect on other proinflammatory cytokines, the mRNA expression patterns of several representative proinflammatory cytokines were analyzed in IFN γ /LPS-stimulated RAW264.7 cells. After stimulation with LPS, gene expression of TNF α peaked in less than 1 h in the control group, followed by an increase in IL-1 β , IL-12p40, and IL-6 expression over the following 4 h (Fig. 9 B). In the AS2677131-treated group, the mRNA expression of IL-12p40 and IL-1 β was strongly suppressed and that of IL-6 was partially suppressed, while that of TNF α was not (Fig. 9 B). I next checked whether this unique cytokine selectivity profile was also shown at the protein level. Thioglycolate-induced peritoneal macrophages were stimulated with IFN γ and LPS, and bone marrow-derived DCs were stimulated in combination with IFN γ , LPS, and muramyl dipeptide (MDP). The concentrations of proinflammatory cytokines in the supernatant were

measured by ELISA. The results showed that AS2677131 and AS2795440 selectively inhibited the production of IL-12p40 and IL-6 (Fig. 9 C), and also inhibited IL-1 β in RAW264.7 cells (data not shown). In contrast, these compounds had no effect on TNF α protein production. Inactive compound did not inhibit the production of any cytokine (IC₅₀ values, >10 μ M).

I next examined the *in vivo* anti-inflammatory effect of these compounds using Toll-like receptor (TLR) ligand-induced inflammation models. To simultaneously detect IL-12p40, IL-6, and TNF α levels, I intravenously injected Poly(I:C), a TLR3 ligand, to MDP-primed rats, and then measured their cytokine plasma concentrations at 2 h after Poly(I:C) injection by ELISA. AS2677131 and AS2795440 were orally administered to rats at 1 h before Poly(I:C) injection. Both compounds significantly decreased the plasma levels of IL-12p40, IL-6, and TNF α in a dose-dependent manner (Fig. 9 D). Interestingly, TNF α production was abrogated in AS2677131 and AS2795440-treated rats, unlike findings in the *in vitro* study (Fig. 9 D).

B cell function was inhibited by AS2677131 and AS2795440.

I next investigated the effect of these agents on immune regulatory function, particularly in B cells. First, I investigated their effect on intracellular Ca²⁺ signaling in a human B cell line, Ramos cells. Cells stimulated with anti-IgM showed an immediate increase in Ca²⁺ influx. AS2677131 or AS2795440 had little or no effect on Ca²⁺ influx up to 10 μ M (Fig. 10 A). This result suggests that these compounds do not directly affect BCR-mediated Ca²⁺ signaling. I next examined whether the compounds

affect B cell activation state. I evaluated the expression level of cell surface MHC class II on CD45R⁺ B cells in anti-IgM-stimulated whole blood from rats treated with AS2795440. The results showed that AS2795440 significantly reduced MHC class II expression by 43.6%, 54.8%, and 83.1% at doses of 1, 3, 10 mg/kg, respectively, compared with the control (CT) group (Fig. 10 B). Similar effect was observed when I used AS2677131 (data not shown). To evaluate the effect on antibody production *in vivo*, TNP-Ficoll, a T cell-independent antigen, was injected intraperitoneally into rats on day 0 and the effect on anti-TNP IgM antibody production from day 4 to day 7 was examined. AS2795440 was used in this model owing to its better physical properties for *in vivo* examination than those of AS2677131. AS2795440 significantly decreased serum antibody levels by 9.0%, 42.5%, and 84.4% at doses of 1 to 10 mg/kg (Fig 10 C). These results indicate that AS2677131 and AS2795440 play an important role in BCR-mediated B cell activation without affecting Ca²⁺ signaling, leading to the inhibition of T cell-independent antibody production.

PIKfyve was identified as a target protein of AS2677131 and AS2795440.

Although these results indicated that AS2677131 and AS2795440 inhibit proinflammatory cytokine production and B cell activation, the mechanism of this regulation remained unclear. To elucidate the direct target protein of these compounds, I used a photoreactive affinity pull down method [56]. I prepared two compounds, which were structurally related to the AS compounds but with different inhibitory activity for IL-12p40, and had a

photoreactive linker (Fig. 11). IC₅₀ values of the high and low activity probes for IL-12p40 production are 1.2 nM and > 1,000 nM, respectively. The tool compounds and linker were connected by a carbodiimide-mediated amidation reaction for use as photoreactive affinity probes. The probes were incubated with cell lysate prepared from RAW264.7 cells with or without an excess amount of a competitor, the tool compound High. After activation of an azide group of the probes by UV light irradiation, formed protein-probe complex was isolated using avidin-immobilized beads. The captured proteins were digested with trypsin and the generated peptide mixture was analyzed by liquid chromatography coupled with tandem mass spectrometry. Overall, 380 proteins were identified (Table 7), but only three of these, PIKfyve, Blvrb, and Nqo2, met my criteria, namely identification with two or more peptides on the high activity probe without a competitor, and also was not identified with a competitor (Table 8). Nqo2 was captured by both the high and low activity probes but PIKfyve and Blvrb were not captured by the low activity probe (Table 8). These results suggested that PIKfyve and Blvrb have the potential to specifically bind to the high activity probe. To confirm if AS2677131 and AS2795440 actually modulate PIKfyve or Blvrb activity, I constructed enzyme assays and evaluated their activity against them. Regarding PIKfyve, both AS2677131 and AS2795440 inhibited the production of PI(3,5)P₂ from PI(3)P by more than 90% at 200 nM (Fig. 12 A). In contrast, no changes in Blvrb activity were observed until both compounds were at 10 μM (data not shown). As expected, a series of compounds with a similar structure showed strong correlations of PIKfyve inhibition with

IL-12p40 inhibition (Fig. 12 B). Similarly, IL-6 inhibition or B cell activation inhibition were confirmed to correlate with PIKfyve inhibitory activity (Fig. 13). These results suggest that AS2677131 and AS2795440 may regulate immune function through PIKfyve, although the contribution of other kinases cannot be ruled out. I then checked the selectivity profile of other lipid kinases of the PI3K family, but found that no compounds affected the enzyme activity of PI3K α , β , or δ until 10 μ M (Table 9). I also confirmed that a structurally related compound (Compound X) selectively inhibited the enzyme activity of PIKfyve without affecting other 148 serine/threonine or tyrosine kinases (Table 10).

PIKfyve is a mammalian type III PI kinase which plays an important role in the PI3-kinase/Akt pathway. I investigated the effect of AS2677131 or AS2795440 on Akt phosphorylation in IFN γ /LPS-stimulated RAW264.7 cells. Consistent with a previous study with a kinase-dead mutant [57], inhibition of PIKfyve activity by AS2677131 or AS2795440 reduced the amount of p-Akt to non-stimulated levels, while the inactive compound showed the same level as the IFN γ /LPS-stimulated DMSO control (Fig. 12 C). Given that other studies have also reported that PIKfyve dysfunction of PIKfyve^{K1831E} mutant or siRNA treatment induces endosome enlargement or profound cytoplasmic vacuolation in many cell types [45, 46, 58], I examined if my compounds show the same phenotype. When RAW264.7 cells were incubated in the presence of DMSO or inactive compound for 2 h, cytoplasmic vacuolation was not observed in both cells. In contrast, treatment with AS2677131 or AS2795440 greatly changed morphology, with

an increase in cell size and the appearance of many small vesicles in the cytoplasm (Fig. 12 D). Taken together, these data clearly indicate that AS2677131 and AS2795440 are selective PIKfyve inhibitors, and that their anti-inflammatory effect and anti-humoral response are caused by the inhibition of PIKfyve activity.

A novel PIKfyve inhibitor regulated the expression of IL-12p40 by the 0.3 kb upstream promoter region in IFN γ /LPS-stimulated RAW264.7 cells.

To elucidate the PIKfyve-mediated regulatory mechanism of IL-12p40 production, I analyzed its intracellular signaling pathway in RAW264.7 cells using AS2677131 as a representative compound on the basis that both AS2677131 and AS2795440 showed the same *in vitro* profile. Previous studies have shown that both IFN γ - and LPS-induced IRF and NF κ B activation are necessary for maximum expression of IL-12p40, but it was unknown which signal was more strongly linked to PIKfyve. To determine which signaling pathway is inhibited by my PIKfyve inhibitor, I investigated the difference in the effect on IL-12p40 production between LPS and IFN γ /LPS stimulation. Consequently, similar IC₅₀ values were observed in the presence or absence of IFN γ stimulation (data not shown), suggesting that PIKfyve might contribute to the LPS/TLR4 signal transduction pathway. It is generally recognized that LPS-induced activation of NF κ B plays a crucial role in IL-12p40 expression in macrophages [42], and that the phosphorylation state of I κ B α reflects the level of activation of the NF κ B pathway. I detected phosphorylated I κ B α with Western blot using specific

antibodies. After IFN γ /LPS stimulation, the rate of I κ B α phosphorylation clearly increased, whereas AS2677131 and inactive compound induced almost no change in DMSO control (Fig. 14 A), suggesting that AS2677131 is likely to regulate either downstream signaling of I κ B α modification or a I κ B α -independent pathway. I then investigated the promoter activity of IL-12p40 by luciferase reporter assay. Stimulation of RAW264.7 cells with IFN γ /LPS elevated the transcriptional activity of IL-12p40, but AS2677131 significantly reduced the promoter activity (*; $p < 0.05$ and **; $p < 0.01$, respectively) in a concentration-dependent manner (Fig. 14 B). In contrast, the inactive compound had no effect. These data were consistent with the results of Fig. 9 B, in which AS2677131 regulated the expression of IL-12p40 at the transcriptional level. I next examined whether AS2677131 affects the nuclear translocation of transcription factors such as p65, p50, c-Rel, PU.1, and IRF-8, which have the potential to bind to the ~0.3 kb promoter of IL-12p40. RAW264.7 cells were stimulated with IFN γ /LPS in the presence or absence of DMSO or compound, and nuclear extract was isolated and immunoblotted with the specific antibodies for indicated transcription factors or internal control gene, PARP. The amount of nuclear translocation of c-Rel, p65, and p50 was significantly increased by treatment with IFN γ /LPS in DMSO control cells, while there were little change in PU.1, IRF-8, or PARP (Fig. 14 C). Further, AS2677131-treated cells also showed a closely similar band pattern between the presence and absence of IFN γ /LPS stimulation, indicating that AS2677131 did not influence nuclear translocation of the indicated transcription factors. Taken together, these

data suggest that AS2677131 might regulate intranuclear but not cytosolic events, such as the binding of transcriptional factors to IL-12p40 promoter after its nuclear translocation.

A PIKfyve inhibitor selectively blocked IFN γ /LPS-induced c-Rel binding activity on IL-12p40 and IL-1 β promoter.

To next determine whether AS2677131 regulates the binding activity of transcription factors to IL-12p40 promoter, I focused on c-Rel among the transcription factors described above on the basis that deletion of c-Rel in macrophages selectively reduced IL-12p40 production whereas TNF α was unaffected [42], a similar pattern to those of my compounds. Two c-Rel-specific siRNAs were synthesized, and confirmed to suppress the expression of mRNA and protein of c-Rel (Fig. 15 A). Consistent with previous reports, specific knockdown of c-Rel by targeted siRNA in RAW264.7 cells canceled IFN γ /LPS-induced upregulation of IL-12p40, whereas no difference was seen in the expression of TNF α (Fig. 15 A). I then determined whether AS2677131 affected binding activity of c-Rel to IL-12p40 promoter in RAW264.7 cells. Cells were stimulated with IFN γ /LPS in the presence or absence of AS2677131 or inactive compound and incubated for 2 h, following which crosslinking by formaldehyde and DNA-protein interaction was detected by ChIP analysis. As expected, AS2677131 decreased the amount of c-Rel on the IL-12p40 promoter, whereas inactive compound had no effect, suggesting that inhibition of the binding activity of c-Rel by AS2677131 is depend on PIKfyve (Fig. 15 C).

Further, I examined whether AS2677131 inhibited the binding of other transcriptional factors to IL-12p40 promoter. PU.1 has its responsive site near the c-Rel binding site on IL-12p40 promoter (Fig. 15 B), but AS2677131 did not affect the binding activity of PU.1 (Fig. 15 C), indicating that AS2677131 selectively inhibited the binding activity of c-Rel. Because c-Rel also binds to IL-1 β promoter and is necessary for its transcriptional activity, I examined the effect on the binding activity of c-Rel on the IL-1 β promoter as well as on IL-12p40 in RAW264.7 cells. As expected, AS2677131 inhibited the binding activity of c-Rel in a concentration-dependent manner whereas the inactive compound did not (Fig. 15 D). These results demonstrate that my PIKfyve inhibitor AS2677131 regulates the binding activity of c-Rel to the response site, and thereby inhibits the expression of c-Rel-regulated genes such as IL-12p40 and IL-1 β .

A PIKfyve inhibitor prevented the development of experimental arthritis.

Based on the results of *in vitro* study, I next examined the effect of my PIKfyve inhibitor on the development of experimental arthritis in rats. Adjuvant-induced arthritis (AIA) is the most frequently used chronic inflammation model, and is considered to be caused by the hyperproduction of various inflammatory cytokines, such as TNF α and IL-1, and by lymphocyte activation [59]. AS2795440 was used for this assay for the same reason that AS2795440 had better physical properties than AS2677131. Treatment with AS2795440 significantly reduced paw swelling at 3 and 10 mg/kg doses (34.3%, 78.3% decrease for 3, 10 mg/kg versus control), and also

induced the recovery of body weight loss at the 10 mg/kg dose (Fig. 16, A and B). In addition, AS2795440 inhibited joint inflammation and bone loss, and reduced clinical scores (bone destruction, cartilage destruction, synovial thickening, and inflammatory cell infiltration) (Fig. 16 C). To further determine the effect of AS2795440 on B cell response, the expression of a cell surface CD62L in CD3⁺CD45RA⁺ B cells was analyzed from whole blood on day 25. CD62L expression was downregulated in accordance with the development of AIA and the percentage of CD62L^{low} cells was measured as a B cell activation marker. AIA rats showed an increased rate of CD62L^{low} B cells (46.9%) in whole blood compared with normal (11.1%), whereas AS2795440 significantly decreased the rate of CD62L^{low} B cells in a dose-dependent manner (Fig. 16, D and E), which was consistent with the data in Fig. 10. Thus, my findings demonstrated that AS2795440, a novel PIKfyve inhibitor, prevented the development of AIA, in which inflammation and B cell activation were suppressed.

Discussion

In this study, I found that AS2677131 and AS2795440, novel small molecule inhibitors of proinflammatory cytokine upregulation, including IL-12p40, IL-6, IL-1 β but not TNF α , demonstrated anti-inflammatory effects both *in vitro* and *in vivo*. I also found that the compounds inhibited BCR-mediated B cell activation and antibody production *in vivo*. Analysis of the inhibitory mechanism of the compounds revealed that PIKfyve, a mammalian type III PI kinase, is a target protein of AS2677131 and AS2795440. In addition, the compounds selectively regulated the binding activity of c-Rel to IL-12p40 and IL-1 β promoter in IFN γ /LPS-stimulated RAW264.7 cells. With regard to therapeutic effect, I found that AS2795440 significantly prevented the development of AIA in rats.

AS2677131 and AS2795440 were discovered by phenotypic screening using IFN γ /LPS-activated RAW264.7 cells as IL-12p40 production inhibitors without inhibitory effect on TNF α production. The mechanism of how these compounds regulate IL-12p40 production and other immune functions was therefore initially unknown. I synthesized two photoreactive linker-conjugated probes with different activity, and incubated the probes with cell lysate collected from RAW264.7 cells. As a result, three binding proteins, PIKfyve, Blvrb, and Nqo2 were identified. Among of these proteins, the enzyme activity of only PIKfyve was inhibited by AS2677131 and AS2795440. I further examined whether these compounds showed typical cellular phenotypes observed under the loss of PIKfyve activity, such as

downregulation of phosphorylation on Akt Ser473 and a vacuolated cellular phenotype [57, 58]. As expected, the compounds induced these characteristic phenotypes (Fig. 12 C and D). In order to exclude the possibility of the contribution of other kinases, the effects of AS compounds on other lipid kinases, serine/threonine or tyrosine kinases were investigated, but the results showed no effect on any other protein kinases (Table 9 and 10). These data support the idea that my compounds are extremely selective inhibitors for PIKfyve. The previously reported PIKfyve inhibitors YM201636 and Apilimod have demonstrated selectivity profiles for a limited number of kinase proteins [45, 60], albeit based on much less data than my present extensive data, suggesting the possibility that my compounds are more selective for PIKfyve than YM201636 and Apilimod. I therefore consider that AS2677131 and AS2795440 are novel selective inhibitors of PIKfyve.

Interestingly, my findings do prove a novel immune regulatory function of PIKfyve. PIKfyve is a member of an evolutionarily conserved gene family of PI(3,5)P₂-synthesizing enzymes from mice to humans. This gene was originally cloned as a GLUT4 transporter from a mouse F442A adipocyte library through screening for transcripts. In mammalian cells, the most prominent cellular phenotype under the loss of PI(3,5)P₂-synthesizing activity of PIKfyve is aberrant endomembrane swelling and vacuolation, which are progressively exacerbated in a dose- and treatment time-dependent manner of PIKfyve inhibitors [44-47]. PIKfyve has therefore been extensively studied, mainly in endosomal membrane systems and in insulin signaling [57, 61]. Recently, PIKfyve was identified as a target

molecule of Apilimod, an IL-12/23 specific production inhibitor, demonstrating that PIKfyve is associated with TLR-induced IL-12p40 production [60]. However, it remains unclear how PIKfyve regulates IL-12p40 production and whether PIKfyve contributes to other immune functions. Here, I found that a number of characteristic immune functions are regulated through a PIKfyve-dependent pathway. First, PIKfyve was found to be involved in the production of proinflammatory cytokines, including IL-12p40 and IL-6 in IFN γ /LPS-stimulated macrophages and DCs, and in Poly(I:C)-stimulated rats (Fig. 9), because the inhibitory activity on PIKfyve was closely correlated with that on IL-12p40 or IL-6 production (Fig. 12 B and 13 A). As in the case of IL-12p40 and IL-6, the production of IL-1 β mRNA and protein in RAW264.7 cells was inhibited by AS2677131 (Fig. 9 B and data not shown). In contrast, TNF α production was differently regulated between *in vitro* and *in vivo* conditions. My PIKfyve inhibitors had no effect on *in vitro* TNF α production from various types of cells, but decreased the level of plasma TNF α in a dose-dependent manner in rats injected with MDP/Poly(I:C) (Fig. 9). This may partially depend on the differences in stimulus type or cell source. Elucidating the contribution of PIKfyve in TNF α production will require more detailed analysis. Collectively, my data suggest that PIKfyve positively regulates a particular kind of proinflammatory cytokine production in activated-immune cells *in vitro* (IL-12p40, IL-6, and IL-1 β) and/or *in vivo* (IL-12p40, IL-6, and TNF α). Second, PIKfyve was found to play a critical role in humoral immune response, because AS2795440 dose-dependently suppressed the expression level of B cell activation marker

induced by anti-IgM (Fig. 10 B). This effect was confirmed by several PIKfyve inhibitors with different activity, which showed the close correlation between the inhibitory activity on B cell activation and that on PIKfyve (Fig. 13). Further examination of the effect on B cell function *in vivo* demonstrated that PIKfyve is involved in TNP-Ficoll-induced antibody responses (Fig. 10 C). Consistent with these results, AS2795440 dose-dependently decreased the number of activated-B cells in the blood in an experimental arthritis model (Fig. 16, D and E). These data thus strongly suggest that PIKfyve is involved in BCR downstream signaling and plays a crucial role in humoral immune response both *in vitro* and *in vivo*. My findings also support many previous reports that the PI3K signaling pathway is important for B cell response to antigen [62, 63]. I therefore consider that the preventive effect of AS2795440 on the development of AIA is attributable to its anti-inflammatory activity via PIKfyve inhibition.

Maximum expression of IL-12p40 in macrophages is generally recognized to require the activation of both the LPS-NF κ B and IFN γ -IRF pathways. LPS and IFN γ -activated cells induce nuclear translocation of transcription factors, such as p65, p50, c-Rel, IRF8, and PU.1, and subsequent coordinated protein binding on the promoter, resulting in gene expression of IL-12p40 [41]. To elucidate the regulatory mechanism of IL-12p40 production by PIKfyve inhibition, intracellular signal transduction was analyzed in IFN γ and LPS-stimulated RAW264.7 cells, particularly with regard to the effects of AS2677131 on the phosphorylation and degradation status of I κ B α , promoter activity, nuclear translocation of transcriptional factors, and their

promoter-binding activity. The results showed that AS2677131 specifically inhibited c-Rel binding activity but not PU.1 to IL-12p40 promoter in macrophages (Fig. 15 C). Similarly, AS2677131 exhibited the dose-dependent inhibition of c-Rel binding to the IL-1 β promoter (Fig. 15 D). These results are consistent with previous reports that c-Rel plays a crucial role in the regulation of expression of many cytokines, such as IL-12p40 and IL-1 β [64, 65]. I cannot rule out the possibility that other mechanisms contributed to IL-12p40 transcription, because the binding activity of other transcription factors described above apart from c-Rel and PU.1 on IL-12p40 promoter has not been investigated. Given that some studies indicate that TLR ligand-induced IL-6 production in macrophages or DCs is necessary for p50 [42, 66, 67], my PIKfyve inhibitors might affect the DNA binding activity of p50 as well as c-Rel. On the other hand, the question whether PIKfyve regulates c-Rel DNA binding ability directly remains to be determined. Zhou D and others reported that PI3K activation is essential for TLR-induced nucleosome remodeling of IL-12p40 promoter [68], and that PIKfyve may be involved in the function of ATP-dependent remodeling complex. A second possibility is that PIKfyve phosphorylates c-Rel and regulates its transactivating activity, because c-Rel phosphorylation is necessary for binding to the target gene promoter [69]. Further studies are needed to determine the mechanism by which c-Rel DNA binding ability is regulated. In contrast, although the regulatory mechanism of B cell is not still confirmed, many studies have indicated that activation of the PI3K pathway is necessary for B cell activation [70], and that c-Rel is required for the

humoral immune response and protection from apoptosis of B cells [71]. c-Rel-deficient mice are resistant to the development of arthritis, in which antigen-induced antibody production is impaired [72]. In agreement with these data, I demonstrated here that PIKfyve inhibition prevented the development of AIA, and that this inhibition involved the suppression of B cell activation (Fig. 16, D and E).

In conclusion, my finding of the novel, highly selective, and orally available PIKfyve inhibitors AS2677131 and AS2795440 has provided evidence that PIKfyve plays a crucial role in inflammatory cytokine production and B cell activation. Further, I revealed that AS compounds inhibited c-Rel DNA binding activity through PIKfyve inhibition. These data suggest that the blockade of PIKfyve might be a potential therapeutic approach in the treatment of inflammatory diseases.

Tables and Figures

Table 3.

List of antibodies

Antibody	Supplier	Catalog No.	Lot	Use
Akt	CST	9272	22	WB
p-Akt (Ser473)	CST	4060	5	WB
I κ B α	CST	4812	6	WB
p-I κ B α (Ser32)	CST	2859	7	WB
NF κ B p65	SantaCruz	sc-372	J2209	WB
NF κ B p50	Abcam	ab7971	813867	WB
c-Rel	SantaCruz	sc-71	J0609	WB
c-Rel	SantaCruz	sc-71X	E2510	ChIP
PU.1	CST	2258	10	WB, ChIP
IRF-8	SantaCruz	sc-13043	A1806	WB
PARP	CST	9542	10	WB
Normal Rabbit IgG	CST	2729	5	EA, ChIP
PIP5K3	Protein Tech	13361-1-AP	1	EA

CST, Cell Signaling Technology; WB, Western Blot; ChIP, Chromatin Immunoprecipitation; EA, Enzyme Assay.

Table 4.

Primers used for RT-PCR or ChIP analysis.

Gene symbol	Forward primer	Reverse primer
<i>Rel</i>	5'-ACATCACCCACCAGCCATAC-3'	5'-AGTCACTGGTGGCCAGCTT-3'
<i>Actb</i>	5'-GGTCATCACTATTGGCAACGA-3'	5'-GAAGGAAGGCTGGAAAAGAGC-3'
<i>Il12b</i>	5'-ACATCACCCACCAGCCATAC-3'	5'-TGAAAAC TAGTGTCAAAACATTCTGG-3'
<i>Il1b</i>	5'-TTGCCGCCTCTATTACCTT-3'	5'- TCTGGGTGTGCATCTACGTGCC -3'

Table 5.**siRNA sequences used for c-Rel**

Accession	Gene name	siRNA name	Sense (upper), Antisense (lower)
-	Negative	siNC	CGGCUGCAAUCGAUUGAUAGC UAUCAAUUCGAUUGCAGCCGAA
NM_009044	c-Rel	si-c-Rel_1	AUAGCAUGUUGACAUCAGAGAUACU AGUAUCUCUGAUGUCAACAUGCUAU
NM_009044	c-Rel	si-c-Rel_2	AAGAUUGAUGCUCACAAGUCUUGGG CCCAAGACUUGUGAGCAUCAAUUU

Table 6.

Scoring criteria of each evaluation index in AIA joint.

Evaluation index	Scoring criteria
Bone destruction	0: normal
	1: localized bone destruction in a single site
	2: bone destruction in multiple sites, but bone structure is kept
	3: bone destruction over a wide area, and bone structure is lost
Cartilage destruction	0: normal
	1: localized small erosion
	2: erosion over a wide area
	3: almost all cartilage destroyed or lost
Synovial thickening	0: normal
	1: localized slight
	2: localized moderate outgrowth or slight outgrowth over a wide sphere
	3: severe outgrowth or moderate outgrowth over a wide area
Inflammatory cell infiltration	0: normal
	1: slight local inflammatory cell infiltration
	2: moderate inflammatory cell infiltration over a wide area
	3: severe inflammatory cell infiltration over a wide area

Table 7.

List of 380 identified proteins and number of identified peptides for each protein in 4 pull down experiments

REFSEQ Accession	protein name	number of identified peptides				gene name
		High + Linker/ -competition	High + Linker/ +competition	Low + Linker/ -competition	Low + Linker/ +competition	
NP_079739	hypothetical protein LOC66276 [Mus musculus]	5	4	5	3	1810009A15Rik
NP_075822	lysinogen 7 [Mus musculus]	1	1	1	1	12210010C04Rik
NP_082487	hypothetical protein LOC72357 [Mus musculus]	2	2	0	0	12210016L2TRik
NP_077172	multiple myeloma tumor-associated protein 2 homolog [Mus musculus]	3	3	4	4	2310033P09Rik
NP_080791	PCNA-associated factor [Mus musculus]	4	4	5	4	2810417H13Rik
NP_808385	hypothetical protein LOC239673 [Mus musculus]	3	5	0	0	4732456N10Rik
NP_001014836	hypothetical protein LOC432479 [Mus musculus]	0	0	0	0	14930404N1TRik
NP_075745	keratin, type I cytoskeletal 20 [Mus musculus]	0	0	0	0	29030623C06Rik
NP_766549	4-aminobutyrate aminotransferase, mitochondrial isoform 1 precursor [Mus musculus]	0	0	0	0	1Abat
NP_038882	ATP-binding cassette sub-family F member 1 [Mus musculus]	1	1	1	1	1Abcf1
NP_033724	tyrosine-protein kinase ABL1 isoform b [Mus musculus]	1	1	0	0	1Abf1
NP_579938	acetyl-CoA carboxylase 1 [Mus musculus]	16	12	19	17	17Acaca
NP_598665	acetyl-Coenzyme A carboxylase beta [Mus musculus]	2	3	3	3	3Acacb
NP_058566	acyl-coenzyme A synthetase ACSM3, mitochondrial [Mus musculus]	1	0	0	0	0Acsm3
NP_031418	actin, aortic smooth muscle [Mus musculus]	6	5	3	2	2Acta2
NP_031419	actin, cytoplasmic 1 [Mus musculus]	8	7	5	3	3Actb
NP_780706	beta-actin-like protein 2 [Mus musculus]	2	3	1	0	0Actbl2
NP_081406	AFG3-like protein 2 [Mus musculus]	1	0	1	0	0Afg3l2
NP_033773	AHNAK nucleoprotein isoform 1 [Mus musculus]	97	98	90	89	89Ahnak
NP_666148	activator of 90 kDa heat shock protein ATPase homolog 1 [Mus musculus]	0	0	1	0	0Ahsa1
NP_031952	aminoacyl-tRNA synthetase complex-interacting multifunctional protein 1 [Mus musculus]	1	0	0	0	0Aimp1
NP_001075425	splicing factor, arginine/serine-rich 17b [Mus musculus]	0	0	1	1	1Akap17b
NP_083055	AMP deaminase 2 [Mus musculus]	0	0	0	0	1Ampd2
NP_780584	multiple ankyrin repeats, single KH-domain homolog [Mus musculus]	0	1	0	0	0Ankhf1
NP_112148	ankyrin repeat domain-containing protein 17 isoform a [Mus musculus]	2	2	1	2	2Ankrd17
NP_031486	AP-3 complex subunit delta-1 [Mus musculus]	1	1	1	1	0Ap3d1
NP_789819	arginine and glutamate-rich protein 1 [Mus musculus]	3	3	4	2	2Arglu1
NP_059098	rho guanine nucleotide exchange factor 7 isoform c [Mus musculus]	1	1	0	0	0Arhgf7
NP_653092	ADP-ribosylation factor-like protein 6-interacting protein 4 [Mus musculus]	4	3	2	3	3Arf6ip4
NP_001004364	arf-GAP with SH3 domain, ANK repeat and PH domain-containing protein 2 isoform b [Mus musculus]	1	1	0	0	1Asap2
NP_080259	ATP synthase subunit epsilon, mitochondrial [Mus musculus]	1	0	0	0	0Atp5e
NP_033556	transcriptional regulator ATRX [Mus musculus]	1	0	0	0	0Atrx
NP_997614	hypothetical protein LOC270156 [Mus musculus]	2	2	2	2	2AU019823
NP_079614	aurora kinase A-interacting protein [Mus musculus]	0	1	1	1	1Aurkap1
NP_666084	hypothetical protein LOC212547 [Mus musculus]	2	2	1	1	1BC027231
NP_001025478	H/ACA ribonucleoprotein complex subunit 4 [Mus musculus]	1	1	1	1	1BC068171
NP_722482	bcl-2-associated transcription factor 1 isoform 2 [Mus musculus]	1	1	1	1	1Blaf1
NP_659172	flavin reductase [Mus musculus]	3	0	0	0	0Blvrb
NP_001074891	bioregeneration of chromosomes in cell division 1-like [Mus musculus]	1	1	0	0	2Bodf1
NP_071304	CDK5 and ABL1 enzyme substrate 1 isoform 2 [Mus musculus]	0	0	1	0	0Cables1
NP_081657	hypothetical protein LOC70312 [Mus musculus]	2	0	1	1	1Cactin
NP_031625	macrophage-capping protein isoform 1 [Mus musculus]	0	0	0	0	0Cag9
NP_064321	cyclin-L1 [Mus musculus]	1	0	0	0	0Cenl1
NP_690023	cell division cycle 5-related protein [Mus musculus]	0	0	0	0	1Cdc5l
NP_031687	cell division protein kinase 11 [Mus musculus]	2	1	0	0	1Cdk11b
NP_031698	cerebellar degeneration-related protein 2 [Mus musculus]	0	0	0	0	1Cdr2
NP_666131	chromodomain helicase DNA-binding protein 3 [Mus musculus]	3	5	6	6	6Chd3
NP_666091	chromodomain-helicase DNA-binding protein 4 [Mus musculus]	26	26	25	29	29Chd4
NP_001074845	chromodomain helicase DNA binding protein 5 isoform 1 [Mus musculus]	6	7	7	8	8Chd5

Table 7.

List of 380 identified proteins and number of identified peptides for each protein in 4 pull down experiments

NP_080130	corepressor interacting with RBPJ 1 [Mus musculus]	1	0	0	0	0	Cir1	
NP_084455	CAP-Gly domain-containing linker protein 4, isoform 1 [Mus musculus]	1	0	0	0	0	Cjlp4	
NP_001013409	cleavage and polyadenylation specificity factor subunit 6 [Mus musculus]	4	4	4	4	4	Cpsf6	
NP_035934	protein CREG1 [Mus musculus]	0	0	0	0	1	Creg1	
NP_031819	cystatin-B [Mus musculus]	0	0	0	0	0	Cstb	
NP_085037	pre-mRNA-splicing factor CWC22 homolog [Mus musculus]	1	0	0	0	1	Cwc22	
NP_080410	cyclin-1 [Mus musculus]	0	0	0	0	1	Cycl1	
NP_001156337	cyclin, basic protein of sperm head cytoskeleton 2 [Mus musculus]	0	1	1	0	1	Cycl2	
NP_001007572	cytidic cell tumor 10 kDa protein homolog [Mus musculus]	1	1	1	2	2	D8Erfdf38e	
NP_001074450	probable ATP-dependent RNA helicase DDX23 [Mus musculus]	8	6	7	9	9	Ddx23	
NP_038960	ATP-dependent RNA helicase DDX25 [Mus musculus]	1	0	0	0	0	Ddx25	
NP_694705	probable ATP-dependent RNA helicase DDX27 [Mus musculus]	0	0	0	0	1	Ddx27	
NP_666087	probable ATP-dependent RNA helicase DDX46 [Mus musculus]	32	33	32	33	33	Ddx46	
NP_080176	protein DEK [Mus musculus]	14	12	14	14	11	Dek	
NP_081263	DEAH (Asp-Glu-Ala-His) box polypeptide 16 [Mus musculus]	0	0	0	0	1	Dhx16	
NP_031884	protein diaphanous homolog 1 [Mus musculus]	1	0	0	0	0	Diap1	
NP_001152833	disco-interacting protein 2 homolog B, isoform 1 [Mus musculus]	0	1	0	0	1	Dip2b	
NP_579943	dynein heavy chain 5, axonemal [Mus musculus]	1	0	0	0	0	Dnah5	
NP_033610	dnaJ homolog subfamily C member 2 [Mus musculus]	3	4	4	0	0	Dnajc2	
NP_084322	DnaJ (Hsp40) homolog, subfamily C, member 21 [Mus musculus]	0	2	1	3	3	Dnajc21	
NP_034196	DNA (cytosine-5)-methyltransferase 1 [Mus musculus]	24	26	26	26	26	Dnmt1	
NP_780500	dedicator of cytokinesis protein 10 [Mus musculus]	0	0	1	1	0	Dock10	
NP_001041519	dual specificity phosphatase 16, isoform B1 [Mus musculus]	0	0	0	0	1	Dusp16	
NP_034236	elongation factor 1-alpha 1 [Mus musculus]	8	11	8	8	8	Eef1a1	
NP_031932	elongation factor 1-alpha 2 [Mus musculus]	5	7	5	5	5	Eef1a2	
NP_080283	elongation factor 1-gamma [Mus musculus]	2	2	2	0	0	Eef1g	
NP_031933	elongation factor 2 [Mus musculus]	6	3	1	1	1	Eef2	
NP_001103465	116 kDa U5 small nuclear ribonucleoprotein component isoform b [Mus musculus]	1	0	0	0	0	Eftud2	
NP_080306	eukaryotic translation initiation factor 2 subunit 2 [Mus musculus]	2	1	1	0	1	Eif2s2	
NP_666312	eukaryotic translation initiation factor 3 subunit C [Mus musculus]	1	0	0	0	1	Eif3c	
NP_001152964	G patch domain containing 8 [Mus musculus]	1	1	1	0	0	1	ENSMUSG00000075516
NP_808489	E1A binding protein p300 [Mus musculus]	1	1	1	0	0	Ep300	
NP_084011	functional aminoacyl-tRNA synthetase [Mus musculus]	7	7	7	3	4	Epr3	
NP_001035966	hypothetical protein LOC68152 [Mus musculus]	1	1	1	1	1	Fam133b	
NP_032016	40S ribosomal protein S30 precursor [Mus musculus]	1	3	2	3	3	Fau	
NP_001116075	Fc fragment of IgG binding protein [Mus musculus]	1	0	0	0	0	Fcgbp	
NP_035943	flt3-interacting zinc finger protein 1 [Mus musculus]	1	0	1	1	1	Fiz1	
NP_035841	formin-like protein 3 [Mus musculus]	1	1	1	1	1	Fmnl3	
NP_038550	protein FRG1 [Mus musculus]	1	0	0	0	0	Frg1	
NP_079586	putative rRNA methyltransferase 3 [Mus musculus]	0	1	0	0	0	Ftsj3	
NP_476513	far upstream element-binding protein 1 [Mus musculus]	1	0	0	0	0	Fubp1	
NP_001124492	glial fibrillary acidic protein isoform 1 [Mus musculus]	1	1	1	1	2	Gfap	
NP_613061	glycine dehydrogenase [decarboxylating], mitochondrial precursor [Mus musculus]	0	0	0	1	1	Gldc	
NP_079650	lactylglutathione lyase [Mus musculus]	1	0	0	0	0	Glo1	
NP_001177285	40S ribosomal protein S24-like [Mus musculus]	1	1	1	1	1	Gm4832	
NP_001003664	hypothetical protein LOC331392 [Mus musculus]	1	1	1	1	1	Gm5124	
NP_001003670	type II keratin K514 [Mus musculus]	1	1	1	1	1	Gm5409	
NP_001177187	predicted gene, ENSMUSG0000050621 [Mus musculus]	2	2	0	0	0	Gm5414	
NP_663527	nuclear GTP-binding protein 2 [Mus musculus]	1	1	1	1	1	Gm9846	
NP_705775	guanine nucleotide-binding protein-like 3, long isoform [Mus musculus]	0	1	1	1	1	Gnl2	
NP_080457	G patch domain-containing protein 1 [Mus musculus]	2	1	0	1	3	Gpatch1	
NP_780709	glypican-5 precursor [Mus musculus]	0	0	0	0	1	Gpc5	
NP_032182	phosphatidylinositol-glycan-specific phospholipase D [Mus musculus]	1	1	1	0	0	Gpld1	
NP_598562	general transcription factor, IIF subunit 1 [Mus musculus]	9	8	11	8	11	Gtf2f1	
NP_081276	nucleolar GTP-binding protein 1 [Mus musculus]	0	1	1	0	0	Gtbbp4	

Table 7.

List of 380 identified proteins and number of identified peptides for each protein in 4 pull down experiments

NP_849209	trifunctional enzyme subunit alpha, mitochondrial precursor [Mus musculus]	1	0	0	0	1	Hacha
NP_032259	hepatoma-derived growth factor-related protein 2 [Mus musculus]	2	3	4	4	6	Hdgfrp2
NP_766334	HIRA-interacting protein 3 [Mus musculus]	11	14	11	11	12	Hirip3
NP_085112	histone H1.1 [Mus musculus]	4	3	3	3	3	Hist1h1a
NP_064418	histone H1.5 [Mus musculus]	2	3	2	2	2	Hist1h1b
NP_056601	histone H1.2 [Mus musculus]	4	3	2	2	5	Hist1h1c
NP_663759	histone H1.3 [Mus musculus]	5	4	3	3	5	Hist1h1d
NP_056602	histone H1.4 [Mus musculus]	6	4	3	3	5	Hist1h1e
NP_034507	histone H11 [Mus musculus]	2	2	1	1	2	Hist1h1t
NP_291074	histone H4 [Mus musculus]	1	1	1	1	0	Hist2h4
NP_034569	high mobility group protein B2 [Mus musculus]	1	0	2	0	0	Hmqb1
NP_032278	high mobility group protein B1 [Mus musculus]	1	1	0	0	0	Hmqb2
NP_598595	heterogeneous nuclear ribonucleoprotein F [Mus musculus]	1	0	0	0	0	Hnmpf
NP_079555	heterogeneous nuclear ribonucleoprotein K [Mus musculus]	1	1	0	0	0	Hnmpk
NP_058085	heterogeneous nuclear ribonucleoprotein U [Mus musculus]	1	0	0	0	0	Hnmpu
NP_034600	heterochromatin protein 1-binding protein 3 isoform 1 [Mus musculus]	3	2	1	1	0	Hnpb3
NP_542365	Hermansky-Pudlak syndrome 3 protein homolog isoform 1 [Mus musculus]	1	0	0	0	0	Hps3
NP_032328	heat shock protein HSP 90-beta [Mus musculus]	4	2	1	1	1	Hsp90ab1
NP_035761	endoplasmic reticulum protein [Mus musculus]	1	1	0	0	0	Hsp90bb1
NP_034608	heat shock 70 kDa protein 1B [Mus musculus]	1	0	0	0	0	Hspa1b
NP_001002012	heat shock-related 70 kDa protein 2 [Mus musculus]	2	1	0	0	1	Hspa2
NP_071705	78 kDa glucose-regulated protein precursor [Mus musculus]	5	3	1	1	3	Hspa5
NP_112442	heat shock cognate 71 kDa protein [Mus musculus]	0	2	0	0	0	Hspa8
NP_034607	60 kDa heat shock protein, mitochondrial [Mus musculus]	1	1	0	0	0	Hspd1
NP_038590	interferon-related developmental regulator 1 [Mus musculus]	1	1	1	1	1	Ifrd1
NP_940803	inverted formin-2 [Mus musculus]	0	0	0	0	0	Irf2
NP_852858	importin-7 [Mus musculus]	1	0	0	0	0	Ipo7
NP_057930	ras GTPase-activating-like protein IQGAP1 [Mus musculus]	38	32	35	35	32	Iqgap1
NP_081987	ras GTPase-activating-like protein IQGAP2 [Mus musculus]	1	1	1	1	0	Iqgap2
NP_001028656	IQ motif containing GTPase activating protein 3 [Mus musculus]	2	2	2	2	1	Iqgap3
NP_034704	irradiation-induced protein 1 [Mus musculus]	0	0	0	0	0	Irx2
NP_666095	potassium voltage-gated channel subfamily A member 5 [Mus musculus]	5	3	1	1	0	Kcna5
NP_034743	far upstream element-binding protein 2 [Mus musculus]	5	3	1	1	2	Khsip
NP_608301	kinesin-like protein KIF-ZC [Mus musculus]	0	0	0	0	0	Krifzc
NP_032472	chromosome-associated kinesin KIF4 [Mus musculus]	1	1	1	1	1	Kif4
NP_663580	kelch domain-containing protein 4 [Mus musculus]	1	1	1	1	2	Klhoc4
NP_034790	keratin, type I cytoskeletal 10 [Mus musculus]	7	9	7	7	8	Krt10
NP_058654	keratin, type I cytoskeletal 14 [Mus musculus]	3	5	0	0	4	Krt11-14
NP_032495	keratin, type I cytoskeletal 15 [Mus musculus]	2	2	2	2	3	Krt11-15
NP_034792	keratin, type I cytoskeletal 13 [Mus musculus]	2	2	2	2	4	Krt13
NP_032496	keratin, type I cytoskeletal 16 [Mus musculus]	3	2	0	0	0	Krt16
NP_034793	keratin, type I cytoskeletal 17 [Mus musculus]	2	4	0	0	3	Krt17
NP_032497	keratin, type I cytoskeletal 19 [Mus musculus]	0	0	0	0	2	Krt19
NP_034798	keratin, type II cytoskeletal 2 epidermal [Mus musculus]	3	3	2	2	3	Krt2
NP_032499	keratin, type II cytoskeletal 1 [Mus musculus]	0	0	0	0	2	Krt2-1
NP_766534	keratin-like protein KRT22 [Mus musculus]	0	0	0	0	1	Krt22
NP_034796	keratin, type II cytoskeletal 27 [Mus musculus]	1	1	1	1	1	Krt27
NP_032501	keratin, type II cytoskeletal 4 [Mus musculus]	2	2	1	1	3	Krt4
NP_001034755	keratin, type I cytoskeletal 40 [Mus musculus]	1	0	0	0	1	Krt40
NP_997648	keratin, type I cytoskeletal 42 [Mus musculus]	3	5	0	0	4	Krt42
NP_081287	keratin, type II cytoskeletal 5 [Mus musculus]	9	9	5	5	8	Krt5
NP_032502	keratin, type II cytoskeletal 6A [Mus musculus]	4	8	2	2	6	Krt6a
NP_034799	keratin, type II cytoskeletal 6B [Mus musculus]	3	7	0	0	5	Krt6b
NP_149064	keratin, type II cytoskeletal 7 [Mus musculus]	2	2	0	0	3	Krt7
NP_064340	keratin, type II cytoskeletal 71 [Mus musculus]	2	2	2	2	0	Krt71
NP_998893	keratin, type II cytoskeletal 72 [Mus musculus]	2	3	0	0	2	Krt72

Table 7.

List of 380 identified proteins and number of identified peptides for each protein in 4 pull down experiments

NP_997850	keratin, type II cytoskeletal 73 [Mus musculus]	3	3	3	3	3	Krt73
NP_579935	keratin, type II cytoskeletal 75 [Mus musculus]	4	5	0	0	0	Krt75
NP_001028349	keratin, type II cytoskeletal 2, oral [Mus musculus]	3	4	2	2	5	Krt76
NP_001003667	keratin, type II cytoskeletal 1b [Mus musculus]	4	3	2	2	3	Krt77
NP_997852	keratin Kc40 [Mus musculus]	1	1	1	1	2	Krt78
NP_666175	keratin, type II cytoskeletal 79 [Mus musculus]	4	4	2	4	4	Krt79
NP_112447	keratin, type II cytoskeletal 8 [Mus musculus]	3	3	1	4	4	Krt8
NP_001003668	keratin, type II cytoskeletal Hb3 [Mus musculus]	0	0	0	1	1	Krt83
NP_032500	keratin, type II cuticular Hb4 [Mus musculus]	0	2	0	0	0	Krt84
NP_613059	la-related protein 7 [Mus musculus]	1	1	1	1	3	Larp7
NP_598576	lamin-B receptor [Mus musculus]	2	2	2	2	2	Lbr
NP_032905	plastin-2 [Mus musculus]	7	5	0	1	0	Lcp1
NP_034829	L-lactate dehydrogenase A chain isoform 1 [Mus musculus]	0	1	0	0	0	Ldha
NP_080529	leucine-rich repeat-containing protein 18, isoform 1 [Mus musculus]	0	1	1	1	1	Lrrc18
NP_957878	leucine-rich repeat-containing protein 47 [Mus musculus]	2	1	1	1	1	Lrrc47
NP_001104781	leucine-rich repeat flightless-interacting protein 1 isoform 1 [Mus musculus]	3	3	2	2	2	Lrrfp1
NP_080157	protein LTV1 homolog [Mus musculus]	2	4	2	3	2	Ltv1
NP_080172	putative RNA-binding protein Luc7-like 1 isoform 1 [Mus musculus]	6	6	6	6	6	Luc7l
NP_619821	putative RNA-binding protein Luc7-like 2 isoform 1 [Mus musculus]	5	7	7	7	7	Luc7l2
NP_080589	Luc7-like protein 3 [Mus musculus]	8	9	8	8	7	Luc7l3
NP_079557	cell growth-regulating nuclear protein [Mus musculus]	7	7	6	6	7	Lyar
NP_033730	microtubule-actin cross-linking factor 1 [Mus musculus]	4	5	3	3	2	Macf1
NP_034497	membrane-associated guanylate kinase, WW and PDZ domain-containing protein 1 isoform a [Mus musculus]	1	1	3	3	3	Magi1
NP_032859	microtubule-associated protein 4 [Mus musculus]	3	4	2	4	2	Map4
NP_076133	methylcrotonyl-CoA carboxylase subunit alpha, mitochondrial [Mus musculus]	14	19	17	17	18	Mccc1
NP_035975	probable E3 ubiquitin-protein ligase MID2 [Mus musculus]	0	0	0	0	1	Mid2
NP_663354	mas-related G-protein coupled receptor member F [Mus musculus]	0	0	1	1	0	Mrgprf
NP_080072	39S ribosomal protein L33, mitochondrial [Mus musculus]	1	1	0	0	0	Mrp133
NP_036015	28S ribosomal protein S12, mitochondrial precursor [Mus musculus]	2	2	1	2	2	Mrs12
NP_032864	bifunctional methylenetetrahydrofolate dehydrogenase/cyclohydrolase, mitochondrial [Mus musculus]	5	4	0	0	0	Mthfd2
NP_032735	N-myc proto-oncogene protein [Mus musculus]	1	1	0	0	0	Mycn
NP_001155247	myosin-11, isoform 2 [Mus musculus]	0	1	0	0	0	Mvh11
NP_071855	myosin-9, isoform 1 [Mus musculus]	2	3	1	1	3	Mvh9
NP_056557	myosin-Xb, isoform 3 [Mus musculus]	1	0	0	0	0	Myo9b
NP_038636	nascent polypeptide-associated complex subunit alpha isoform b [Mus musculus]	1	1	1	1	1	Naca
NP_075783	kinetochore protein NDC80 homolog [Mus musculus]	1	1	0	0	1	Ndc80
NP_079717	serologically defined colon cancer antigen 1 homolog [Mus musculus]	4	5	3	6	6	Nemf
NP_079995	NFKB activating protein-like [Mus musculus]	0	0	0	0	1	Nkapl
NP_032733	glycopeptide N-tetradecanoyltransferase 1 [Mus musculus]	1	1	1	2	2	Nmt1
NP_032734	glycopeptide N-tetradecanoyltransferase 2 [Mus musculus]	0	0	0	0	1	Nmt2
NP_076043	nucleolar protein 7 [Mus musculus]	1	0	0	0	0	Nol7
NP_001034440	nucleolar and coiled-body phosphoprotein 1 isoform B [Mus musculus]	21	22	22	22	22	Nolc1
NP_848720	nucleolar protein 16 [Mus musculus]	6	5	6	6	6	Nop16
NP_032748	nucleophosmin [Mus musculus]	1	2	1	1	1	Npm1
NP_064678	ribosyl(dihydroxycinnamide dehydrogenase (quinone) isoform 1 [Mus musculus]	6	0	4	0	0	Nqo2
NP_032760	pro-neuregulin-3, membrane-bound isoform isoform 1 [Mus musculus]	0	1	0	0	0	Nrg3
NP_795942	5-nucleotidase domain-containing protein 1 [Mus musculus]	1	0	0	0	0	Nt5dc1
NP_780503	nuclear ubiquitin casein and cyclin-dependent kinases substrate isoform 1 [Mus musculus]	0	1	0	0	0	Nucks1
NP_598612	nucleolar and spindle-associated protein 1 isoform a [Mus musculus]	3	2	2	2	2	Nusap1
NP_035162	protein disulfide-isomerase precursor [Mus musculus]	17	17	2	3	3	P4hb
NP_032800	polyadenylate-binding protein 1 [Mus musculus]	0	1	0	0	0	Pabpc1
NP_031441	poly (ADP-ribose) polymerase 1 [Mus musculus]	1	2	1	2	1	Parp1
NP_659093	propionyl-CoA carboxylase alpha chain, mitochondrial precursor [Mus musculus]	23	24	23	23	23	Pcca
NP_032823	pyruvate carboxylase, mitochondrial isoform 2 [Mus musculus]	22	24	21	23	23	Pcx
NP_031978	protein disulfide-isomerase A3 precursor [Mus musculus]	3	3	1	3	1	Pdia3

Table 7.

List of 380 identified proteins and number of identified peptides for each protein in 4 pull down experiments

NP_033917	protein disulfide-isomerase A4 [Mus musculus]	1	0	0	0	0	Pdia4
NP_082235	protein disulfide-isomerase A6 [Mus musculus]	1	2	0	0	0	Pdia6
NP_742146	pyridoxal kinase [Mus musculus]	1	0	0	0	0	Pdkk
NP_032852	6-phosphofruktokinase, liver type [Mus musculus]	1	0	0	0	0	Pfk
NP_084340	PHD finger protein 23 [Mus musculus]	1	0	0	1	0	Pfhd23
NP_001074549	PHD finger protein 3 [Mus musculus]	0	0	0	1	0	Pfhd3
NP_058662	D-3-phosphoglycerate dehydrogenase [Mus musculus]	1	2	0	0	0	Pfhdh
NP_035216	1-phosphatidylinositol-3-phosphate 5-kinase [Mus musculus]	11	0	0	0	0	Pktyve
NP_035386	membrane-associated phosphatidylinositol transfer protein [Mus musculus]	1	0	0	0	0	Pip4k2a
NP_001093249	pyruvate kinase isozymes M1/M2 [Mus musculus]	0	1	0	0	0	Pipkm2
NP_035229	pyruvate kinase isozymes M1/M2 [Mus musculus]	8	10	0	1	0	Pkkr
NP_001028491	liprin-alpha-1 isoform B [Mus musculus]	0	1	1	1	0	Pplia1
NP_035279	peptidyl-prolyl cis-trans isomerase B precursor [Mus musculus]	1	1	0	0	0	Ppib
NP_080417	peptidyl-prolyl cis-trans isomerase-like 4 [Mus musculus]	4	2	2	2	0	Ppila4
NP_082308	serine/threonine-protein phosphatase 2A 55 kDa regulatory subunit B alpha isoform [Mus musculus]	1	1	0	0	0	Ppp2r2a
NP_051164	peroxiredoxin-1 [Mus musculus]	6	6	3	0	0	Ppx1
NP_035693	peroxiredoxin-2 [Mus musculus]	1	2	0	0	0	Ppx2
NP_058044	peroxiredoxin-4 [Mus musculus]	2	2	1	1	0	Ppx4
NP_766285	pre-mRNA-splicing factor 38A [Mus musculus]	1	0	1	0	0	Ppf38a
NP_080121	pre-mRNA-splicing factor 38B [Mus musculus]	9	9	9	9	0	Ppf38b
NP_598709	PC4 and SFRS1-interacting protein [Mus musculus]	0	0	0	1	0	Ppsp1
NP_033001	protein tyrosine phosphatase type IVA 3 isoform 1 [Mus musculus]	0	0	1	0	0	Ptp4a3
NP_663433	PX domain-containing protein kinase-like protein long isoform [Mus musculus]	0	0	1	0	0	Ppk
NP_033022	ras-related protein Rab-1A [Mus musculus]	0	1	0	0	0	Rab1
NP_033037	UV excision repair protein RAD23 homolog B [Mus musculus]	1	1	1	1	0	Rad23b
NP_033039	RAD51-associated protein 1 [Mus musculus]	1	1	0	0	0	Rad51ap1
NP_035377	E3 ubiquitin-protein ligase RBBP6 isoform 1 [Mus musculus]	2	1	2	0	0	Rbbp6
NP_081625	RNA-binding protein 25 [Mus musculus]	1	1	0	0	0	Rbm25
NP_573505	RNA-binding protein 39 [Mus musculus]	6	5	4	4	0	Rbm39
NP_776282	protein RCC2 [Mus musculus]	4	5	2	2	0	Rcc2
NP_077204	serine/threonine-protein kinase RIO1 [Mus musculus]	2	3	0	0	0	Rio1
NP_033096	RNA-binding protein with serine-rich domain 1 isoform 1 [Mus musculus]	2	2	2	2	0	Rnps1
NP_061209	RNA polymerase II-associated protein 1 isoform 1 [Mus musculus]	1	1	1	1	0	Rp9
NP_796268	RNA polymerase II-associated protein 1 isoform 1 [Mus musculus]	0	0	0	0	0	Rp9
NP_443067	60S ribosomal protein L10 [Mus musculus]	2	2	3	2	0	Rpl10
NP_001156405	60S ribosomal protein L10-like [Mus musculus]	1	1	1	1	0	Rpl10l
NP_080195	60S ribosomal protein L11 [Mus musculus]	3	3	3	3	0	Rpl11
NP_058018	60S ribosomal protein L13 [Mus musculus]	1	2	2	2	0	Rpl13
NP_001002239	60S ribosomal protein L17 [Mus musculus]	6	5	5	5	0	Rpl17
NP_033104	60S ribosomal protein L19 isoform 1 [Mus musculus]	2	3	3	3	0	Rpl19
NP_033105	60S ribosomal protein L22 [Mus musculus]	1	1	1	1	0	Rpl22
NP_080793	60S ribosomal protein L22-like 1 [Mus musculus]	1	0	1	1	0	Rpl22l1
NP_075029	60S ribosomal protein L23 [Mus musculus]	2	3	3	3	0	Rpl23
NP_997406	60S ribosomal protein L23a [Mus musculus]	9	8	8	8	0	Rpl23a
NP_077180	60S ribosomal protein L24 [Mus musculus]	2	2	2	2	0	Rpl24
NP_033106	60S ribosomal protein L26 [Mus musculus]	5	7	6	6	0	Rpl26
NP_036105	60S ribosomal protein L27a [Mus musculus]	1	1	1	1	0	Rpl27a
NP_033107	60S ribosomal protein L28 [Mus musculus]	2	2	2	2	0	Rpl28
NP_444487	60S ribosomal protein L31 [Mus musculus]	2	2	2	2	0	Rpl31
NP_081000	60S ribosomal protein L34 isoform 1 [Mus musculus]	0	0	0	0	0	Rpl34
NP_079868	60S ribosomal protein L35 [Mus musculus]	2	2	2	2	0	Rpl35
NP_063918	60S ribosomal protein L36a [Mus musculus]	4	3	3	3	0	Rpl36a
NP_033110	60S ribosomal protein L37a [Mus musculus]	1	1	1	1	0	Rpl37a
NP_075861	60S ribosomal protein L38 [Mus musculus]	6	6	6	6	0	Rpl38
NP_035422	60S ribosomal protein L9 [Mus musculus]	0	0	0	0	0	Rpl9

Table 7.

List of 380 identified proteins and number of identified peptides for each protein in 4 pull down experiments

NP_080239	40S ribosomal protein S10 [Mus musculus]	1	1	1	1	2	Rps10
NP_036753	40S ribosomal protein S11 [Mus musculus]	2	2	2	2	3	Rps11
NP_080809	40S ribosomal protein S13 [Mus musculus]	2	2	2	2	2	Rps13
NP_065625	40S ribosomal protein S14 [Mus musculus]	4	4	4	4	4	Rps14
NP_733769	40S ribosomal protein S15a [Mus musculus]	4	4	4	4	3	Rps15a
NP_038675	40S ribosomal protein S16 [Mus musculus]	4	4	4	4	4	Rps16
NP_033118	40S ribosomal protein S17 [Mus musculus]	2	1	1	1	1	Rps17
NP_035426	40S ribosomal protein S18 [Mus musculus]	5	6	6	6	5	Rps18
NP_075622	40S ribosomal protein S19 [Mus musculus]	5	6	6	6	5	Rps19
NP_032529	40S ribosomal protein S2 [Mus musculus]	1	1	1	1	1	Rps2
NP_060423	40S ribosomal protein S20 [Mus musculus]	2	2	2	2	1	Rps20
NP_077137	40S ribosomal protein S23 [Mus musculus]	5	5	5	5	3	Rps23
NP_035427	40S ribosomal protein S24 isoform 1 [Mus musculus]	4	5	5	5	5	Rps24
NP_077228	40S ribosomal protein S25 [Mus musculus]	4	4	4	4	3	Rps25
NP_038793	40S ribosomal protein S26 [Mus musculus]	3	3	3	3	3	Rps26
NP_001171510	ribosomal protein L26-like [Mus musculus]	3	4	4	4	5	Rps26i
NP_081291	40S ribosomal protein S27 [Mus musculus]	0	0	0	0	2	Rps27
NP_080743	40S ribosomal protein S27-like [Mus musculus]	2	3	3	3	2	Rps27i
NP_033119	40S ribosomal protein S29 [Mus musculus]	1	1	1	1	2	Rps29
NP_036182	40S ribosomal protein S3 [Mus musculus]	1	1	1	1	0	Rps3
NP_058655	40S ribosomal protein S3a [Mus musculus]	5	5	5	5	4	Rps3a1
NP_033120	40S ribosomal protein S4_X isoform [Mus musculus]	3	2	2	2	2	Rps4x
NP_033121	40S ribosomal protein S5 [Mus musculus]	0	1	1	1	1	Rps5
NP_033122	40S ribosomal protein S6 [Mus musculus]	6	6	6	6	5	Rps6
NP_035430	40S ribosomal protein S7 [Mus musculus]	3	3	3	3	1	Rps7
NP_033124	40S ribosomal protein S8 [Mus musculus]	4	4	4	4	5	Rps8
NP_084043	40S ribosomal protein S9 [Mus musculus]	9	8	8	8	9	Rps9
NP_077243	ribosome-binding protein 1 isoform a [Mus musculus]	9	10	10	10	8	Rrbp1
NP_598329	ribosome-binding protein 1 isoform b [Mus musculus]	1	1	1	1	0	Rrbp1
NP_955518	RRP12-like protein [Mus musculus]	1	1	1	1	0	Rrp12
NP_080098	arginine/serine-rich coiled-coil protein 1 [Mus musculus]	6	4	4	4	5	Rsrc1
NP_001005525	arginine/serine-rich coiled-coil protein 2 isoform 1 [Mus musculus]	5	6	7	7	8	Rsrc2
NP_033133	retinoic acid receptor RXR-gamma isoform 1 [Mus musculus]	1	0	0	0	0	Rrxg
NP_035441	protein S100-A4 [Mus musculus]	1	0	0	0	0	S100a4
NP_079640	SAP domain-containing ribonucleoprotein [Mus musculus]	0	0	0	0	1	Samp
NP_780364	SAM and SH3 domain-containing protein 1 [Mus musculus]	1	0	0	0	0	Sash1
NP_082424	splicing factor, arginine/serine-rich 2, interacting protein [Mus musculus]	10	9	9	9	8	Scaf11
NP_766301	protein SDA1 homolog [Mus musculus]	1	1	1	1	0	Sdad1
NP_001076444	epimerase family protein SDR39U1 [Mus musculus]	1	0	0	0	0	Sdr39u1
NP_083555	selenocysteine insertion sequence-binding protein 2 [Mus musculus]	0	1	1	1	0	Secisbp2
NP_080090	plasmalogen activator inhibitor 1 RNA-binding protein isoform 1 [Mus musculus]	0	2	2	2	0	Serbp1
NP_035484	small EDRK-rich factor 2 [Mus musculus]	1	1	1	1	0	Sert2
NP_001074493	histone-lysine N-methyltransferase SETDB2 [Mus musculus]	1	1	1	1	1	Setdb2
NP_079945	splicing factor, arginine/serine-rich 18 [Mus musculus]	7	7	7	7	8	Sfrs18
NP_067481	putative E3 ubiquitin-protein ligase SH3RF1 [Mus musculus]	0	0	0	0	0	Sh3rf1
NP_081774	serine/threonine-protein kinase SIK3 [Mus musculus]	0	0	0	0	1	Siik3
NP_808283	solute carrier family 26 member 10 [Mus musculus]	0	1	1	1	1	Sic26a10
NP_031541	cationic amino acid transporter 3 [Mus musculus]	0	0	0	0	1	Sicr/a3
NP_079941	U4/U6.U5 small nuclear ribonucleoprotein 27 kDa protein [Mus musculus]	3	3	3	3	4	Snmp27
NP_033250	U1 small nuclear ribonucleoprotein 70 kDa [Mus musculus]	0	0	0	0	1	Snmp70
NP_035568	transcription factor SOX-12 [Mus musculus]	0	0	0	0	0	Sox12
NP_849245	spermatogenesis-associated protein 7 homolog [Mus musculus]	0	1	1	1	0	Sspat7
NP_631879	spermatogenesis-associated serine-rich protein 2 [Mus musculus]	1	1	1	1	1	Sspat2
NP_766180	splicing factor, arginine/serine-rich 12 [Mus musculus]	1	1	1	1	1	Srek1
NP_001074506	SLIT-ROBO Rho GTPase-activating protein 1 [Mus musculus]	0	1	1	1	0	Sragap1
NP_001074480	SLIT-ROBO Rho GTPase-activating protein 2 [Mus musculus]	1	2	2	2	1	Sragap2

Table 7.
List of 380 identified proteins and number of identified peptides for each protein in 4 pull down experiments

NP_058079	serine/arginine repetitive matrix protein 1 [Mus musculus]	3	3	3	4	Srm1
NP_780438	serine/arginine repetitive matrix protein 2 [Mus musculus]	9	8	6	11	Srm2
NP_081265	splicing factor, arginine/serine-rich 11 [Mus musculus]	2	3	1	1	Srsf11
NP_035488	splicing factor, arginine/serine-rich 2 [Mus musculus]	3	4	3	3	Srsf2
NP_038691	splicing factor, arginine/serine-rich 3 [Mus musculus]	1	1	1	2	Srsf3
NP_065612	splicing factor, arginine/serine-rich 4 [Mus musculus]	3	2	1	3	Srsf4
NP_001073162	splicing factor, arginine/serine-rich 5 [Mus musculus]	2	2	0	0	Srsf5
NP_080775	arginine/serine-rich splicing factor 6 [Mus musculus]	5	2	0	3	Srsf6
NP_892035	FACT complex subunit SSRP1 isoform 1 [Mus musculus]	6	6	6	6	Ssrp1
NP_035424	activated RNA polymerase II transcriptional coactivator p15 [Mus musculus]	6	7	5	8	Sub1
NP_033324	surfeit locus protein 6 [Mus musculus]	7	7	7	7	Surf6
NP_001034563	transcription elongation regulator 1 [Mus musculus]	0	1	0	0	Tcerg1
NP_035682	treacle protein [Mus musculus]	4	3	3	4	Tcof1
NP_038714	T-complex protein 1 subunit alpha [Mus musculus]	0	1	0	0	Tcp1
NP_081898	testis-expressed protein 19.2 [Mus musculus]	0	0	1	0	Tex19.2
NP_035703	testis expressed gene 264 [Mus musculus]	0	0	1	0	Tex264
NP_848782	transcription factor DP-2 isoform A [Mus musculus]	0	1	0	1	Tfcp2
NP_668265	thyroid hormone receptor-associated protein 3 [Mus musculus]	1	1	0	2	Thrap3
NP_899073	coiled-coil domain-containing protein 72 [Mus musculus]	2	2	2	2	Tma7
NP_001013391	transmembrane protease serine 13 [Mus musculus]	0	0	0	1	Trmprs13
NP_033442	tropomyosin beta chain [Mus musculus]	1	0	0	0	Tpm2
NP_034036	tripeptidyl-peptidase 1 precursor [Mus musculus]	0	0	1	0	Tpp1
NP_035776	trypsin 4 [Mus musculus]	1	1	1	1	Try4
NP_084479	testis-specific Y-encoded-like protein 4 [Mus musculus]	8	8	6	5	Tsrl
NP_796299	pre-rRNA-processing protein TSR1 homolog [Mus musculus]	8	7	7	0	Tuba1a
NP_035783	tubulin alpha-1A chain [Mus musculus]	8	7	8	6	Tuba1a
NP_033474	tubulin alpha-1C chain [Mus musculus]	9	8	8	6	Tuba1c
NP_033472	tubulin alpha-3 chain [Mus musculus]	6	6	6	5	Tuba3a
NP_033473	tubulin alpha-4A chain [Mus musculus]	7	6	5	3	Tuba4a
NP_059075	tubulin alpha-8 chain [Mus musculus]	5	5	0	0	Tuba8
NP_001029051	tubulin alpha chain-like 3 [Mus musculus]	1	1	1	1	Tubal3
NP_001074440	tubulin_beta_1 [Mus musculus]	2	2	1	0	Tubb1
NP_033476	tubulin beta-2A chain [Mus musculus]	7	7	3	4	Tubb2a
NP_075768	tubulin beta-3 chain [Mus musculus]	7	7	4	4	Tubb3
NP_033477	tubulin beta-4 chain [Mus musculus]	6	6	3	3	Tubb4a
NP_666228	tubulin beta-2C chain [Mus musculus]	9	9	0	5	Tubb4b
NP_035785	tubulin beta-5 chain [Mus musculus]	11	11	6	6	Tubb5
NP_080749	tubulin beta-6 chain [Mus musculus]	4	5	0	1	Tubb6
NP_001005506	alpha-taxilin [Mus musculus]	9	9	4	5	Xlna
NP_598432	splicing factor U2AF 65 kDa subunit [Mus musculus]	6	5	5	5	U2af2
NP_080752	U2-associated protein SR140 2 [Mus musculus]	8	8	8	9	U2surp
NP_035820	valyl-tRNA synthetase [Mus musculus]	1	0	0	0	Vais
NP_766126	vezatin [Mus musculus]	1	0	0	0	Vezt
NP_766355	von Willebrand factor A domain-containing protein 5A [Mus musculus]	0	1	0	0	Vvra5a
NP_084510	WD repeat-containing protein 76 [Mus musculus]	0	1	0	0	Wdr76
NP_067369	Z-DNA-binding protein 1 isoform 1 [Mus musculus]	0	0	0	1	Zbp1
NP_064652	transcriptional regulator Kaiso [Mus musculus]	1	1	0	1	Zbnb33
NP_081210	zinc finger CCH domain-containing protein 15 [Mus musculus]	0	1	0	0	Zc3h15
NP_001007461	probable palmitoyltransferase ZDHHC23 [Mus musculus]	1	0	1	0	Zdhhc23
NP_077177	zinc finger protein 593 [Mus musculus]	1	1	1	1	Zfp593
NP_033594	zinc finger protein 94 [Mus musculus]	1	0	0	0	Zfp94
NP_059077	zinc finger Ran-binding domain-containing protein 2 [Mus musculus]	11	9	11	10	Zrmb2

Table 8

Selected list of captured proteins from photoreactive experiments using two types of probes with or without competitor conditions.

Probe	Competition with High	Number of identified peptides		
		PIKfyve	Blvrb	Nqo2
High + Linker	-	11	3	7
High + Linker	+	0	0	0
Low + Linker	-	0	0	3
Low + Linker	+	0	0	0

Two probes possessing differential activity (High, 1.2 nM; Low, > 1000 nM) were used for assay.

Table 9.

Inhibitory activity on PI3K superfamily enzymes (IC₅₀, μM)

Compound	PI3K α	PI3K β	PI3K δ
AS2677131	>10	>10	>10
AS2795440	>10	>10	>10
Inactive	>10	>10	>10

Table 10.

Kinase selectivity profile of Compound X against 148 kinases.

Compound X (1 μ M)					
Kinase	% Inhibition	Kinase	% Inhibition	Kinase	% Inhibition
ABL	7.8	FGR	-2.8	LYNa	1.4
ACK	1.2	FLT1	1.3	MER	0.7
BLK	12.7	FLT3	7.6	MET	-1.4
BMX	1.4	FMS	1.4	MUSK	-6.3
BTK	10.8	FRK	0.2	PDGFRa	5.5
CSK	0.2	FYN	15.2	PYK2	-0.7
CTK	8.6	HCK	14.0	RET	-4.1
EGFR	-0.2	HER2	2.6	ROS	0.8
EPHA1	-0.6	IGF1R	-0.1	SRC	0.6
EPHA2	-4.7	INSR	5.4	SRM	-1.6
EPHA5	-2.6	IRR	-0.3	TEC	3.5
EPHB1	-11.5	ITK	0.6	TIE2	-1.8
EPHB4	-2.0	KDR	2.4	TNK1	-1.9
FAK	-0.5	KIT	-2.5	TRKA	0.7
FER	-2.8	LCK	5.8	TXK	1.6
FGFR1	7.6	LTK	0.1	TYK2	-1.7

Table 10.

Kinase selectivity profile of Compound X against 148 kinases.

Compound X (1 μ M)					
Kinase	% Inhibition	Kinase	% Inhibition	Kinase	% Inhibition
TYRO3	-6.0	CHK1	-23.5	IKKa	0.7
YES	3.2	CK1g1	-0.2	IKKb	4.6
ZAP70	-6.4	CK1e	9.4	IKKe	-4.8
AKT1	0.9	CK2a1/b	0.3	IRAK1	11.6
AKT2	1.5	CLK1	0.1	IRAK4	-6.8
AMPKa1/b1/g1	4.2	COT	13.4	JNK1	3.3
AurC	-4.9	CRIK	-5.4	JNK2	1.7
BMPR1A	0.8	DAPK1	-3.6	JNK3	-3.6
BRAF	1.4	DCAMKL2	-4.1	MAP2K1	14.7
CaMK1a	1.7	DLK	5.9	MAP2K2	7.0
CaMK2a	-2.8	DYRK1A	-14.5	MAP2K3	6.1
CaMK4	0.5	EEF2K	1.3	MAP2K4	-3.4
CDC2	4.8	Erk5	14.8	MAP2K5	-6.2
CDC7	-5.9	GSK3a	-2.1	MAP2K7	-5.3
CDK2/CycA2	0.4	GSK3b	6.8	MAP3K1	-0.7
CDK3	5.2	HGK	9.5	MAP3K2	1.9
CGK2	4.0	HIPK1	4.3	MAP3K3	2.2

Table 10.

Kinase selectivity profile of Compound X against 148 kinases.

Compound X (1 μ M)					
Kinase	% Inhibition	Kinase	% Inhibition	Kinase	% Inhibition
MAP3K4	3.9	p70S6K	-1.5	PKR	4.9
MAP3K5	-0.5	PAK1	-28.1	PLK1	6.4
MAP4K2	0.5	PAK6	-62.2	PRKX	0.5
MAPKAPK2	5.5	PASK	-0.1	RAF1	-1.2
MARK1	12.8	PBK	-2.1	ROCK1	0.2
MELK	8.8	PDHK2	-1.1	RSK1	7.0
MINK	-0.4	PEK	18.9	RSK2	14.6
MLK1	4.3	PGK	-1.3	SGK	5.1
MNK1	5.9	PIM1	18.5	SLK	-1.3
MRCKa	-1.6	PKACa	20.1	TAK1-TAB1	-10.6
MST1	-2.1	PKCa	4.3	TAOK2	-2.1
NDR1	-0.4	PKCb1	3.5	TSSK1	-1.9
NEK2	-1.6	PKCg	-1.3	TTK	4.4
NuaK1	-17.7	PKCd	3.9	WEE1	-1.4
p38b	-5.3	PKCq	2.6	WNK1	-1.2
p38g	-7.3	PKD2	16.0	PIKfyve	95.9 (0.2 μM)
p38d	-1.4	PKN1	-4.7	PIKfyve	48.7 (0.05 μM)

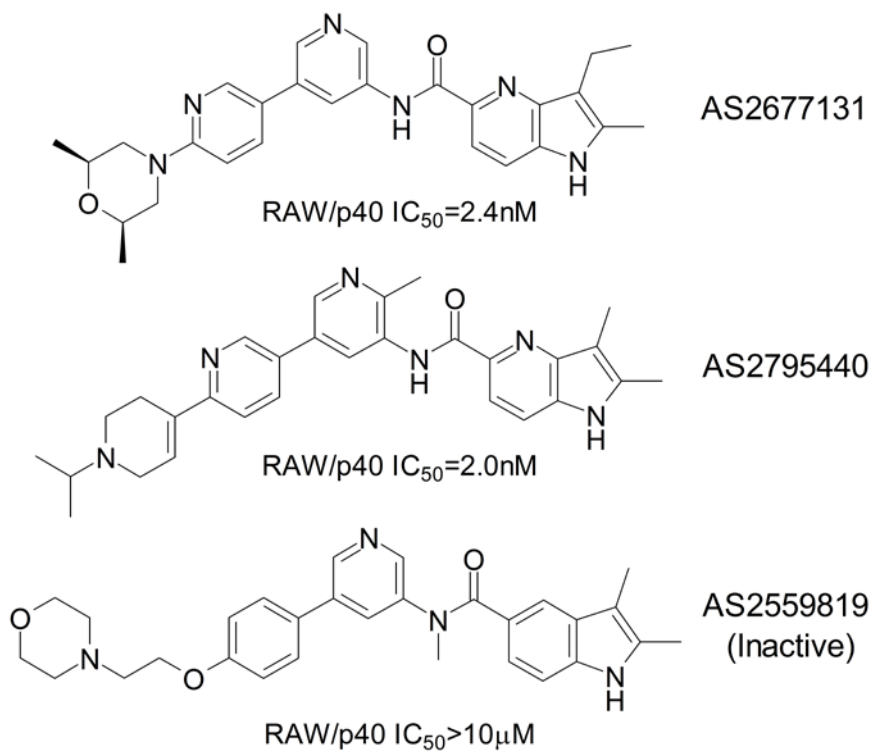


Fig. 8. Chemical structures and pharmacological activity of AS2677131, AS2795440, and AS2559819. Two active compounds, AS2677131 and AS2795440, and an inactive compound, AS2559819. Inhibitory activity of AS compounds on IL-12p40 production in IFN γ /LPS-stimulated RAW264.7 cells is shown.

Fig. 9. AS2677131 and AS2795440 inhibit proinflammatory cytokine production. (A) Inhibitory activity of the AS compounds on IL-12p40 production in IFN γ /LPS-stimulated RAW264.7 cells. Cells were prestimulated with IFN γ , followed by addition of compounds and stimulation with LPS. IL-12p40 levels were measured by ELISA. Data are presented as percentage of DMSO-treated control cells (100%). A representative of three experiments is shown. (B) Kinetics of cytokine mRNA levels in IFN γ /LPS-stimulated RAW264.7 cells treated with AS2677131 (unfilled) or DMSO (filled). Data are normalized relative to β -actin. (C) Effect of the AS compounds on the production of IL-12p40, IL-6, and TNF α in activated macrophages (M ϕ) or DCs (DC). Macrophages were stimulated with IFN γ /LPS. DCs were stimulated with IFN γ /LPS/MDP. Cytokine levels were determined by ELISA. Data are presented as a percentage of DMSO-treated control cells (100%). A representative of three experiments is shown. (D) Inhibitory effect of the AS compounds on the production of IL-12p40, IL-6, and TNF α in TLR ligand-injected rats. AS2677131 (1, 3, 10, 30 mg/kg), AS2795440 (0.3, 1, 3, 10 mg/kg), or vehicle were orally administered to rats ($n = 4$ /group) 1 h before i.v. injection of Poly(I:C) (1 mg/rat) and MDP (20 μ g/rat). Cytokine levels were measured by ELISA in collected plasma 2 h after injection. Values are expressed as mean \pm S.E.M. Significant differences between the vehicle and treated groups: *: $p < 0.05$, **: $p < 0.01$, ***: $p < 0.001$ (Dunnet multiple comparison test).

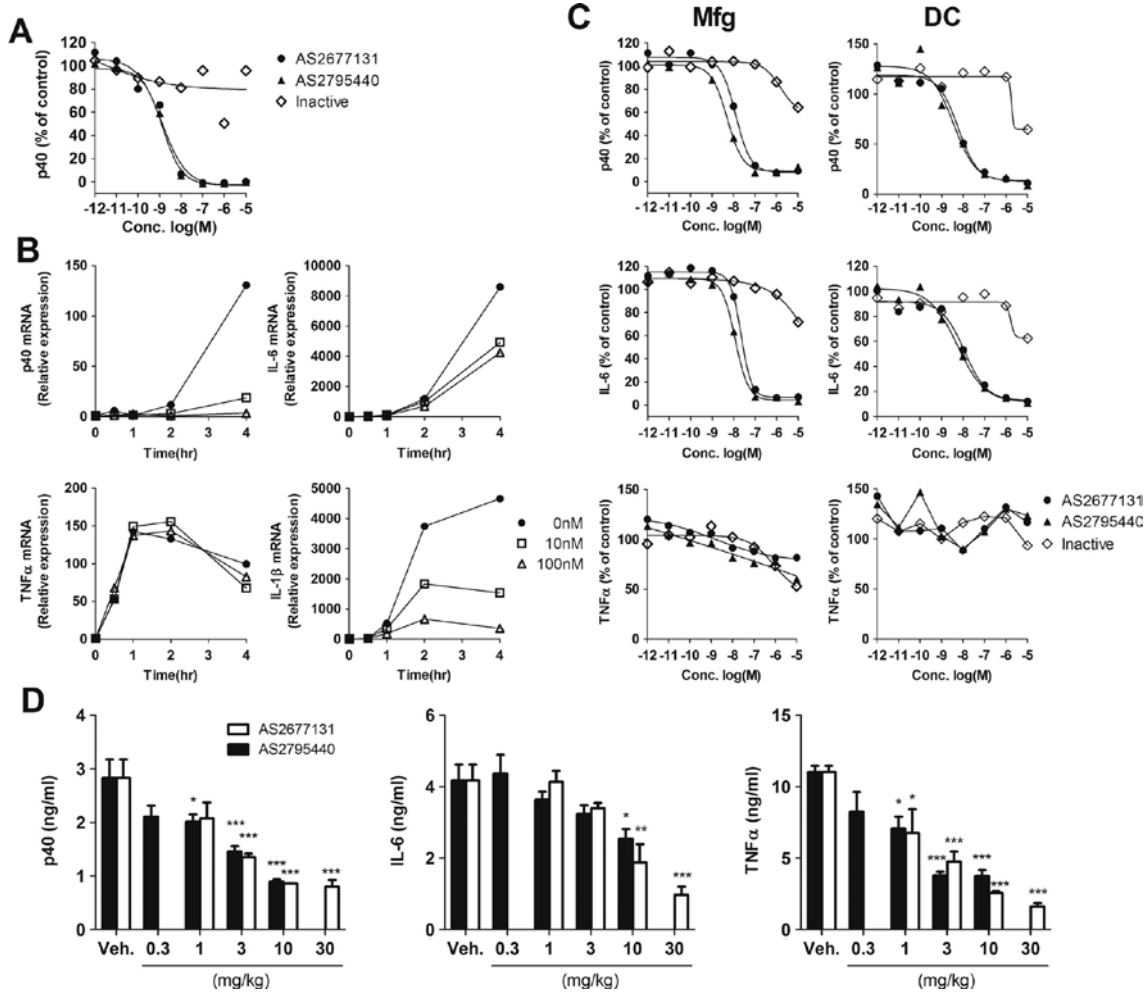


Fig. 9.

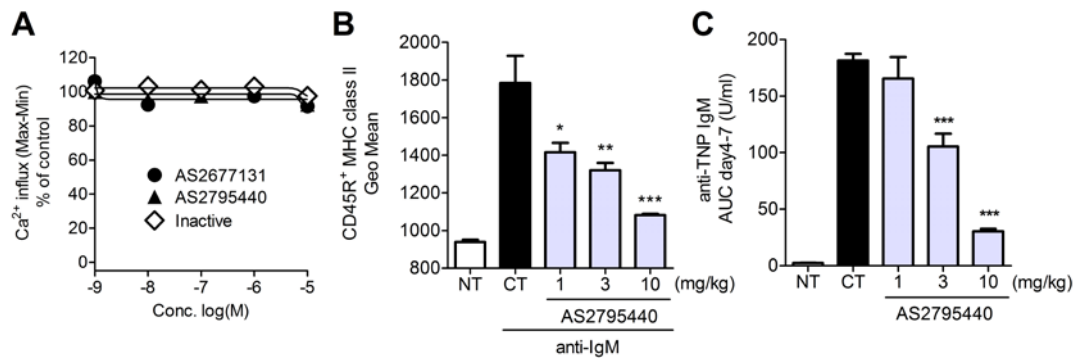


Fig. 10. AS2677131 and AS27795440 inhibit B cell activation and antibody production. (A) BCR-mediated calcium mobilization in anti-IgM-stimulated Ramos cells with the AS compounds or DMSO. Following baseline acquisition, Ca^{2+} influx (Max-Min) was calculated. Data are presented as percent of control (DMSO-treated cells). A representative of three experiments is shown. (B) Expression levels of MHC class II in CD45R^+ B cells in anti-IgM-stimulated whole blood from rats treated with AS2795440 or vehicle. Whole blood was collected 2 h after treatment with AS2795440 (1-10 mg/kg, p.o.) or 0.5% methyl cellulose (MC). 0.5% MC-treated group was used as a control (CT). Mean \pm S.E.M.; $n = 3$. (C) Plasma levels of anti-TNP IgM antibody in TNP-Ficoll-immunized rats with AS2795440 (1-10 mg/kg, p.o., u.i.d.) or 0.5% MC (CT). Data are presented as AUC from day 4 to day 7 (day 4-7) values. Mean \pm S.E.M.; $n = 5$. Significant differences between control and treated groups: *: $p < 0.05$, **: $p < 0.01$, ***: $p < 0.001$ (Dunnet multiple comparison test).

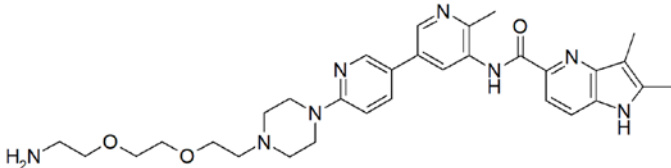
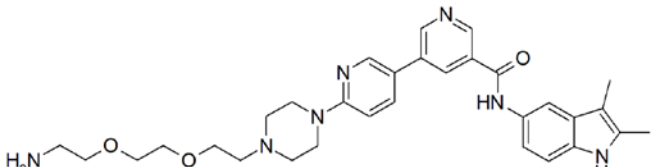
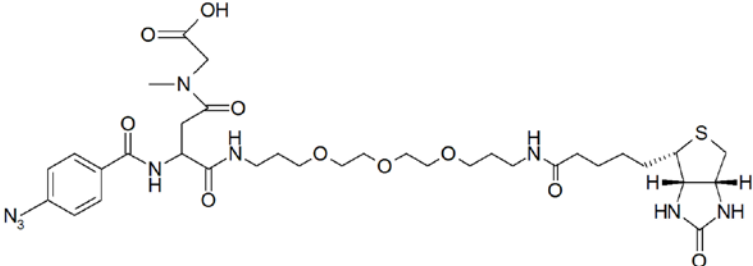
Tool compound	Structure	p40 inhibition IC ₅₀ , nM
High		1.2
Low		>1000
Linker		

Fig. 11. Chemical structures and pharmacological activity of probes or linker. Structures of two different activity probes, High and Low, that are structurally related to AS compounds, or linker. Inhibitory activity of High and Low for IL-12p40 production in IFN γ /LPS-stimulated RAW264.7 cells are shown.

Fig. 12. AS2677131 and AS2795440 are novel PIKfyve inhibitors. (A) Inhibitory activity of three AS compounds for the immunoprecipitated PIKfyve from RAW264.7 cell lysate. Activity was shown as the percent ratio of the control. (B) Correlation between PIKfyve inhibition and IL-12p40 production inhibition for 12 compounds, namely AS2677131, AS2795440, inactive, and nine other structural analogs (A-I). Percentage of inhibition on PIKfyve activity at 200 nM and inhibitory activity on IL-12p40 production (IC₅₀ values in RAW264.7 cells) were plotted. Inactive (p40; IC₅₀ >10 μ M) is indicated as 0% at 10 μ M. (C) Western blotting for p-Akt and total-Akt in RAW264.7 cells treated with the AS compounds or DMSO. Cells pretreated with IFN γ (100 μ g/mL) were treated with AS compounds or DMSO with LPS (10 μ g/mL) for 2 h. Inhibitor concentrations were as follows: AS2677131, AS2795440 (100 nM), and inactive (1 μ M). (D) Phase-contrast images of RAW264.7 cells treated with the AS compounds or DMSO. Inhibitor concentrations were as follows: AS2677131, AS2795440 (100 nM), and inactive (1 μ M). Scale bars: 10 μ m.

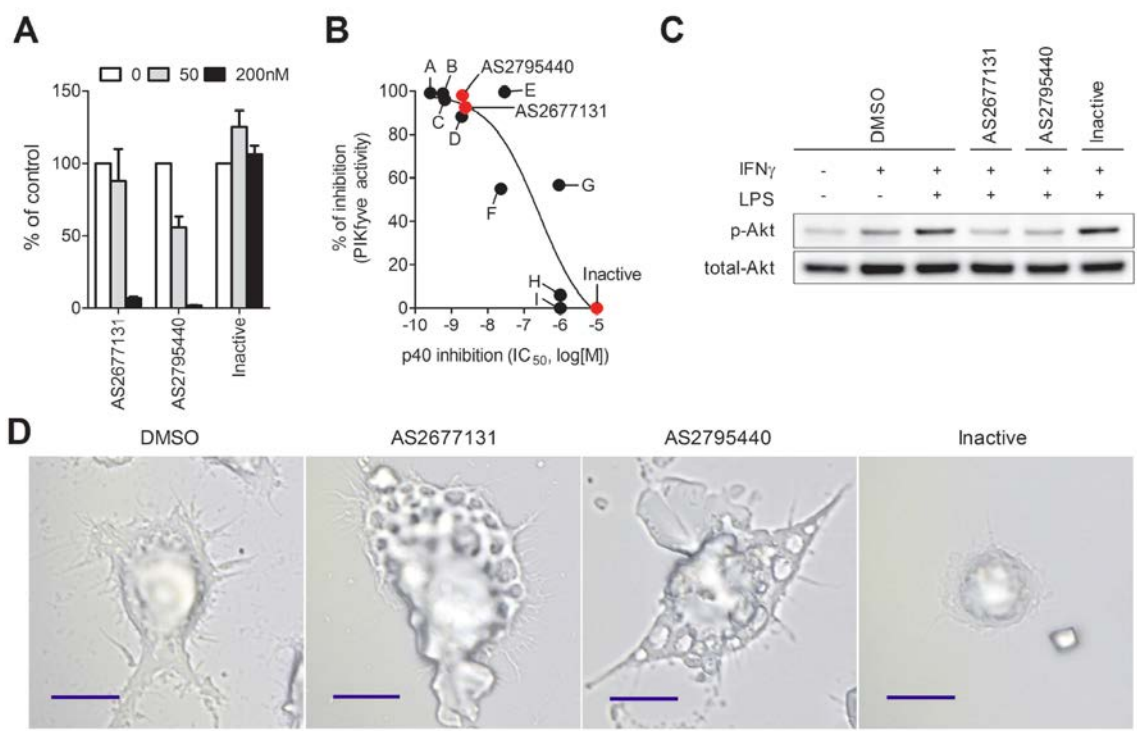


Fig. 12.

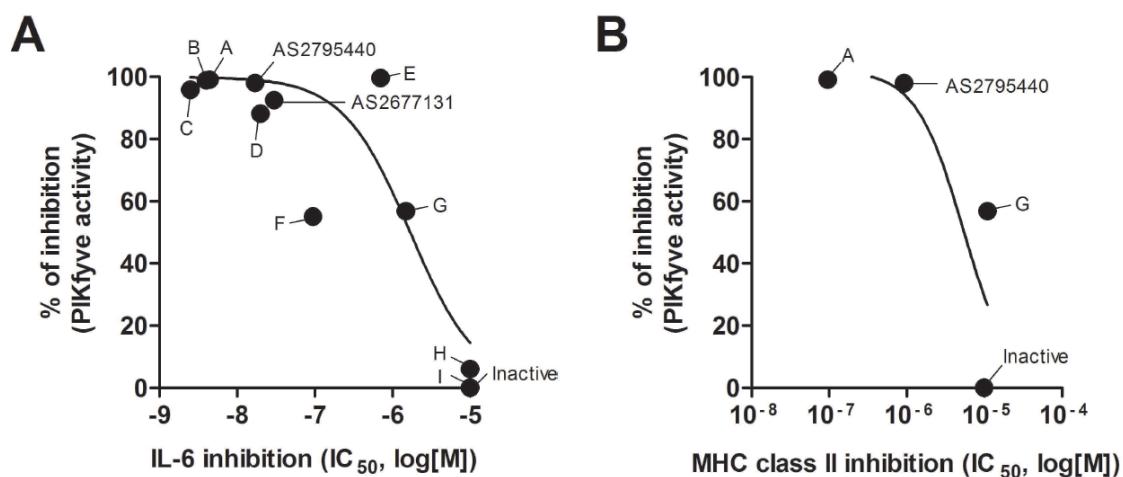


Fig. 13. Correlation between inhibition of PIKfyve activity and IL-6 production or MHC class II expression. Percentage of inhibition on PIKfyve activity at 200 nM (A) and inhibitory activity on IL-12p40 production (IC₅₀ values in RAW264.7 cells) (B) by 12 compounds. Test compounds: AS2677131, AS2795440, inactive, and nine other structural analogs (A-I). Inactive (p40; IC₅₀ >10 μM) was indicated as 0% at 10 μM.

Fig. 14. AS2677131 regulates IL-12p40 expression without affecting I κ B α phosphorylation or nuclear translocation. (A) Western blotting for p-I κ B α and total- I κ B α in RAW264.7 cells treated with the AS compounds or DMSO. Cells pretreated with IFN γ (100 μ g/mL) were restimulated with LPS (10 μ g/mL) for 0.5 h in the presence of AS2677131 (100 nM), inactive (1 μ M), or DMSO. (B) Transient transfection assay of luciferase reporters containing fragments of IL-12p40 promoter (~0.3 kb). IFN γ -primed RAW264.7 cells were stimulated with LPS in the presence of AS2677131 (10, 100 nM), inactive (100 nM), or DMSO. Luciferase activity was measured 6 h after stimulation. Relative promoter activity was calculated by normalizing luciferase activity against Renilla activity. Values are expressed as mean \pm S.E.M. Significant differences are shown as *: $p < 0.05$, **: $p < 0.01$ (Dunnett multiple comparison test, vs IFN γ /LPS-stimulated DMSO control) (C) Western blotting for six proteins in RAW264.7 cells treated with AS2677131 (100 nM) or DMSO. Cells were stimulated with IFN γ and LPS as described above for 1 h and then nuclear fraction was isolated, and immunoblotted with anti-p65, p50, c-Rel, PU.1, IRF-8, and PARP.

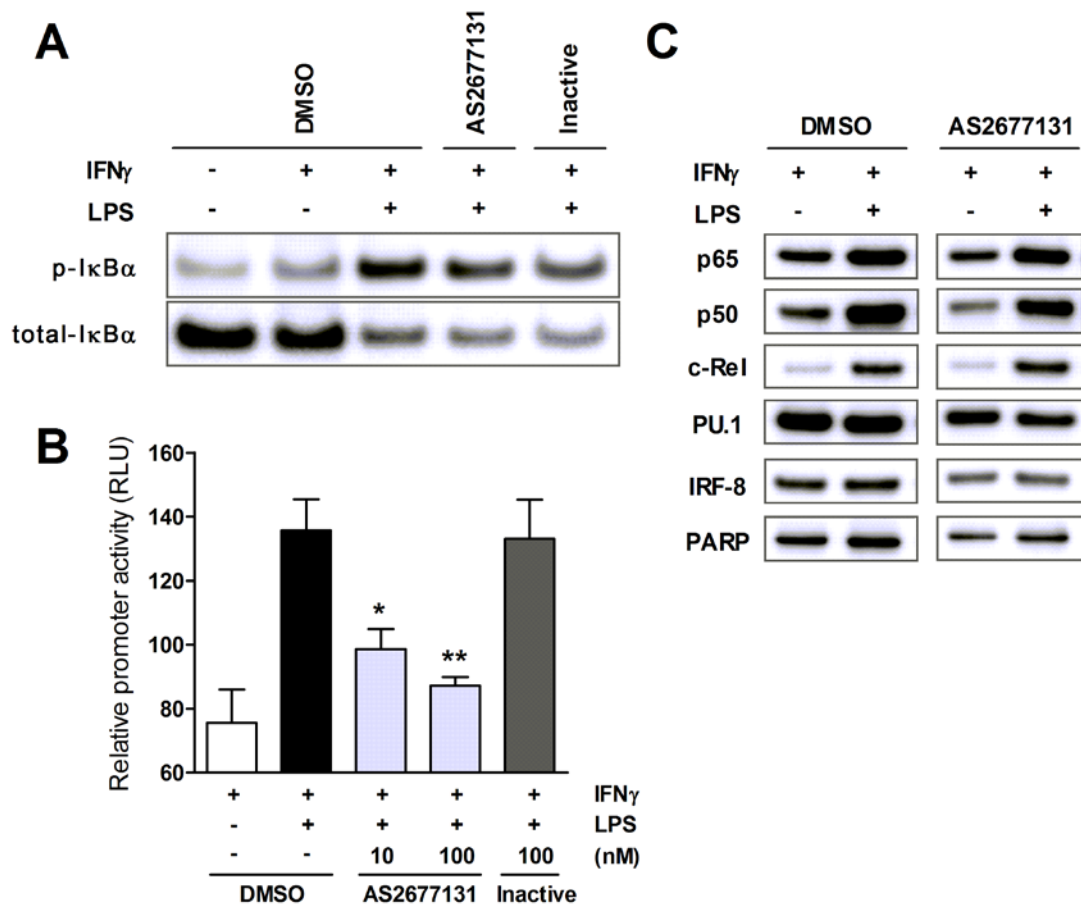


Fig. 14.

Fig. 15. AS2677131 selectively inhibits DNA-binding affinity of c-Rel to IL-12p40 and IL-1 β promoter. (A) Effect of c-Rel knockdown on IL-12p40 and TNF α production in IFN γ /LPS-stimulated RAW264.7 cells. Cells were transfected with siRNAs (si-c-Rel) or scrambled siRNA (si-NC) for 48 h, and the expression levels of c-Rel were detected by real-time PCR or Western blotting. After further incubation with IFN γ (100 ng/mL) and LPS (10 μ g/mL), cytokines in supernatants were measured by ELISA. Mean \pm S.E.M. (B) Schematic representation of endogenous mouse IL-12p40 promoter and the annealing positions of primers for quantification of ChIP assay. (C) ChIP assay of c-Rel and PU.1 to endogenous IL-12p40 promoter in IFN γ /LPS-stimulated RAW264.7 cells treated with the AS2677131 (100 nM), inactive (100 nM), or DMSO. Quantification of DNA bound to c-Rel or PU.1 was performed by real-time PCR (% input mean \pm SD. $n = 3$). (D) ChIP assay of c-Rel to endogenous IL-1 β promoter in IFN γ /LPS-stimulated RAW264.7 cells treated with AS2677131 (1, 10, 100 nM), inactive (100 nM), or DMSO. Quantification was performed as described above.

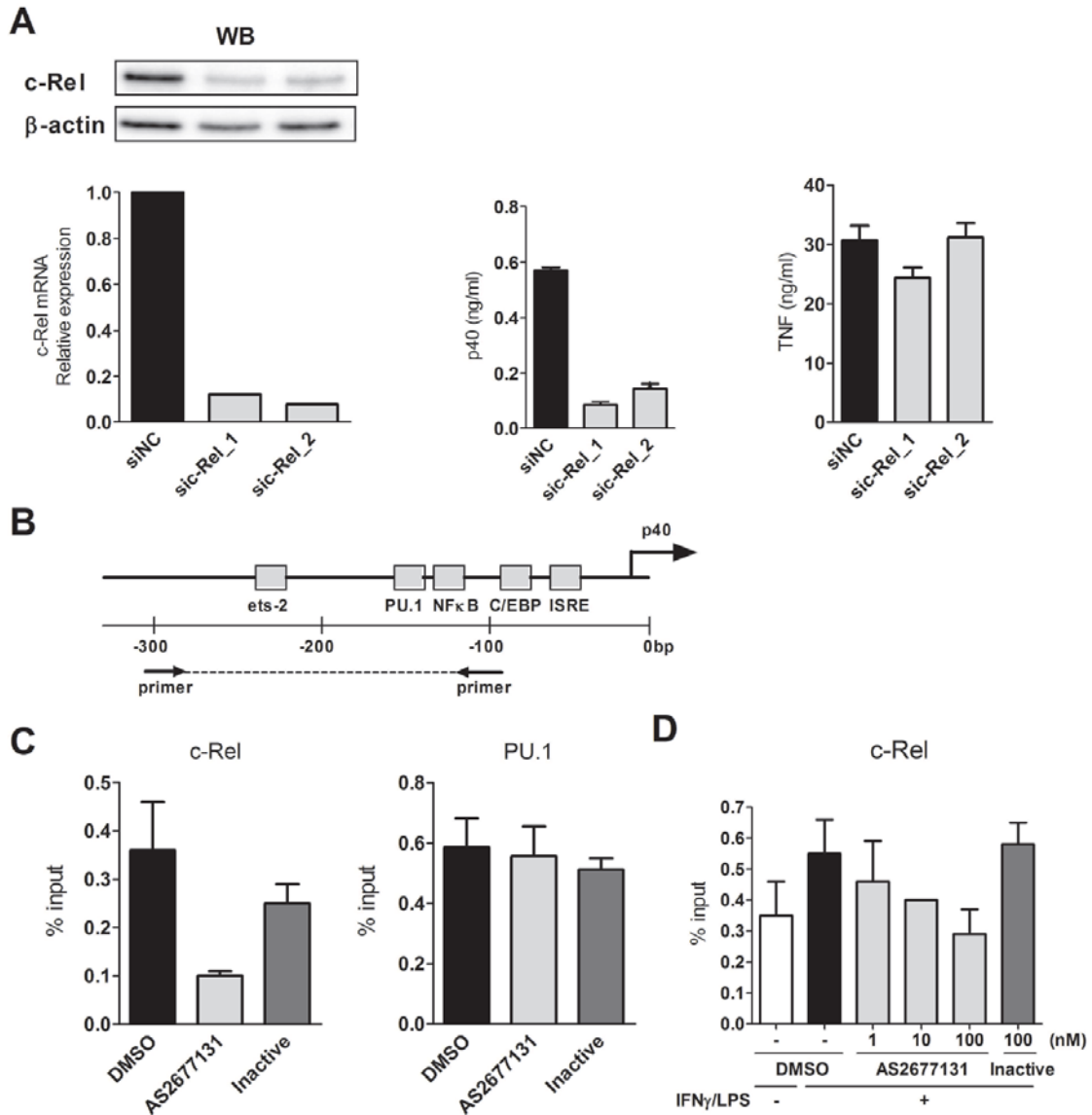


Fig. 15.

Fig. 16. AS2795440 prevents development of AIA. AIA was induced by a subcutaneous injection of CFA at day 0 and treated with AS2795440 (1, 3, 10 mg/kg) or vehicle from day 1 to 24 (control; $n = 10/\text{group}$, AS; $n = 5/\text{group}$). (A) Time course of changes in paw volume in AIA or normal rats treated with AS2795440 or vehicle. The bar graph indicates values at the end of the study (day 25). (B) Body weight of AIA or normal rats at day 25. (C) Histological changes in joint from AIA and normal rats treated with AS2795440 or vehicle. Representative images (HE staining) are shown. Clinical scores were calculated for bone destruction, cartilage destruction, synovial thickening, and inflammatory cell infiltration. Values are expressed as mean \pm S.E.M. (D) Expression levels of CD62L on CD3⁺CD45RA⁺ B cells in whole blood from AIA or normal rats treated with AS2795440, vehicle (blue), or normal (grey). (E) Percentages of CD3⁺CD45RA⁺ CD62L^{low} B cells in whole blood from AIA or normal rats treated with AS2795440 or vehicle. Values are expressed as mean \pm S.E.M. Significant differences between AS2795440 and vehicle-treated (CT) groups: *: $p < 0.05$, **: $p < 0.01$, ***: $p < 0.001$ (Dunnett multiple comparison test)

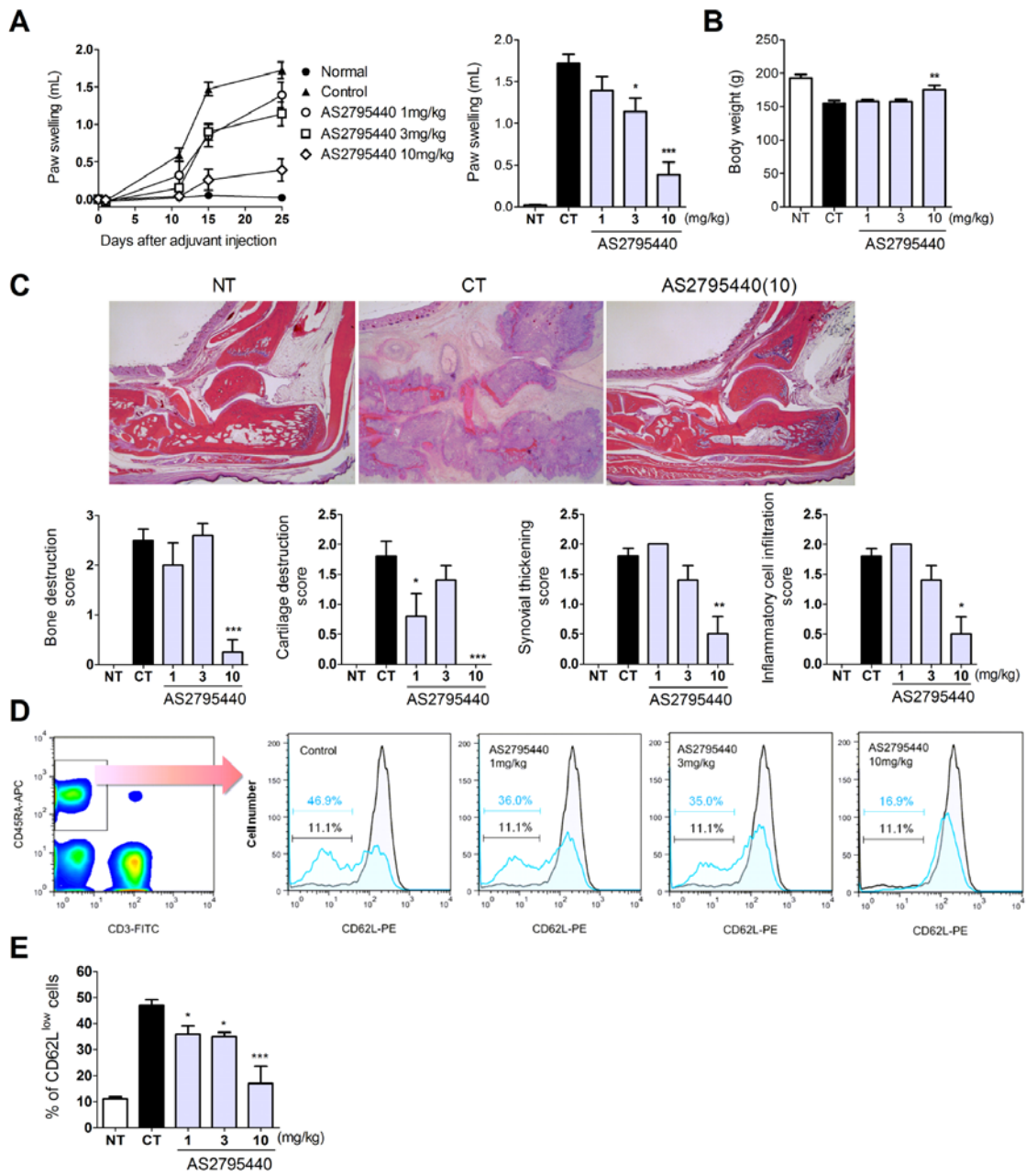


Fig. 16.

General discussion

To elucidate the immunological mechanisms of chronic inflammation and identify potential targets for novel anti-inflammatory drugs, in this study, I have focused on the intracellular signaling pathway regulating proinflammatory cytokine production in macrophages, because it has been reported that many biologic drugs, which can neutralize inflammatory cytokine activity, show excellent therapeutic effect on various chronic inflammatory diseases [2-4]. However, biological therapy is generally expensive and inconvenient to administer, and therefore I have screened and identified the small molecule inhibitors for two different targets, p38 MAPK (Chapter I) and PIKfyve (Chapter II), which have crucial roles in the inflammatory responses, including proinflammatory cytokine production in activated macrophages/monocytes and dendritic cells. This study has also revealed some roles of p38 MAPK and PIKfyve in the development of chronic inflammation by analyzing the pharmacological profiles of the newly identified inhibitors.

In the first chapter, I screened a small molecule inhibitor of p38 MAPK that is responsible for the production and activation signal of proinflammatory cytokines such as TNF α , IL-1 β , and IL-6, and a novel p38 MAPK inhibitor, AS1940477 was identified. Functional characterization regarding the anti-inflammatory properties of AS1940477 in both *in vitro* and *in vivo* has indicated that its potency and selectivity against p38 MAPK is superior to those of previously reported p38 MAPK inhibitors (Fig. 2-7, and Table 1-2). Especially, it is remarkable that AS1940477 can reduce the production of LPS-induced TNF α and IL-6 production in rats at doses below

0.1 mg/kg (Fig. 6A-C) and its inhibitory effect lasts for 20h after oral administration (Fig. 7). Following completion of the current study, Toru-Asano et al. also reported that AS1940477 prevented the development of experimental arthritis in rats [73], which is supporting that the inhibition of p38 MAPK may be useful for the treatment of chronic inflammatory diseases. On the other hand, some clinical studies on p38 programs showed that early suppressive effect on CRP was not sustained and rebounded by 2-4 weeks, and others also have the opinion that it is preferable to combine inhibition of p38 with other targets in parallel inflammatory signaling pathway to achieve the desired efficacy in chronic inflammatory disease [74]. In that regard, it may be necessary to obtain further clinical data using potent and high selectivity inhibitors such as AS1940477.

In the second chapter, I firstly screened small molecule inhibitors for the production of IL-12p40 in IFN γ /LPS-stimulated macrophages, and identified two potent and selective IL-12p40 production inhibitors, AS2677131 and AS2795440. Functional characterization has indicated that these compounds show inhibitory activity against proinflammatory cytokine production (IL-12p40, IL-6, IL-1 β but not TNF α) and BCR-mediated B cell activation (Fig. 9 and 10), and a significant preventive effect was also confirmed on experimental arthritis in rats (Fig. 16). Furthermore, molecular biological analysis using photoreactive linker-conjugated probes has shown that PIKfyve is a direct target and selectively regulates the binding activity of c-Rel to the promoter of proinflammatory cytokines, including IL-12p40 and IL-1 β (Fig. 12-15 and Table 8-10). These results indicate that PIKfyve is a

key signaling molecule for proinflammatory cytokine production and BCR-mediated B cell activation, but this study has unveiled only a part of the immune regulatory mechanism of PIKfyve. It remains unknown whether PIKfyve directly or indirectly controls c-Rel activity and whether the mechanisms of proinflammatory cytokine production and B cell activation are mediated by membrane trafficking or autophagy system.

Mammalian PIKfyve that was originally discovered from mouse adipocytes in screening as one of transcripts like GLUT4 transporter controls pleiotropic expression cell function. The best-characterized role of PIKfyve is membrane trafficking pathway, especially, many studies on endosome formation have been reported. On the other hand, there has been no major report on PIKfyve involvement in immune system until recently, although PI3K, one of the family protein regulating PI metabolism same as PI5K including PIKfyve, is known to be an important molecule in immune system [75]. The report of Cai X et al in 2013 showed that PIKfyve was the target of apilimod, an IL-12/IL-23 inhibitor, and it was firstly revealed that PIKfyve contributed to the inflammatory response [60]. Thereafter, several studies has been reported that PIKfyve is involved in TLR-mediated type I IFN production [76], allergic inflammatory reaction [77], and immune system in neutrophil [78], but understanding of molecular mechanisms including cytokine production is still insufficient. The findings in this study that PIKfyve regulates proinflammatory cytokine production via c-Rel are consistent with the previous reports that deletion of c-Rel in macrophages selectively decreased IL-12p40 production [42], which has greatly

contributed to the correct understanding of the mechanism of chronic inflammation.

In conclusion, the current study has demonstrated that p38 MAPK and PIKfyve play key roles in the development of chronic inflammation, and the inhibition of their kinase activity by novel small molecule inhibitors (AS1940477, AS2677131, and AS2795440) could be a new therapeutic approach for treating chronic inflammatory diseases. It is also expected that new molecules as anti-inflammatory drug targets will be found in future from PIKfyve-c-Rel pathway.

Acknowledgements

I would like to express my greatest appreciation to Associate Prof. Kazuichi Sakamoto (Faculty of Life and Environmental Sciences, University of Tsukuba) for his valuable guidance and support.

I also specially thank Prof. Akito Tanaka. (Hyogo University of Health Science) for providing the Linker compound.

Further, I thank Drs. Shunichiro Matsumoto, Sadao Kuromistu, Taro Masunaga, Yasuaki Shimizu, and Nobuo Seki, Astellas Pharma Inc., for helpful discussions and encouragement.

I also thank Mamoru Tasaki, Dr. Tomoko Kawashima, Dr. Takeshi Ishikawa, Emiko Imamura, Dr. Makoto Ogino, Dr. Takashi Matsuda, Dr. Hiroshi Nagata, Ikue Sato, Narumi Kamata and many colleagues in Astellas Pharma Inc. for their technical support and valuable discussion.

Finally, I would like to appreciate my family for their continuous encouragement and support.

References

1. Freund, A., et al., *Inflammatory networks during cellular senescence: causes and consequences*. Trends Mol Med, 2010. **16**(5): p. 238-46.
2. Schett, G., et al., *How cytokine networks fuel inflammation: Toward a cytokine-based disease taxonomy*. Nat Med, 2013. **19**(7): p. 822-4.
3. Mease, P.J. and C.E. Antoni, *Psoriatic arthritis treatment: biological response modifiers*. Ann Rheum Dis, 2005. **64 Suppl 2**: p. ii78-82.
4. Bresnihan, B. and M. Cobby, *Clinical and radiological effects of anakinra in patients with rheumatoid arthritis*. Rheumatology (Oxford), 2003. **42 Suppl 2**: p. ii22-8.
5. Dong, C., R.J. Davis, and R.A. Flavell, *MAP kinases in the immune response*. Annu Rev Immunol, 2002. **20**: p. 55-72.
6. Sbrissa, D., O.C. Ikononov, and A. Shisheva, *PIKfyve, a mammalian ortholog of yeast Fab1p lipid kinase, synthesizes 5-phosphoinositides. Effect of insulin*. J Biol Chem, 1999. **274**(31): p. 21589-97.
7. Firestein, G.S., *Evolving concepts of rheumatoid arthritis*. Nature, 2003. **423**(6937): p. 356-61.
8. Lowes, M.A., A.M. Bowcock, and J.G. Krueger, *Pathogenesis and therapy of psoriasis*. Nature, 2007. **445**(7130): p. 866-873.
9. Xavier, R.J. and D.K. Podolsky, *Unravelling the pathogenesis of inflammatory bowel disease*. Nature, 2007. **448**(7152): p. 427-434.
10. Bohm, C., et al., *The alpha-isoform of p38 MAPK specifically regulates arthritic bone loss*. J Immunol, 2009. **183**(9): p. 5938-5947.
11. O'Keefe, S.J., et al., *Chemical genetics define the roles of p38alpha and p38beta in acute and chronic inflammation*. J Biol Chem, 2007. **282**(48): p. 34663-34671.
12. Miyazawa, K., et al., *Regulation of interleukin-1beta-induced interleukin-6 gene expression in human fibroblast-like synoviocytes by p38 mitogen-activated protein kinase*. J Biol Chem, 1998. **273**(38): p. 24832-24838.
13. Zhang, J., B. Shen, and A. Lin, *Novel strategies for inhibition of the p38 MAPK pathway*. Trends Pharmacol Sci, 2007. **28**(6): p. 286-295.

14. Hope, H.R., et al., *Anti-inflammatory properties of a novel N-phenyl pyridinone inhibitor of p38 mitogen-activated protein kinase: preclinical-to-clinical translation*. J Pharmacol Exp Ther, 2009. **331**(3): p. 882-895.
15. Beyaert, R., et al., *The p38/RK mitogen-activated protein kinase pathway regulates interleukin-6 synthesis response to tumor necrosis factor*. EMBO J, 1996. **15**(8): p. 1914-1923.
16. Minden, A., et al., *c-Jun N-terminal phosphorylation correlates with activation of the JNK subgroup but not the ERK subgroup of mitogen-activated protein kinases*. Mol Cell Biol, 1994. **14**(10): p. 6683-8.
17. Traenckner, E.B., et al., *Phosphorylation of human I kappa B-alpha on serines 32 and 36 controls I kappa B-alpha proteolysis and NF-kappa B activation in response to diverse stimuli*. EMBO J, 1995. **14**(12): p. 2876-2783.
18. Raingeaud, J., et al., *Pro-inflammatory cytokines and environmental stress cause p38 mitogen-activated protein kinase activation by dual phosphorylation on tyrosine and threonine*. J Biol Chem, 1995. **270**(13): p. 7420-7426.
19. Schindler, J.F., J.B. Monahan, and W.G. Smith, *p38 pathway kinases as anti-inflammatory drug targets*. J Dent Res, 2007. **86**(9): p. 800-811.
20. Goldstein, D.M., et al., *Selective p38alpha inhibitors clinically evaluated for the treatment of chronic inflammatory disorders*. J Med Chem, 2010. **53**(6): p. 2345-2353.
21. Damjanov, N., R.S. Kauffman, and G.T. Spencer-Green, *Efficacy, pharmacodynamics, and safety of VX-702, a novel p38 MAPK inhibitor, in rheumatoid arthritis: results of two randomized, double-blind, placebo-controlled clinical studies*. Arthritis Rheum, 2009. **60**(5): p. 1232-1241.
22. Kuma, Y., et al., *BIRB796 inhibits all p38 MAPK isoforms in vitro and in vivo*. J Biol Chem, 2005. **280**(20): p. 19472-19479.
23. Hill, R.J., et al., *Pamapimod, a novel p38 mitogen-activated protein kinase inhibitor: preclinical analysis of efficacy and selectivity*. J Pharmacol Exp Ther, 2008. **327**(3): p. 610-619.
24. Labuda, T., A. Sundstedt, and M. Dohlsten, *Selective induction of p38*

- mitogen-activated protein kinase activity following A6H co-stimulation in primary human CD4(+) T cells.* Int Immunol, 2000. **12**(3): p. 253-261.
25. Westra, J. and P.C. Limburg, *p38 mitogen-activated protein kinase (MAPK) in rheumatoid arthritis.* Mini Rev Med Chem, 2006. **6**(8): p. 867-874.
 26. Morrison, D.C. and J.L. Ryan, *Endotoxins and disease mechanisms.* Annu Rev Med, 1987. **38**: p. 417-432.
 27. Lichtman, A.H., G.B. Segel, and M.A. Lichtman, *The role of calcium in lymphocyte proliferation. (An interpretive review).* Blood, 1983. **61**(3): p. 413-422.
 28. Ward, S.G., et al., *A p38 MAP kinase inhibitor SB203580 inhibits CD28-dependent T cell proliferation and IL-2 production.* Biochem Soc Trans, 1997. **25**(2): p. 304S.
 29. Zhang, J., et al., *p38 mitogen-activated protein kinase mediates signal integration of TCR/CD28 costimulation in primary murine T cells.* J Immunol, 1999. **162**(7): p. 3819-3829.
 30. Rincon, M., et al., *Interferon-gamma expression by Th1 effector T cells mediated by the p38 MAP kinase signaling pathway.* EMBO J, 1998. **17**(10): p. 2817-2829.
 31. Chopra, P., et al., *Pharmacological profile of AW-814141, a novel, potent, selective and orally active inhibitor of p38 MAP kinase.* Int Immunopharmacol, 2010. **10**(4): p. 467-473.
 32. Nikas, S.N. and A.A. Drosos, *SCIO-469 Scios Inc.* Curr Opin Investig Drugs, 2004. **5**(11): p. 1205-1212.
 33. Cohen, S.B., et al., *Evaluation of the efficacy and safety of pamapimod, a p38 MAP kinase inhibitor, in a double-blind, methotrexate-controlled study of patients with active rheumatoid arthritis.* Arthritis Rheum, 2009. **60**(2): p. 335-344.
 34. Genovese, M.C., et al., *A 24-week, randomized, double-blind, placebo-controlled, parallel group study of the efficacy of oral SCIO-469, a p38 mitogen-activated protein kinase inhibitor, in patients with active rheumatoid arthritis.* J Rheumatol, 2011. **38**(5): p. 846-54.
 35. Hynes, J., Jr., et al., *The discovery of (R)-2-(sec-butylamino)-N-(2-methyl-5-(methylcarbamoyl)phenyl)*

- thiazole-5-carboxamide (BMS-640994)-A potent and efficacious p38alpha MAP kinase inhibitor*. *Bioorg Med Chem Lett*, 2008. **18**(6): p. 1762-1767.
36. Genovese, M.C., et al., *Proof of concept study for a potent p38 MAPK dual action inhibitor BMS-582949 in subjects with RA receiving concomitant methotrexate. [abstract]*. *Arthritis Rheum*, 2010. **62**(suppl 10): p. 1119.
 37. Schieven, G., et al., *BMS-582949 is a dual action p38 kinase inhibitor well suited to avoid resistance mechanisms that increase p38 activation in cells. [abstract]*. *Arthritis Rheum*, 2010. **62**(suppl 10): p. 1513.
 38. Langrish, C.L., et al., *IL-12 and IL-23: master regulators of innate and adaptive immunity*. *Immunol Rev*, 2004. **202**: p. 96-105.
 39. Murphy, C.A., et al., *Divergent pro- and antiinflammatory roles for IL-23 and IL-12 in joint autoimmune inflammation*. *J Exp Med*, 2003. **198**(12): p. 1951-1957.
 40. Lee, E., et al., *Increased expression of interleukin 23 p19 and p40 in lesional skin of patients with psoriasis vulgaris*. *J Exp Med*, 2004. **199**(1): p. 125-30.
 41. Goriely, S., M.F. Neurath, and M. Goldman, *How microorganisms tip the balance between interleukin-12 family members*. *Nat Rev Immunol*, 2008. **8**(1): p. 81-6.
 42. Sanjabi, S., et al., *Selective requirement for c-Rel during IL-12 P40 gene induction in macrophages*. *Proc Natl Acad Sci U S A*, 2000. **97**(23): p. 12705-12710.
 43. Skwarek, L.C. and G.L. Boulianne, *Great expectations for PIP: phosphoinositides as regulators of signaling during development and disease*. *Dev Cell*, 2009. **16**(1): p. 12-20.
 44. Rutherford, A.C., et al., *The mammalian phosphatidylinositol 3-phosphate 5-kinase (PIKfyve) regulates endosome-to-TGN retrograde transport*. *J Cell Sci*, 2006. **119**(Pt 19): p. 3944-57.
 45. Jefferies, H.B., et al., *A selective PIKfyve inhibitor blocks PtdIns(3,5)P(2) production and disrupts endomembrane transport and retroviral budding*. *EMBO Rep*, 2008. **9**(2): p. 164-70.
 46. Shisheva, A., *PIKfyve: Partners, significance, debates and paradoxes*. *Cell Biol Int*, 2008. **32**(6): p. 591-604.

47. de Lartigue, J., et al., *PIKfyve regulation of endosome-linked pathways*. *Traffic*, 2009. **10**(7): p. 883-93.
48. Hattori, K., et al., *The synthetic procedure and structure-activity relationship of novel IL-12(p40) production inhibitors*, in *30th Medicinal Chemistry Symposium*. 2012, The Pharmaceutical Society of Japan, Division of Medicinal Chemistry: Japan. p. 86.
49. Ouyang, X., et al., *Cooperation between MyD88 and TRIF pathways in TLR synergy via IRF5 activation*. *Biochem Biophys Res Commun*, 2007. **354**(4): p. 1045-51.
50. Rappsilber, J., Y. Ishihama, and M. Mann, *Stop and go extraction tips for matrix-assisted laser desorption/ionization, nanoelectrospray, and LC/MS sample pretreatment in proteomics*. *Anal Chem*, 2003. **75**(3): p. 663-70.
51. Tsuruta, F., et al., *PIKfyve regulates CaV1.2 degradation and prevents excitotoxic cell death*. *J Cell Biol*, 2009. **187**(2): p. 279-94.
52. Nonami, H., et al., *beta-Carboline alkaloids as matrices for UV-matrix-assisted laser desorption/ionization time-of-flight mass spectrometry in positive and negative ion modes. Analysis of proteins of high molecular mass, and of cyclic and acyclic oligosaccharides*. *Rapid Commun Mass Spectrom*, 1998. **12**(6): p. 285-96.
53. Ma, X., et al., *Identification and characterization of a novel Ets-2-related nuclear complex implicated in the activation of the human interleukin-12 p40 gene promoter*. *J Biol Chem*, 1997. **272**(16): p. 10389-10395.
54. Zhu, C., et al., *Activation of the murine interleukin-12 p40 promoter by functional interactions between NFAT and ICSPB*. *J Biol Chem*, 2003. **278**(41): p. 39372-39382.
55. Magari, K., et al., *Comparison of anti-arthritic properties of leflunomide with methotrexate and FK506: effect on T cell activation-induced inflammatory cytokine production in vitro and rat adjuvant-induced arthritis*. *Inflamm Res*, 2004. **53**(10): p. 544-50.
56. Luo, Y., et al., *The cAMP capture compound mass spectrometry as a novel tool for targeting cAMP-binding proteins: from protein kinase A to potassium/sodium hyperpolarization-activated cyclic nucleotide-gated channels*. *Mol Cell Proteomics*, 2009. **8**(12): p. 2843-56.

57. Ikonomov, O.C., et al., *Requirement for PIKfyve enzymatic activity in acute and long-term insulin cellular effects*. *Endocrinology*, 2002. **143**(12): p. 4742-54.
58. Ikonomov, O.C., D. Sbrissa, and A. Shisheva, *Mammalian cell morphology and endocytic membrane homeostasis require enzymatically active phosphoinositide 5-kinase PIKfyve*. *J Biol Chem*, 2001. **276**(28): p. 26141-7.
59. Stolina, M., et al., *The evolving systemic and local biomarker milieu at different stages of disease progression in rat adjuvant-induced arthritis*. *J Clin Immunol*, 2009. **29**(2): p. 158-74.
60. Cai, X., et al., *PIKfyve, a class III PI kinase, is the target of the small molecular IL-12/IL-23 inhibitor apilimod and a player in Toll-like receptor signaling*. *Chem Biol*, 2013. **20**(7): p. 912-21.
61. Berwick, D.C., et al., *Protein kinase B phosphorylation of PIKfyve regulates the trafficking of GLUT4 vesicles*. *J Cell Sci*, 2004. **117**(Pt 25): p. 5985-93.
62. Okkenhaug, K. and B. Vanhaesebroeck, *PI3K in lymphocyte development, differentiation and activation*. *Nat Rev Immunol*, 2003. **3**(4): p. 317-30.
63. Hodson, D.J. and M. Turner, *The role of PI3K signalling in the B cell response to antigen*. *Adv Exp Med Biol*, 2009. **633**: p. 43-53.
64. Hiscott, J., et al., *Characterization of a functional NF-kappa B site in the human interleukin 1 beta promoter: evidence for a positive autoregulatory loop*. *Mol Cell Biol*, 1993. **13**(10): p. 6231-40.
65. Murphy, T.L., et al., *Regulation of interleukin 12 p40 expression through an NF-kappa B half-site*. *Mol Cell Biol*, 1995. **15**(10): p. 5258-67.
66. O'Keeffe, M., et al., *Distinct roles for the NF-kappaB1 and c-Rel transcription factors in the differentiation and survival of plasmacytoid and conventional dendritic cells activated by TLR-9 signals*. *Blood*, 2005. **106**(10): p. 3457-64.
67. Lu, Y.C., et al., *Differential role for c-Rel and C/EBPbeta/delta in TLR-mediated induction of proinflammatory cytokines*. *J Immunol*, 2009. **182**(11): p. 7212-21.
68. Zhou, D., et al., *Protein tyrosine phosphatase SHP-1 positively regulates TLR-induced IL-12p40 production in macrophages through inhibition of*

- phosphatidylinositol 3-kinase*. J Leukoc Biol, 2010. **87**(5): p. 845-55.
69. Sanchez-Valdepenas, C., et al., *NF-kappaB-inducing kinase is involved in the activation of the CD28 responsive element through phosphorylation of c-Rel and regulation of its transactivating activity*. J Immunol, 2006. **176**(8): p. 4666-74.
70. Baracho, G.V., et al., *Emergence of the PI3-kinase pathway as a central modulator of normal and aberrant B cell differentiation*. Curr Opin Immunol, 2011. **23**(2): p. 178-83.
71. Hsia, C.Y., et al., *c-Rel regulation of the cell cycle in primary mouse B lymphocytes*. Int Immunol, 2002. **14**(8): p. 905-16.
72. Campbell, I.K., et al., *Distinct roles for the NF-kappaB1 (p50) and c-Rel transcription factors in inflammatory arthritis*. J Clin Invest, 2000. **105**(12): p. 1799-806.
73. Asano, T., et al., *Identification, synthesis, and biological evaluation of 6-[(6R)-2-(4-fluorophenyl)-6-(hydroxymethyl)-4,5,6,7-tetrahydropyrazolo[1,5-a]pyrimidin-3-yl]-2-(2-methylphenyl)pyridazin-3(2H)-one (AS1940477), a potent p38 MAP kinase inhibitor*. J Med Chem, 2012. **55**(17): p. 7772-85.
74. Xing, L., *Clinical candidates of small molecule p38 MAPK inhibitors for inflammatory diseases*. MAP Kinase 2015, 2015. **4**(5508): p. 24-30.
75. Fruman, D.A., et al., *The PI3K pathway in human disease*. Cell, 2017. **170**(4): p. 605-635.
76. Cai, X., et al., *PIKfyve, a class III lipid kinase, is required for TLR-induced type I IFN production via modulation of ATF3*. J Immunol, 2014. **192**(7): p. 3383-9.
77. Kawasaki, T., et al., *Deletion of PIKfyve alters alveolar macrophage populations and exacerbates allergic inflammation in mice*. EMBO J, 2017. **36**(12): p. 1707-1718.
78. Dayam, R.M., et al., *The Lipid Kinase PIKfyve Coordinates the Neutrophil Immune Response through the Activation of the Rac GTPase*. J Immunol, 2017. **199**(6): p. 2096-2105.